The Vulnerability of Nuclear Reactors to Attack By Nuclear Weapons

Steve Fetter

Program in Science and Technology for International Security

Report No. 7

Department of Physics
Massachusetts Institute of Technology
Cambridge, Massachusetts 02139

August 1982

INTRODUCTION

Steve Fetter is now a graduate student at the University of California, Berkeley. While still a fourth-year undergraduate at M.I.T., he undertook to examine the vulnerability of nuclear reactors to the various effects of a nuclear detonation, as his senior thesis topic. A year earlier he had examined (with Kosta Tsipis) what would be the effects of a direct nuclear hit on a reactor, without attempting to relate the probability that the reactor would collapse to the various parameters of the attacking nuclear weapon. The results of this earlier study were published in PSTIS Report #5 under the title Catastrophic Nuclear Radiation Releases. In a sense, then, this report is a sequel to Report #5 and completes the discussion of a nuclear attack on a nuclear reactor.

K. Tsipis
Co-Director, PSTIS

August 1982

TABLE OF CONTENTS

CHAPTER 1

Description of the Problem

Energy production facilities have always been targets in war, because energy is needed for the healthy functioning of any economy and for the support of a war effort. In fact, after World War II some German officials stated that the chief error made by the United States was their failure to attack energy facilities, and that the war might have been ended a year earlier if they were bombed. For this reason alone, it seems wise to consider the possibility that nuclear reactors might become target in future wars, and even future nuclear wars.

But there is another more compelling reason to study this problem - nuclear reactors contain vast amounts of radioactive materials, which if distributed effeciently would contaminate tens of thousands of square miles of land. A typical reactor contains as many long-lived fission products as fifty one-megaton weapons. A successful attack on a reactor with a nuclear weapon may prove to be a very effective means of desolating large areas of adjacent land, destroying crops, and crippling the economy.

The question before us is "can this happen?" Are nuclear reactors vulnerable to an attack by nuclear weapons? To answer this question we must define two measures of "vulnerability": the attacker must be able to destroy the reactor (physical vulnerability), and the attack must produce a significantly greater amount of damage than that produced by attacks on more conventional targets (strategic vulnerability). Only if both of

these criteria are met will the reactor be vulnerable to attack.

The first part of this report will deal exclusively with the physical vulnerability of the reactor to the destructive effects of a large nuclear weapon, which include nuclear and thermal radiations (Chap. 2), air blast (Chap. 3), cratering (Chap. 4), and ground shock (Chap. 5). The result of this analysis will be an estimate of the miss distance of a weapon which is needed to inflict a given level of damage to the reactor. The discussion is limited to a one-megaton thermonuclear weapon and a 1000 megawatt nuclear reactor because they are typical of what exists, but the results can be applied to different situations also.

In general, there are five levels of physical damage of interest here, and they are listed in order of increasing severity: 1) the weapon does not cause a reactor meltdown, but causes a loss of power; 2) the weapon causes a meltdown, but the containment structure is not breached; 3) the weapon breaches the containment structure, and radioactivity from the core escapes after one-half hour; 4) the weapon completely destroys the reactor facilities, and volatile fission products are released immediately; and 5) the weapon ruptures the pressure vessel and entrains some or all of the reactor core and spent fuel in the radioactive cloud of the weapon.

In the second part of the report, the additional damage caused by each type of attack is estimated. The most obvious consequence of a successful attack is the loss of electric power and perhaps the capital investment represented by the reactor. Even more potentially damaging may be the releases of radioactivity that follow the attack. The most severe damage is caused when

reactor fission products are released during the first few minutes after the attack, when the radioactive material can join with the weapon debris and increase the resulting fallout (Chap. 7). Chapter 8 estimates the damage from radioactive materials released after the winds have subsided, in the manner of a meltdown. Subsequent chapters try to estimate the social and economic impacts that this increased damage may have.

What immediately follows is a brief description of the forces at work in a nuclear detonation, and the reactor buildings which must resist these effects.

The Effects of Nuclear Weapons in Brief

The vast amounts of energy liberated in the detonation of a nuclear weapon are due to the processes of fission and fusion, in which the nuclei of certain atoms are changed. In fission, the nucleus of a Uranium or Plutonium atom is split into two or more parts after being bombarded with neutrons, and in the process two or three new neutrons are produced, along with about 200 MeV of energy. In fusion, the nucleus of an isotope of Hydrogen or Lithium is fused together with another nucleus. usually producing a neutron and several MeV of energy.

The first weapons produced, including those dropped on Hiroshima and Nagasaki, were entirely fission weapons, and had total energy yields equivalent to about twenty thousands tons of TNT (20kt). If a country with unsophisticated nuclear weapons or a terrorist group were to attack a nuclear reactor, it would probably be with a weapon of this type, with a yield between 0.05 and 50 kt. The weapons which comprise the arsenals of the United States, the Soviet Union, and China utilize both fission and fusion, and achieve yields above 10 million tons of TNT equivalent (10 MT). These devices are called "thermonuclear weapons", because they utilize the extremely high temperatures of a fission reaction to initiate the fusion reaction. In weapons of this type, roughly half of the energy is released by fission, and the other half by fusion processes.

Because temperatures on the order of several million degrees Kelvin are necessary for fusion reactions to take place, thermonuclear weapons must be contructed in such a manner that the

energy from a small fission reaction or "trigger" can be directed onto a target of fusable material, so that the material undergoes fusion before the weapon is blown apart by the extremely high pressures caused by the fission reaction. Because a large amount of high energy neutrons are released in the fusion process, it is common practise to surround the entire assembly with Uranium-238, which will fission and release even more energy when bombarded by these neutrons. These processes continue until the amount of energy released is so great that the weapon vaporizes, and the reactions stop. At this time, which is approximately one-half microsecond, the weapon debris reach pressures of millions of atmospheres and temperatures of tens of millions of degrees Kelvin.

Very small amounts of material are used in producing energy in this manner; only about 9 kilograms of Deuterium and 28 kilograms of Uranium are needed to react to produce one megaton of energy. Thus, the weapon itself may be very small, yielding very high energy densities. This is in contrast to chemical explosions, where large amounts of explosive per unit of energy are needed to transfer energy to the environment.

Immediately after the detonation, the weapon materials are in a dense, hot vapor, with nearly all the atoms completely ionized. If the detonation occurs near the surface of the earth, these ionized electrons will not be distributed symmetrically about the point of burst, and in about one-half microsecond a tremendous current surge will occur in the vertical direction as the electrons redistribute themselves. This surge is called the

"Electromagnetic pulse" or EMP, and radiates long-wavelength radiation for hundreds of miles from the burst.

Charged particles released by the reactions will not travel far in the weapon debris, and will be quickly thermalized. Even though they are not charged, over 90% of the neutrons produced by fission and fusion will be absorbed by the dense vapor; the remainder travel so fast that they escape in much less than one millisecond, and can travel considerable distances in air. Gamma rays produced by the reactions and by the decaying fission products will also be strongly absorbed by the debris.

The hot vapor almost immediately starts to emit photons as electrons reattach to atoms and return from their excited states. Most of these photons have an energy of a few keV, which is far above the visible and corresponds to "soft" x-rays. Air at ordinary temperatures absorbs soft x-rays very quickly, and so as the weapon debris radiates the x-rays they are absorbed immediately by the surrounding cold air, which then heats the air and causes it to become transparent to the x-rays. In this way, subsequent radiation can travel farther to a new layer of cold air, heat that air, and so on. The air heated in this manner becomes so hot that it becomes incandescent, and for this reason it is called the fireball. At one millisecond, the fireball is about 250 feet in radius and has an internal temperature of 5×10^5 degrees Kelvin. This process by which the early fireball grows is called "radiative growth", because it is fueled by the absorption of radiation emitted by the weapon vapors.

Only a small fraction of the energy escapes in the form of

visible and infra-red radiation at this stage of development, and this small amount reaches a peak at about one millisecond, after which it declines due to the increasing opacity of the front.

After a few milliseconds, the surface temperatures have dropped to the point at which radiative growth no longer becomes important, and the driving mechanism behind the growth of the fireball is pressure-volume work done by very dense air at the shock front on the cold air in front of the front. This is called "shock growth".

As the fireball continues to grow, the temperature of the shock front drops until the front inself is no longer luminous. This allows one to look into the hotter interior of the fireball, while the shock front seems to separate and continue to expand. This phenomenon is called "breakaway", and for a one megaton weapon that is surface burst it occurs at about 80 milliseconds, when the fireball radius is about 2,300 feet.

After breakaway, we continue to see further into the fireball to hotter interior temperatures, and so the amount of thermal radiation that is emitted grows rapidly at this time, reaching a maximum at one second. The fireball continues to expand slowly, reaching a maximum diameter of about 5,700 feet after 10 seconds, while also rising into the atmosphere at a rate of 250 to 350 feet per second. The surface temperature continues to drop, and after a minute no visible radiation is emitted.

The shock front, on the other hand, continues expanding at a rapid rate after breakaway. At breakaway, the peak overpressure at the shock front is about 1000 psi, which is great enough to destroy

the very best of shelters. The air shock can be a source of damage to distances of eight miles, where the shock arrives in about 40 seconds with a peak overpressure of one psi. Part of the energy from the air shock is transmitted into the soil, and usually travels ahead of the shock front, causing earthquake-like ground motions.

The fireball and weapon debris also serve in excavating a crater if the weapon is detonated close to the ground, and up to ten million tons of soil can be lifted into the air. Large pieces will be ejected hundreds or thousands of feet from the point of burst, while smaller pieces (up to a few tons) can be lofted into the cloud by the strong updrafts around the cloud. Much of the soil lifted into the cloud will mix with radioactive fission products, and travel with the cloud to a height of about 12 miles in four minutes. During this time, and for hours to come, these radioactive particles will rain back to earth as "fallout", contaminating large amounts of land at lethal dose-rates. Some of the material will be injected into the stratosphere, where it may circle the earth for months or years before returning to the ground.

Description of the Target Reactor

The effects of airblast, ground shock, and nuclear and thermal radiation on a reactor depend very strongly on the dynamic response of the structure and the details of its design. The reactor design chosen for analysis in this report is a commercial pressurized water reactor (PWR), chiefly because two-thirds of the reactors in the United States are of this type.

In a PWR, slightly enriched uranium is arranged in small pellets and inserted in a casing of Zirconium. As fissioning begins, the same reactions which take place in a nuclear weapon occur in these fuel elements, although at a much slower rate. The rate of power production for the reactor considered here is about 3.2×10^9 watts of thermal energy in the reactor core. In constrast, a megaton weapon generates about 10^{22} watts for less than one millionth of a second. The reactor produces power almost continuously, and so the radioactive fission products which decay very quickly are not present in the same proportion as those generated by a weapon.

Ordinary water under high pressure is circulated around the fuel elements in order to tranfer the heat energy of the core. This water passes in a closed loop through the reactor vessel and a heat exchanger, which boils water at normal pressures to generate the steam which turns the turbines and produces electricity. In the end, about 10^9 watts of electricity are generated by the entire reactor.

Even when the fission reaction stops, the fission products will release great amounts of heat, and so it is necessary to

keep the core covered by constantly circulating water. If the water stops circulating, or water is lost from the loop, the core will start to overheat and eventually melt, boiling away large quanities of water and perhaps causing a steam explosion which may rupture the pressure vessel and breach the containment building. If this occurs, radioactive fission products will escape into the atmosphere.

A cross section of the reactor analyzed here is shown in Figure 1-1. Notice the massive construction of the building: the reactor vessel is a 9-inch thick steel cylinder, and it is surrounded by a minimum of 122 inches of heavily reinforced concrete in all directions. Directly outside of the reactor vessel is a 68-inch thick concrete biological shield; surrounding this are the pumps and turbines shielded by at least 12 inches of concrete; the entire assembly is housed in a containment structure with prestressed concrete walls 42 inches thick, with a ¼-inch airtight steel liner attached to the inside. For the purposes of analysis, the containment structure is idealized as a cylinder 130feet in diameter and 145 feet in height, topped by a hemisphere.

Typical containments are designed to withstand severe earthquakes, very high winds (600 mph), and the impact of a car or an airplane. Reactors are usually built in a geologically stable medium, with foundations more massive than those of hundred-story office buildings. Such a reactor is one of the best contructed civilian structures, and consequently it is very resistant to the effects of nuclear weapons.

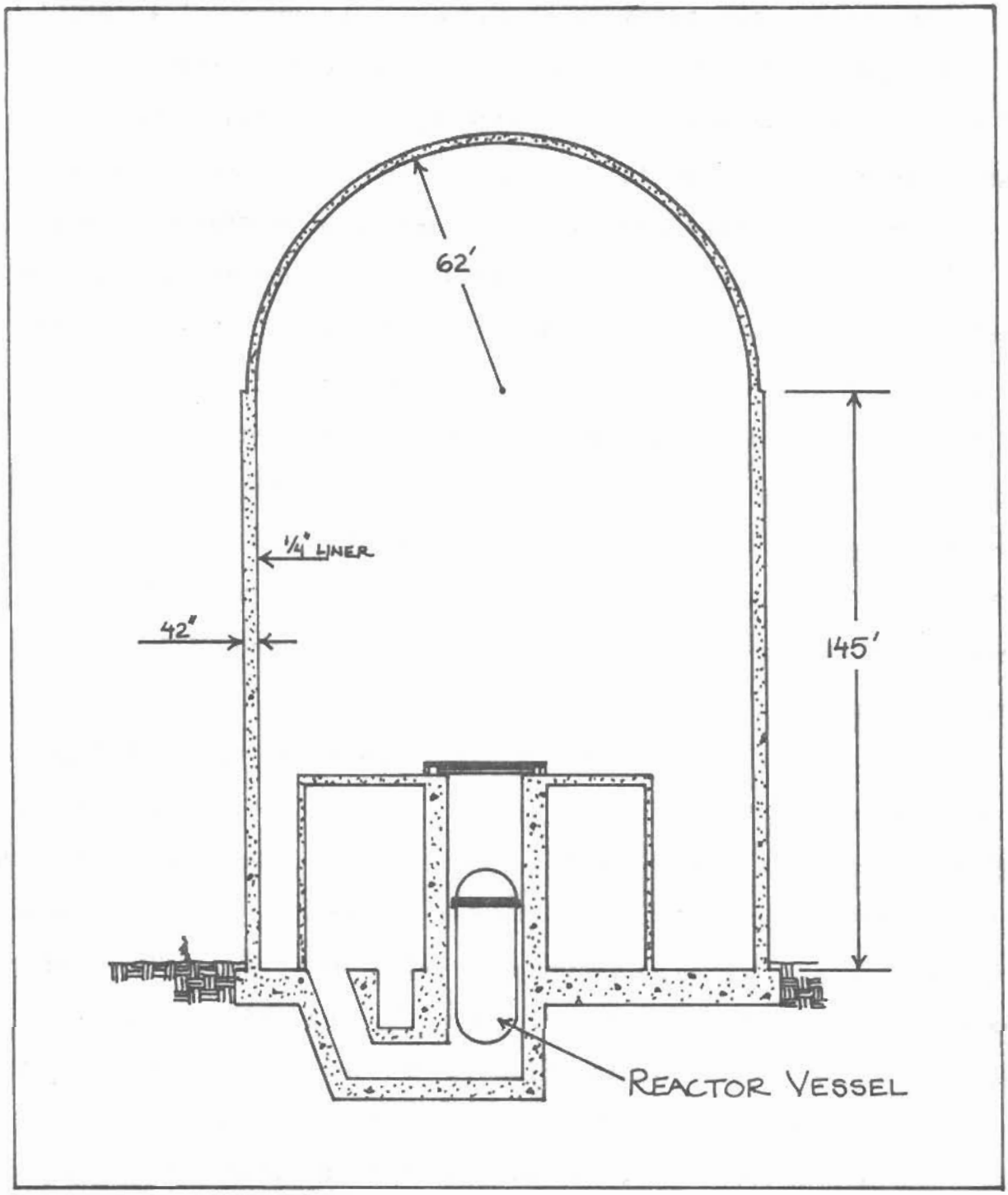

FIGURE 1-1: Section through a typical 1000 megawatt nuclear reactor containment structure.

The containment building is the most important of a group of structures which support the entire production facility. Some of these buildings are directly adjacent to the containment, though usually much smaller, while cooling towers can be much larger than the containment and are located some distance away.

When the fuel elements contain a high proportion of fission products, it is necessary to remove the "spent" fuel and replace it with new fuel. In most reactors, one-third of the core is replaced every year in a single operation, so that at any time, the three regions of the reactor core have different "ages", each separated by about one year. On the average, and for the purposes of the following calculations, the three regions will have been irradiated, or have "burnups" of, 8,800, 17,600, and 26,400 mega-watt-days per metric ton of Uranium.

The fuel that is removed is highly radioactive and generates large amounts of heat due to fission product decay. Immediately after removal from the core the spent fuel is immersed under water in a "spent fuel holding pond", where it remains until it decays to lower levels, usually about six months to a year. When the existing facilities were built, the utilities had planned to reprocess the spent fuel in order to recover the high amounts of unused uranium that are still present. But because the rods also contain Plutonium, which can be used to build nuclear weapons, the United States has stopped reprocessing and plans to dispose of the spent fuel permanently. However, since there are no permanent disposal plans which are agreed upon, temporary storage of the spent fuel in existing spent fuel storage ponds

has been proposed, and probably will be accepted. Present ponds were designed to hold four-thirds core of fuel - one-third in normal operation, and the entire reactor core in the case of an emergency. If used at this rate, all the spent fuel ponds in the United States will quickly be filled, and so plans have been made to enlarge the storage capacity by an average factor of 2.5 at the reactor site. The ponds would then hold seven-thirds of a core in normal operation, and still reserve space for the emergency removal of the reactor core.

The fuel, when placed in these ponds, is quite safe. If the water were to stop circulating because of a pump malfunction, it would take days for the water to boil off and expose the fuel. And even if the fuel is exposed, it takes a considerably longer time to melt and disperse radioactivity into the environment. The only violent release that is possible in the environment of the spent fuel holding ponds is a criticality accident, in which the fuel elements are packed very tightly together, and undergo spontaneous fissioning. It is argued by many that this is extremely unlikely, if not impossible, occurrence.

If a nuclear weapon is to cause a reactor to release radioactivity into the atmosphere, it must disrupt the safety systems of the system, and breach the containment structure, or set into motion a meltdown that will breach the containment. If the weapon is detonated at very close range[a], the core itself may be exposed, along with the spent fuel, to the strong afterwinds which loft debris into the radioactive cloud of the weapon.

CHAPTER 2

NUCLEAR AND THERMAL RADIATION

The early fireball formed immediately after a nuclear detonation is the site of intense radiations of all types. Nuclear radiations refer to the high energy (several MeV) neutrons and photons (Gamma rays) which are emitted during the fission and fusion processes, as well as gamma rays released in secondary nuclear events by the fission products or weapon debris. Thermal radiation refers to the lower energy photons produced by atomic interactions, from energies in the low x-ray range to the infra-red (fractions of an eV to several 100keV). It is unfortunate that history has named both of these phenomena "radiation", because they are really quite different; in one case the word refers to particles emitted by nuclear processes, and in the other case it simply refers to energy in the form of photons.

Nuclear Radiations

Neutrons

The neutron is the uncharged particle which initiates the fission reaction and is released in some fusion reactions. Two or three neutrons are produced in every fissioning of a uranium nucle s. One of these neutrons is needed to sustain the reaction, and the others may either fission additional nuclei or escape from the weapon entirely. In addition, 2 neutrons are produced for every 5 deuterium nuclei that are fused. In all, a net total of more than 10^{27} neutrons are produced by a one-megaton weapon, but a large fraction of these are absorbed by the weapon debris.

Using the data given by Glasstone, the following formula gives the number of neutrons per square centimeter between distances of 1200 and 5000 feet:[1]

$$N(n/cm^2) = \frac{4x10^{23}}{r^2} \text{ EXP}(-r/720) \qquad (2\text{-}1)$$

where r is the distance measured in feet.

Since these neutrons arrive in less than one millisecond, while the shock front is only 250 in radius, it is possible for the neutrons to be absorbed by a target before it is destroyed. If the neutrons deposit sufficient energy in the concrete containment wall, the strength of the wall will decline, and it will be more susceptible to blast loading. The neutron flux at which this occurs, however, is very high: greater than 5×10^{19} neutrons per square centimeter.[2] This high flux occurs within 100 feet of the containment, where such weakening would be utterly neglible.

Since the neutrons may arrive before the shock itself, we may wonder if the neutrons released by the weapon will be able to reach the reactor core in sufficient numbers to fission the uranium and release a significant amount of additional energy. If the weapon is detonated thirty feet from the containment wall, it will be relatively undisturbed as the first neutrons pass through it. If there were no intervening material, the neutron flux would be approximately 10^{20} n/cm^2 at the reactor vessel. There is at least 122 inches of concrete and 10 inches of steel between the outside of the wall and the reactor core. This will reduce the total fluence by a factor of 10^{14} to 10^{17}, depending

on the details of the neutron spectra and the composition of the concrete, bringing the fluence to 10^3 - 10^6 neutrons/cm^2. Even if we adopt this higher number, and if we assume that every neutron intercepted by the core results in a fission, the total amount of energy released is trivial.

Gamma Rays

Gamma-rays are high energy photons produced by nuclear processes. The first gamma-rays emitted in a nuclear detonation are due to the fission and fusion processes, and emission resulting when a neutron is captured by the weapon materials. These are called "prompt" gamma-rays, and they are released in less than 10^{-7} seconds. Neutrons may also transfer part of their energy to the nuclei of of air atoms, and when the nuclei return to the ground state they emit a gamma-ray. Nitrogen also captures neutrons completely, and emits gamma radiation from 10^{-2} to 10^{-1} seconds. After this, the only important source of gamma radiation are the emissions for the fission products as they decay.

The exposure in roentgens to these gamma-rays at a point r from the point of burst is given approximately by:[3]

$$D = \frac{2.4 \times 10^{14}}{r^2} \text{EXP}(-r/974) \quad (r) \qquad (2\text{-}2)$$

When high energy photons strike the surface of a concrete wall, they may either be reflected, absorbed, or transmitted. If the photons are absorbed, they will deposit their energy among the molecules in the substance, and heating will occur. If great

amounts of energy are absorbed, changes may occur in the structure and the properties of the concrete, resulting in a loss of compressive strength and making the wall more vulnerable to the effects of air blast. For all energies and atoms, in general the amount absorbed falls as the energy increases and rises as the atomic number increases. Since gamma rays have a very high energy, and since the average atomic number of concrete is only 11, very little absorption will take place. In fact, only about $0.02 \frac{\text{calories}}{\text{gram}}$ per gram of concrete will be absorbed for every calorie per square centimeter incident on the wall.[4]

From theoretical considerations, damage to the wall should take place when the energy absorbed exceeds 100 cal/gm, corresponding to gamma flux of 5,000 cal/cm^2. This in turn corresponds to exposures in air greater than 10^8 r , which by Equation (2-2) occurs at about 900 feet from the point of burst. The fireball will arrive at this point at about 20 milliseconds at this distance, well after most of the gamma-rays have been emitted.

Even though damge to the concrete through this mechanism is in theory possible, notice that we only reach the threshold of damage (100 cal/gm) at very short ranges, where other weapons effects will be much stronger than the resistance offered by undamaged concrete. We can therefore conclude that this damage will be negligible.

Thermal Radiation

Thermal radiation refers to the photons that are emitted when an excited electron returns to its ground state. The energies

of these photons can range from less than one eV to several keV, or from the infra-red to soft x-rays.

In the first phases of the fireball developement, the energy densities in the vapors are very high, resulting in temperatures as high as 10^7 K. A black-body at this temperature would radiate mostly energies of a few keV, in the soft x-ray range. This is in fact what occurs, and these x-rays are srongly absorbed by the cold air outside of the fireball. This in turn heats the air, making it transparent to x-rays, so that subsequent x-rays can pass to larger volumes of cold air, heat these, and so on. In this way the fireball becomes larger and larger, until the internal temperature drops to about 10^5 K at about 7 milliseconds, at which point this radiative growth becomes unimportant.

An outside observer would not see a spectral distribution even close to a black-body at this temperature during these stages, because the transparency of the air to these radiations has been altered by the neutrons, gamma-rays, and other debris.

When the surface temperature of the fireball drops below 2000 K at about 80 milliseconds, the air is no longer incandescent, and one can "see" into the hotter interior of the fireball. As this continues, the thermal output from the fireball continues to increase, reaching a maximum at about one second. The energy spectrum in this pulse is characteristic of a black-body at a temperature of about 7,000 K, and most of the energy is emitted in the visible, ultraviolet, and infra-red.

The total radiant exposure at any point r is given by:

$$Q = \frac{10^{15} f \Upsilon(r)}{4\pi r^2} \qquad (\text{cal/cm}^2) \qquad (2\text{-}3)$$

where f is the fraction of the weapon's energy converted into thermal energy, r is the distance in centimeters, and $\tau(r)$ is called the "transmittance", and accounts for absorption of radiation by the air. For a surface burst, f = 0.18, and for distances less than 15,000 feet, $\tau(r)$ is between 1.0 and 0.7 for a typical clear day.[5] Converting r from centimeter to feet, we have:

$$Q = \frac{1.54 \times 10^{10} \tau(r)}{r^2} \quad (\text{cal/cm}^2) \qquad (2\text{-}4)$$

Photons of this energy are strongly absorbed by the light elements which compose concrete and body tissue, and so they can raise the temperature significantly. Just as in the case of gamma-rays, if the concrete absorbs over 100 cal/gm, thermochemical changes will take place that will decrease the compressive strength of the concrete. First, for this effect to have any consequence, the thermal energy must be emitted before the blast wave arrives. For a one-megaton weapon, 5% of the energy is emitted before 0.4 sec, 25% before 1.0 sec, 50% after 2.0 sec, and 75% after 6 sec.[6] Figure 2-1 shows the amount of thermal radiation reaching a normal surface at a distance r before the arrival of the shock wave. Notice that this fuction reaches a rather sharp maximum at about 5,500 ft, where the radiance is 170 cal/cm^2. This radiant exposure can lead to surface absorptions as great as 68,000 cal/gm, which is much greater than the 100 cal/gm limit. The energy absorption at any distance into the wall is:

$$Q(x) = 68{,}000 \int_0^\infty g(\epsilon)\ \text{EXP}(-\rho\, \mu(\epsilon) x)\, d\epsilon \qquad (2\text{-}5)$$

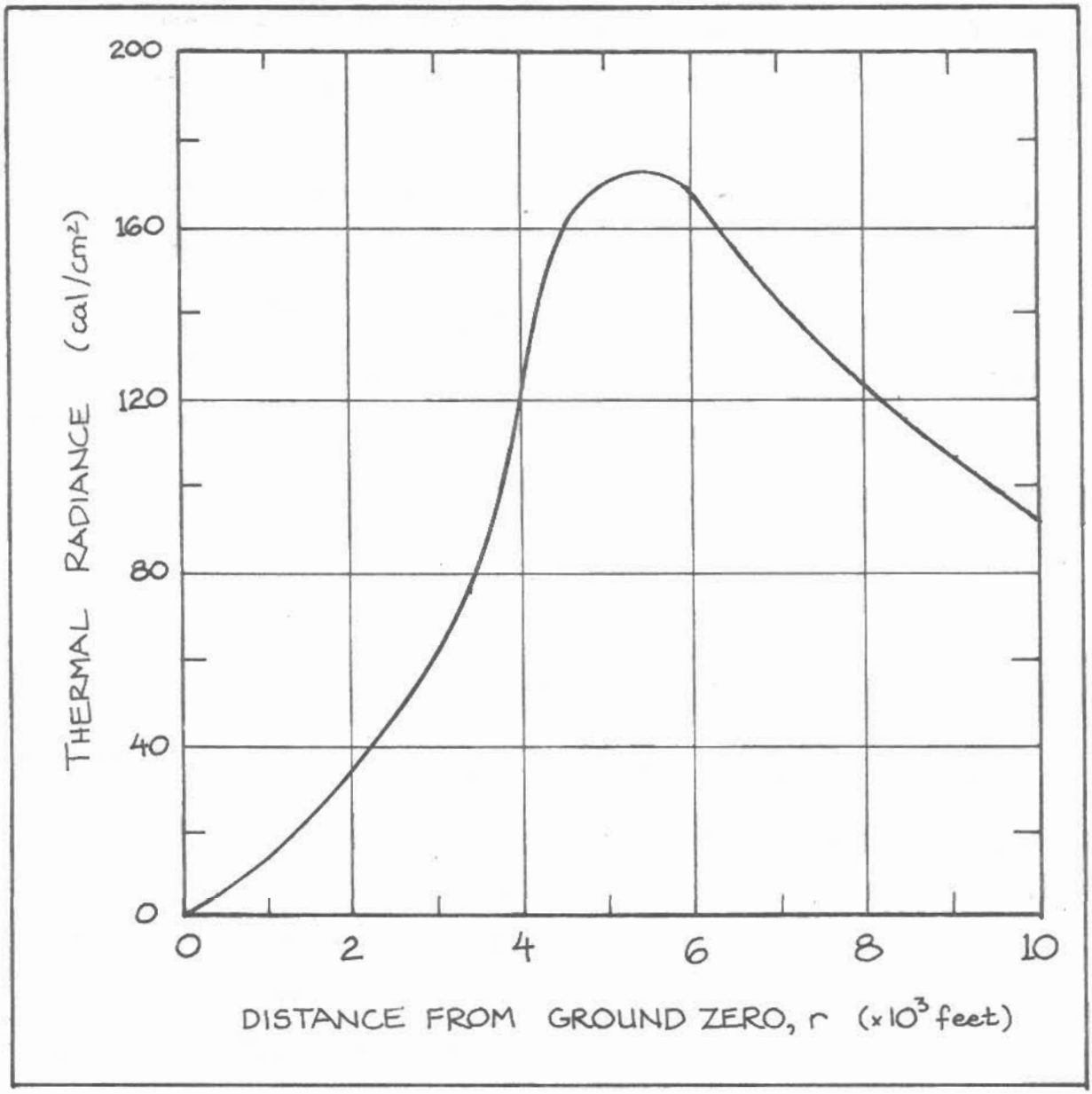

FIGURE 2-1: The amount of thermal radiation falling on a normal surface before the arrival of the shock wave, as a function of distance.

where $g(\epsilon)$ is the fraction of the total energy emitted at energies between ϵ and $d\epsilon$, ρ is the density of the concrete, and $\mu(\epsilon)$ is the mass attenuation co-efficient, which is a function of energy. $g(\epsilon)$ can be given approximately by Planck's black-body equation for a temperature of 7,000 K, which will be strongly peaked at an energy of 3 eV. At these energies, μ is very large - much greater than $10^8 cm^2/gm$, and so the radiation will not diffuse into the concrete very far. The more predictable result is that the surface of the wall will vaporize, forming a vapor that will shield the wall from further radiance.

Brode in fact warns that an analysis such as the one above will overestimate the damage done to the structure, even for much higher photon energies, because of the transient nature of the thermal loads. Actual observations do indeed show that thermal loads are relatively neglible.[7]

The Electromagnetic Pulse

Immediately after a nuclear detonation, the matter inside the fireball is completely ionized, and due to the intense radiation flux through the surrounding air, the air atoms will be ionized for several mean free paths. The electrons, being much lighter than the positively charged nuclei, travel much further after an interaction. In an ideal situation, this will result in a spherical distribution of negative charges. However, if for some reason the distribution is not perfectly symmetrical, then a net current will flow, and the charges will act like a dipole radiator. This current is called the electromagnetic pulse (EMP).

If the burst occurs near the ground, the gamma-rays which travel downward into the ground will ionize atoms, but very little charge separation will occur. On the other hand, gamma-rays which travel upward will produce a significant charge separation, and so a net electron current will be produced in the vertical direction.

The pulse produced in this way will have an electric field of tens of thousands of volts per square meter, and emit frequencies from a fraction of a hertz to a few gigahertz. The current produced in an overhead bare wire near the blast can reach over 10,000 amperes in less than half a microsecond, and can damage unprotected equipment over eight miles from the burst.[8]

It is not known to what extent nuclear power plants are equipped to deal with the electromagnetic pulse. In the absence of long exterior antennas (transmission lines), there would be no damage to the equipment inside the containment structure, because it is surrounded by a continuous metal shield. Some protection is offered by standard lightning arrestors, but most of those already installed will not be sufficient and may suffer flashover. However, there are devices which are effective against EMP. Additional information on the ability of nuclear power plants to withstand EMP is needed.

CHAPTER 3
AIR BLAST

As mentioned earlier, the rapidly expanding hot gases near the point of detonation form a shock wave in the air, and it is this blast wave which causes most of the physical damage observed after a nuclear blast. The blast wave is characterized by a front of high pressure which rises almost instantaneously, and then falls of in an exponential manner. To conserve energy, the maximum overpressure, P_m , must fall off with increasing distance of the shock front from the point of burst. Figure 3-1 depicts the shock wave for various times after detonation.[1]

In addition to this "overpressure" caused by the high density of air in the shock front, there is also a pressure caused by the physical movement of the air molecules that comprise the front. This is called the "dynamic pressure", Q , and it is essentially the same as wind.

The relationship between the peak overpressure and the distance from the burst is well known and appears in many references.[2,3] A composite of this data is shown in Figure 3-2. Brode suggests that the following approximation be used to estimate the peak overpressure from a one-megaton surface burst:[4]

$$P_m = \frac{3.3 \times 10^{12}}{r^3} + \frac{6.07 \times 10^6}{r^{1.5}} \text{ (psi)} \qquad (3\text{-}1)$$

where r is the range in feet, and P_m is the maximum overpressure in psi. This is an excellent approximation for $P_m > 10$ psi.

The peak dynamic pressure can be calculated from the following formulas:[5]

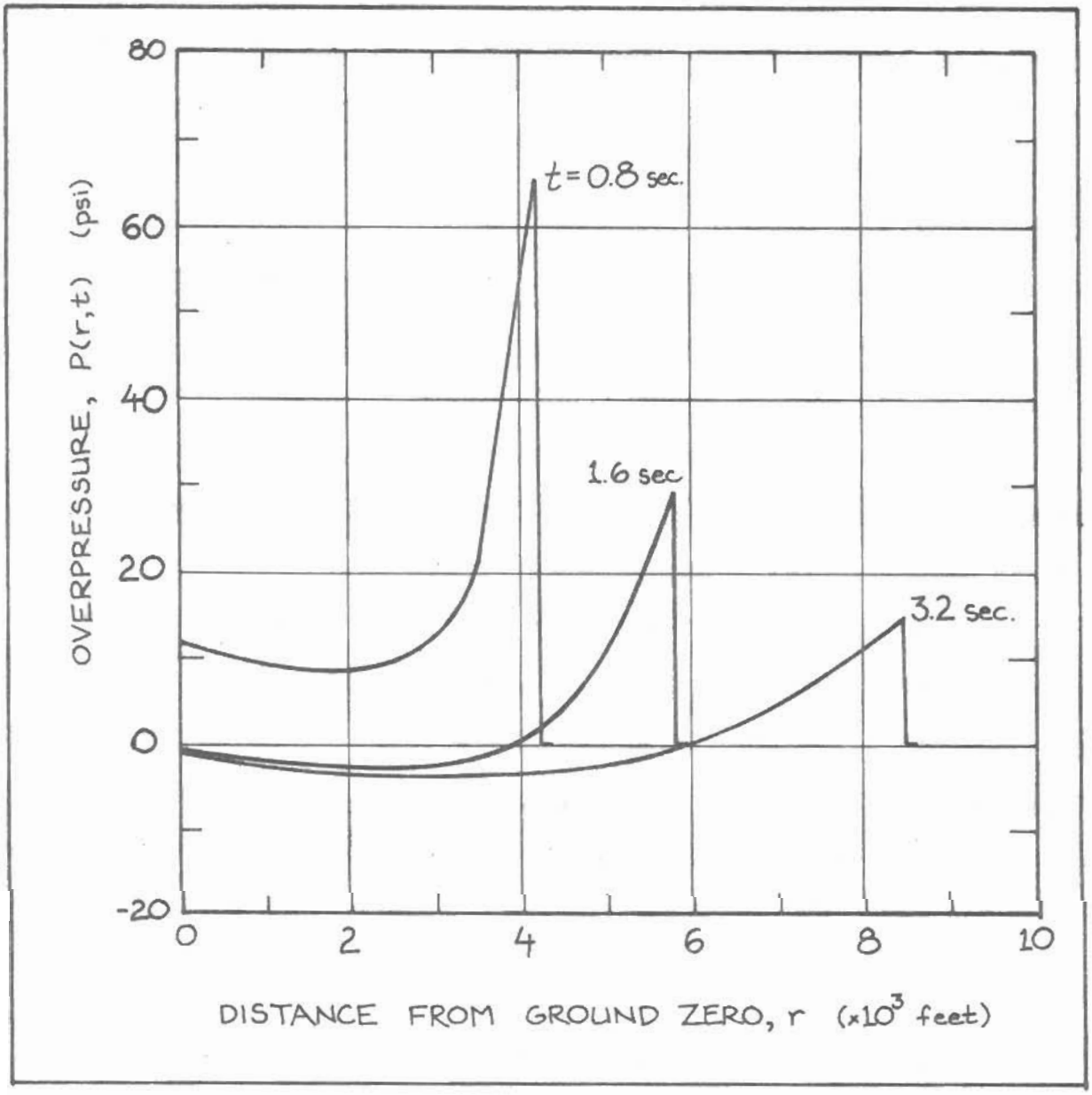

FIGURE 3-1: The overpressure profile of the blast wave for several times after the event.

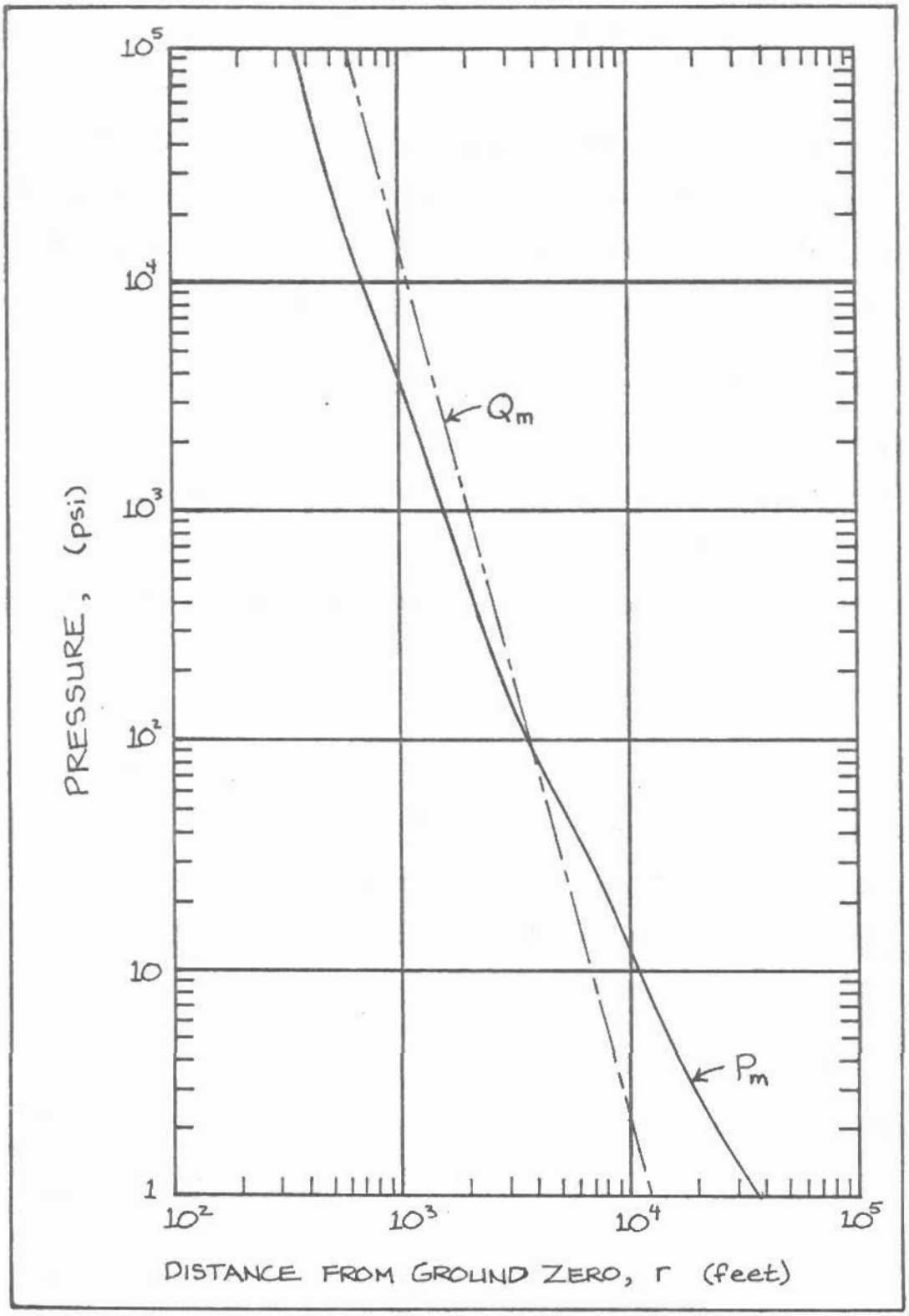

FIGURE 3-2: The maximum overpressure and dynamic pressure as a function of distance for a one-megaton surface burst.

$$Q = \frac{P^2}{2\gamma P_o + (\gamma - 1)P} = \frac{5}{2}\,\frac{P^2}{7P_o + P} \quad (psi) \qquad (3\text{-}2)$$

where P_o is the ambient pressure (14.7 psi at sea level).

The latter expression results when γ is set equal to 1.4, which is a good approximation for $P < 200$ psi. The peak dynamic pressure is plotted vs. distance in Figure 3-2.

When the blast wave strikes a structure, reflections occur that greatly increase the peak instantaneous pressure on the wall. This pressure is called the reflected pressure, P_r, and it is a function of the peak incident overpressure. P_r is given by the following theoretical formula for $P_i < 200$ psi:[6]

$$P_r = 2P + (\gamma + 1)Q = 2P\,\frac{7P_o + 4P_i}{7P_o + P_i} \quad (psi) \qquad (3\text{-}3)$$

where P_i is the incident overpressure on the wall, and the latter expression results when $\gamma = 1.4$. For higher overpressures, air displays its non-ideal nature, and the ratio of P_r / P_i must be expressed by a much more complicated relationship, which is plotted here in Figure 3-3.[7]

The velocity of the shock wave is always greater than the speed of sound, and it is given by the following expression:[8]

$$U = c_o\left[1 + \frac{(\gamma + 1)P}{2\,P_o}\right]^{.5} = c_o\left[1 + \frac{6P}{7P_o}\right]^{.5} \quad (ft/s) \qquad (3\text{-}4)$$

Another important parameter to be considered is the total incident impulse defined as:

$$I_p^+ = \int_0^{t_p^+} P(t)\,dt \qquad (3\text{-}5)$$

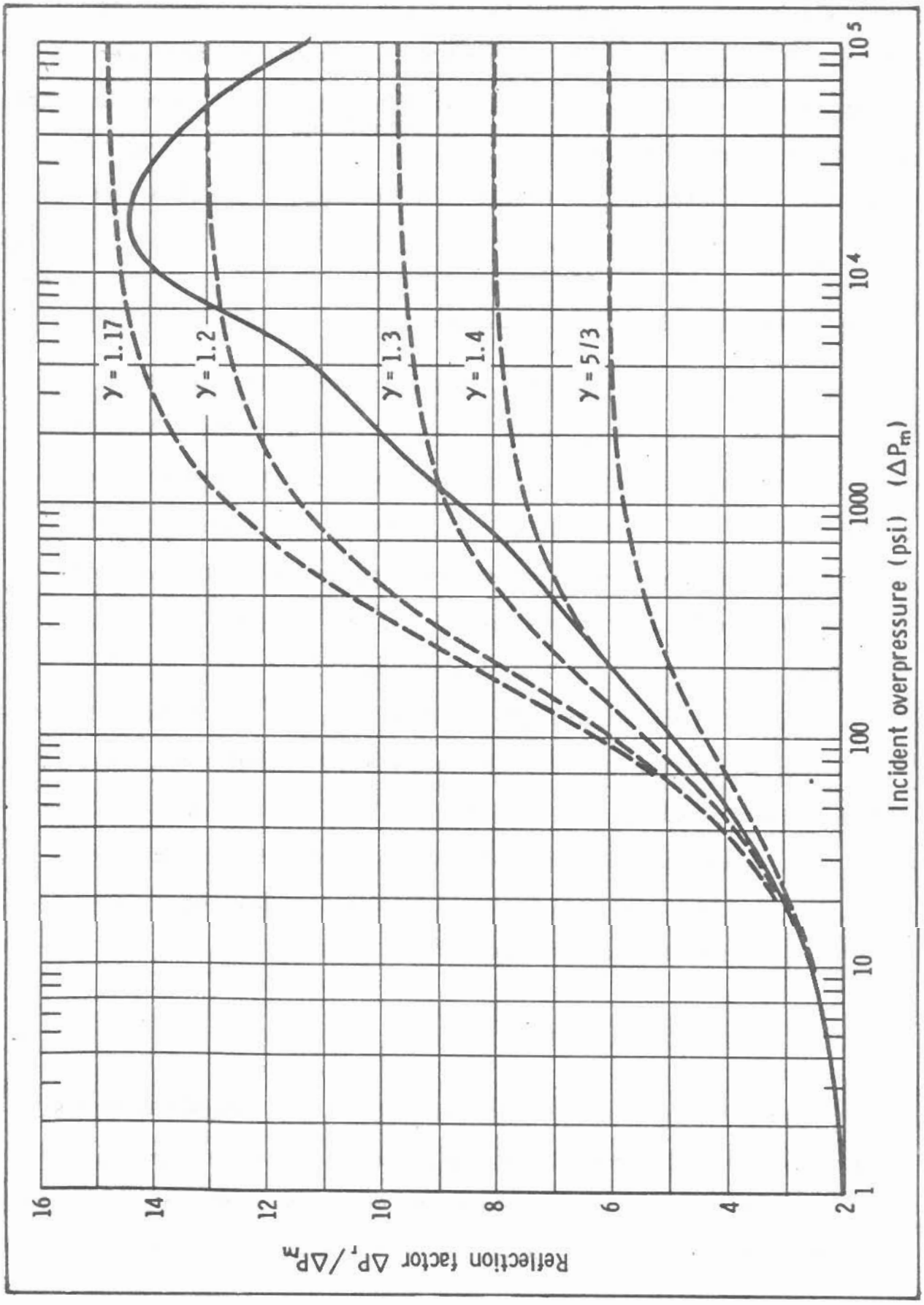

FIGURE 3-3: NORMAL REFLECTION FACTOR AS A FUNCTION OF INCIDENT OVERPRESSURE

where t_p^+ is the duration of the "positive phase" of the blast wave. The positive phase duration of the overpressure is graphed in Figure 3-4, along with the positive phase duration of the dynamic pressure. P(t) is a complicated function, and the equation of motion must be solved numerically; results for various peak overpressures appear in Figure 3-5.[9] A good approximation is:

$$I_p^+ = 1.83P_m^{\frac{1}{2}}(1 + .00385P_m^{\frac{1}{2}}) \qquad (3\text{-}6)$$

Interaction of Air Blast with Structures

For simplicity, we first consider a simple box-like structure of width a, height b, and of arbitrary length, with no windows or other openings. If a blast wave of peak overpressure P_m is normally incident on the face ab of the structure, then reflections will occur, and the pressure at the face will instantaneously rise to the peak reflected pressure, P_r, given by Equation 3-3 or Figure 3-3. It has been observed from laboratory studies that at a characteristic time t_s after the blast wave strikes the structure, the pressure will simply become $P(t_s) + C_d Q(t_s)$, where P(t) and Q(t) are taken from Figure 3-5, and 3-6 and C_d is the "drag coefficient. The time t_s is called the "stagnation time", and it is approximately equal to:[10]

$$t_s = \frac{3S}{U} \qquad (3\text{-}7)$$

where S is equal to the height of the structure or half the width, whichever is less. P_s is the "stagnation prssure", as is given above. The pressure is assumed to diminish linearly from the peak reflected pressure to the stagnation pressure,

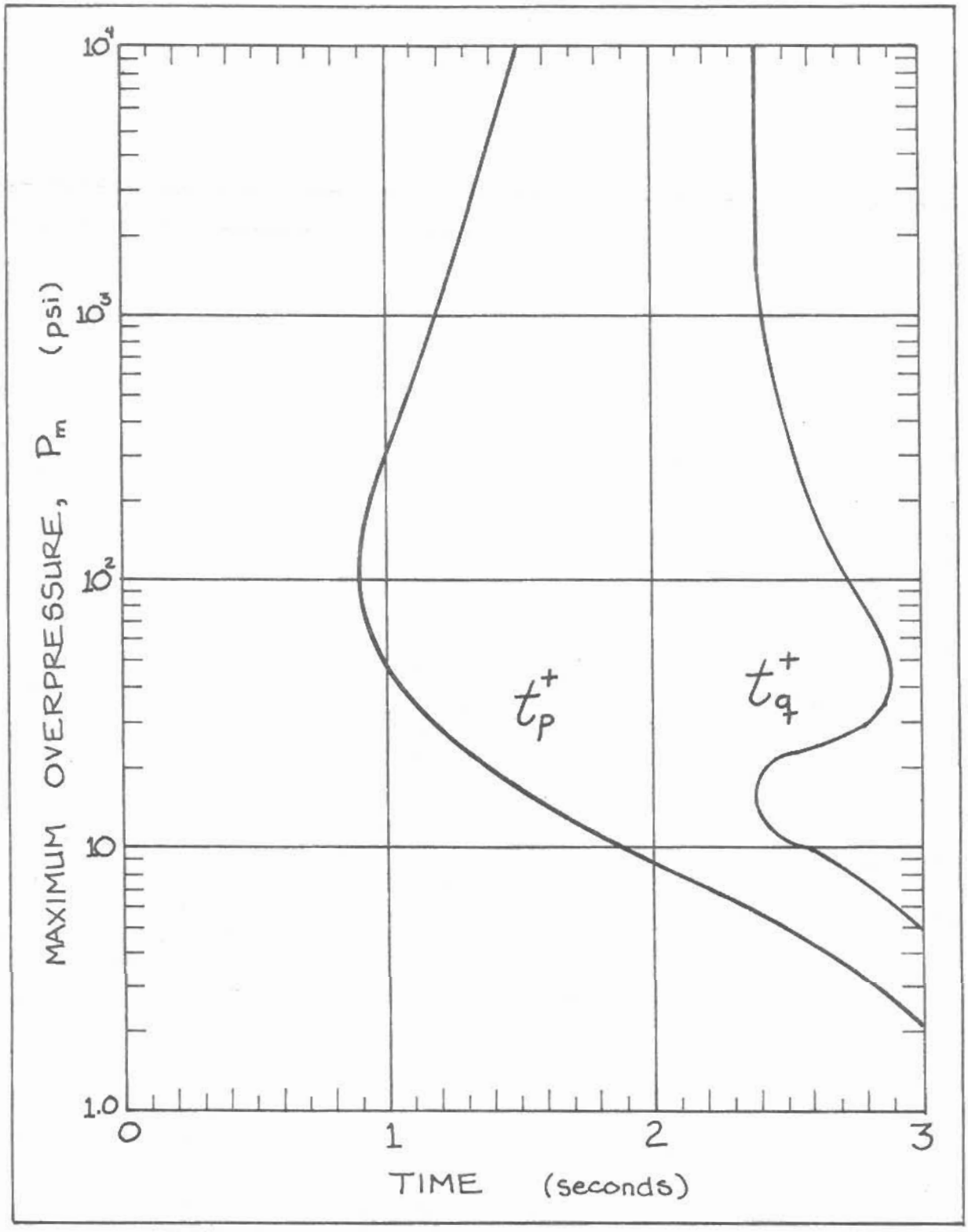

FIGURE 3-4: The positive phase duration of the overpressure, t_p^+, and the positive phase duration of the dynamic pressure, t_q^+, as a function of the maximum overpressure, P_m.

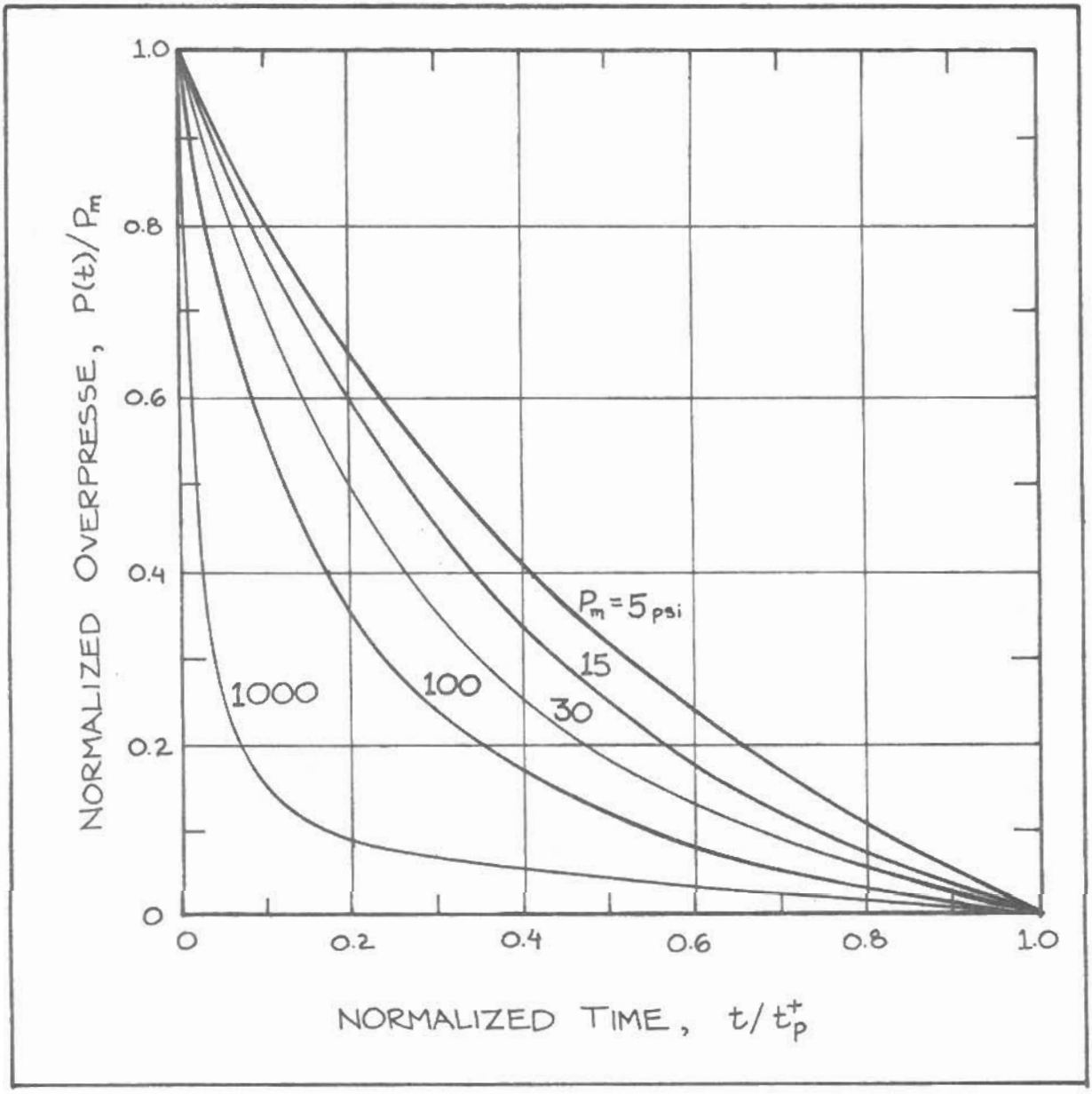

FIGURE 3-5: The decay of the overpressure with time for several values of the maximum overpressure.

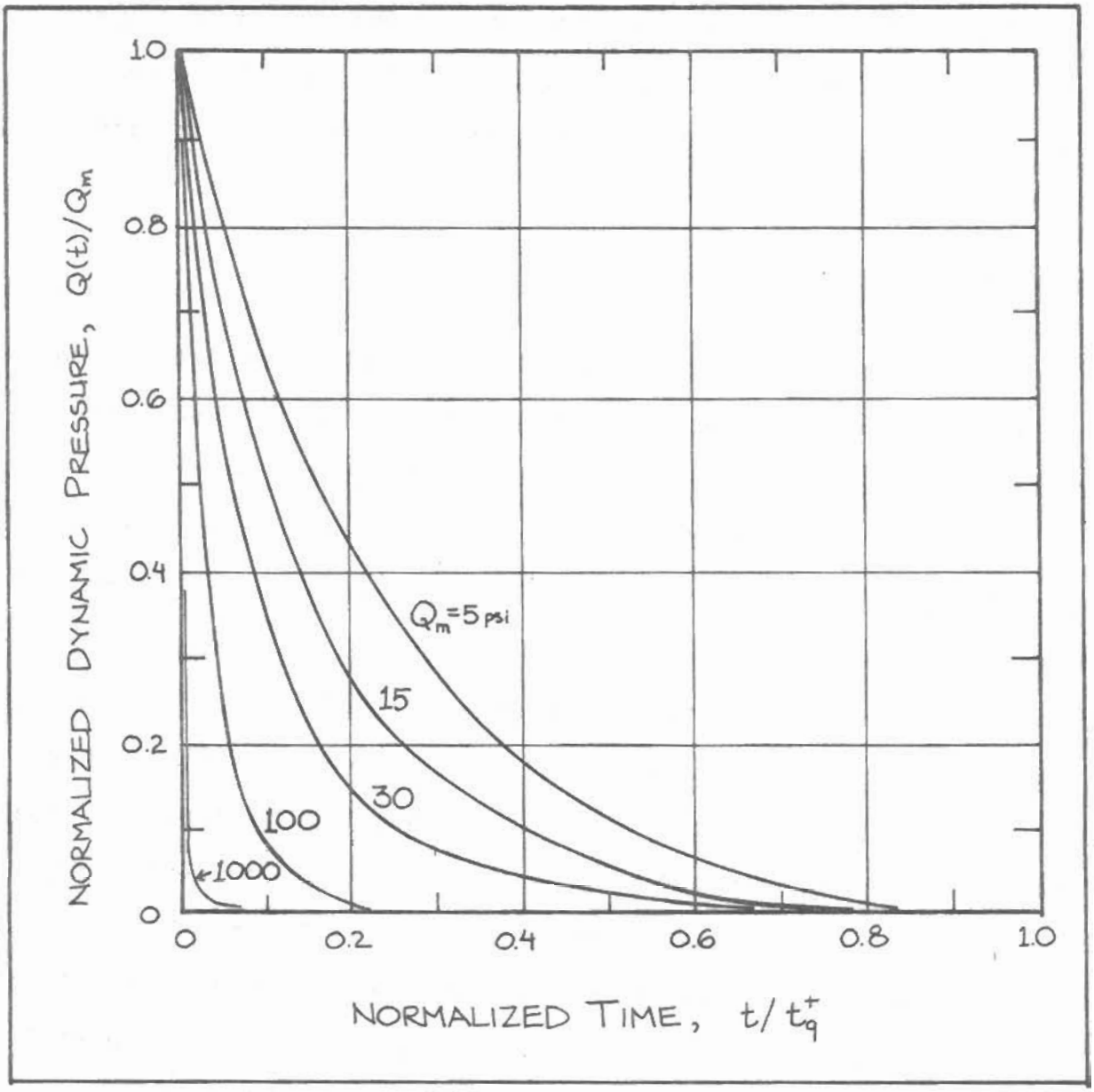

FIGURE 3-6: The decay of the dynamic pressure with time for several values of the maximum dynamic pressure.

and thereafter it is assumed to fall off as $P_t = P(t) + C_d Q(t)$. A typical pressure-time history is shown in Figure 3-7A, for P_m=30psi.

After a pressure-time history has been constructed, the effects on the structure may be analyzed according to the principles of structural dynamics, by approximating the pressure loading on the wall by a number of triangles, making sure to keep the total impluse on the wall equal. This approximation is shown in Figure 3-7B.

TARGETING IMPLICATIONS

Now we apply the above formulas and principles to the task of determining the effects of blast loading on the containment structure of a nuclear reactor. Refering to Figure 1-1,

we can idealize the containment structure to be a simple-supported cylindrical shell with a radius of 65 feet and height of 145 feet, with a wall thickness of 42 inches, topped by a hemisphere with a wall thickness of 30 inches. Unfortunately there are no simple methods avail able to estimate the damage due to blast loading on a vertical aboveground cylindrical shell, and so we must be content with somewhat more crude estimates. The interaction of blast waves with flat walls is well-known, and although a flat wall cannot resist flexure nearly as well as a cylindrical shell, the flat wall analysis will give a useful lower bound. In the same way, the spherical portion of the containment is much more resistant to flexure than a cylindrical shell, and so an analysis of the spherical part of the containment will give a useful upper bound.

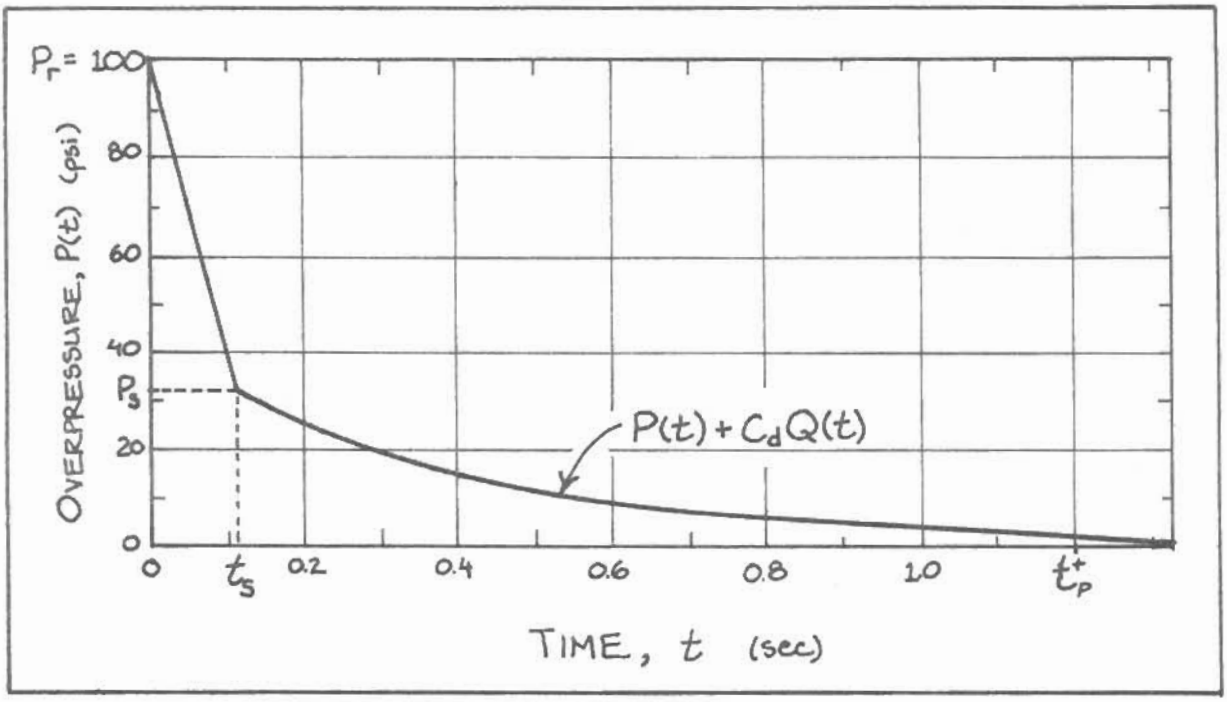

FIGURE 3-7A: Pressure-time history for the front face of a rectangular structure for a maximum overpressure of 30 psi.

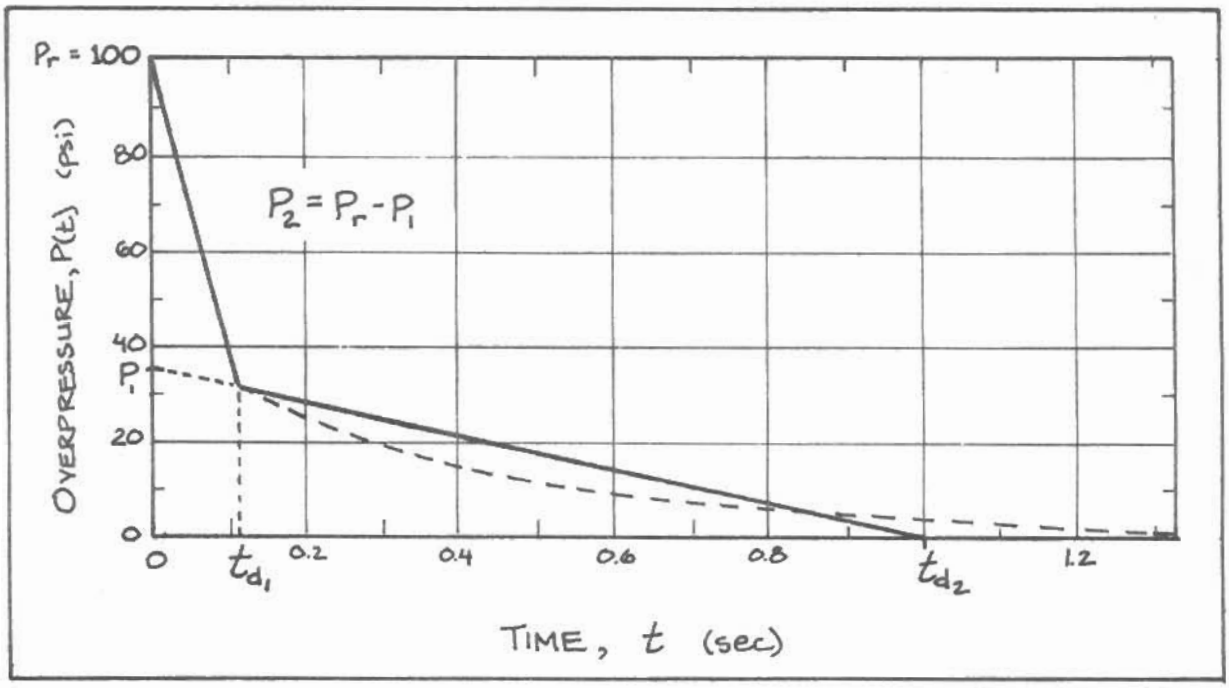

FIGURE 3-7B: An example of approximating the pressure-time history in Figure 3-7A with two triangular pulses.

Flat Wall Analysis

The first task is to determine what the dimensions of an "equivalent flat slab" should be, in order to faithfully represent the reactor containment. It is assumed here that the total reflected impulse on the equivalent flat slab should be about the same as that on the reactor building. Using the methods outlined in Glasstone, the total reflected impulse on the front face of the containment has been computed, and it was found that a wall 210 feet in length and 130 in width will receive about the same impulse.[11] These dimensions seem especially suitable because they are nearly the same as the containment itself.

Methods are available for analyzing a flat slab that is simple-supported, as well as one that is fixed at all sides. Our "equivalent flat slab" is somewhere between these two cases, perhaps acting more like a fixed slab. The method used below compares the pressure loading function to the ultimate resistance of the slab in order to determine the degree of damage done.

As stated in Chapter 1, the containment wall is assumed to be prestressed, making its analysis more difficult than that of a conventionally re-inforced concrete wall. The ultimate moment must be based on the full plastic strength of the prestressing tendons, which are located at 48" intervals in the center of the wall (vertical tendons) and spaced at 27" and 6" from the outside face (horizontal tendons). The physical characteristics of the wall are the computed ultimate moments are summarized in Table 3-1.

TABLE 3-1[12]

Total Wall thickness	D_c = 42"
Effective wall thickness	d = 39"
Concrete compression strength	σ_c = 4500 psi
Steel yield strength	σ_s = 60000 psi
Tendon yield strength	σ_t = 240000 psi
Plastic strength of tendons	2.0×10^6 lb
Tendon spacing - horizontal	27"
vertical	48"
Tendon location - horizontal	6" from outside
- vertical	centerline
Horizontal re-inforcement	1.27 in^2/ft
Steel ratio	f_s = 0.014
Ultimate Moment - vertical tendons, M_{ov}	0.7×10^6 ft-lb/ft
horizontal tendons, M_{oH}	2.0×10^6 ft-lb/ft
horizontal reinforcement, M_o	0.24×10^6 ft-lb/ft
Total positive ultimate moment along short edge M_{pfa}	2.9×10^8 ft-lb
along long edge M_{pfb}	1.5×10^8 ft-lb
Wall width	130 ft
Wall length	210 ft

Simple-Supported Slab - From the tables provided by the U.S. Army Corps of Engineers,[13] we can find the transformation factors that allow us to approximate the motion of the real slab with a simple spring-mass system. For a simple-supported slab with $a/b = 130/210 = 0.62$, we find that the maximum resistance, R_m, is given by

$$R_m = (12M_{Pfa} + 9.4M_{Pfb})/a \quad \text{(lb)} \qquad (3\text{-}8)$$

Substituting the above values in Table 3-1, we find that $R_m = 3.8 \times 10^7$ lb = 9.6 psi.

The natural period of such a slab is given by

$$T = 2\pi\sqrt{\frac{K_{1m} M}{k}} \quad \text{(s)} \qquad (3\text{-}9)$$

where K_{1m} is a transformation factor to convert from the real slab to the spring-mass system, and it is equal to about 0.58 for the plastic behavior considered here; M is the mass of the slab, and k is the equivalent spring constant, which for our slab is given by

$$k = \frac{197EI_a}{a^2} \quad \text{(lb/ft)} \qquad (3\text{-}10)$$

In this expression, E is the modulus of elasticity, and I_a is the moment of inertia of the slab about a, and is given by

$$I_a = \tfrac{1}{2}bd^3(5.5f_s + 0.083) \qquad (3\text{-}11)$$

where f_s is the steel to concrete ratio. Substituting the values of Table 3-1 into these expressions, we find that the natural period of the slab is T = 0.73 s.

These calculations enable us to compute the damage done by blast loading, by assuming a maximum value of the "ductility factor" that can be sustained by the wall without breaching. The ductility ratio, μ , is defined by

$$u = y_m/y_e \qquad (3\text{-}12)$$

where y_m is the maximum displacement, and y_e is the elastic limit of the wall. The corresponding force vs. displacement curve is shown in Figure 3-8.

For a given pressure-time history as shown in Figure 3-7A, we can approximate the loading on the slab by two or more triangles, as in Figure 3-7. The resulting ductility ratio can then be computed by solving the following equation developed by Newmark[14]:

$$\frac{P_1}{R_m} C_1(\mu) + \frac{P_2}{R_m} C_2(\mu) = 1 \qquad (3\text{-}13)$$

where $C_1(\mu)$ and $C_2(\mu)$ are the values of the ratio (R_m/F) that correspond to a certain value of the ductility ratio, and the ratio of the duration of the loading triangle t_d to the period T . $C(\mu)$ can be read directly from Figure 3-9, which represents the numerical solutions to the equations of motion of the slab. For example, if we assume that $\mu = 10$ corresponds to a breach of the containment, and if we are considering a pressure-time history for which $t_{d_1} = 0.11$ s, then $t_d/T = 0.11/0.73 = 0.15$, and from Figure 3-9 we find that $C_1(10) = 0.1$.

All the pertinent blast parameters have been calculated for many values of the peak overpressure; these appear in Table 3-2.

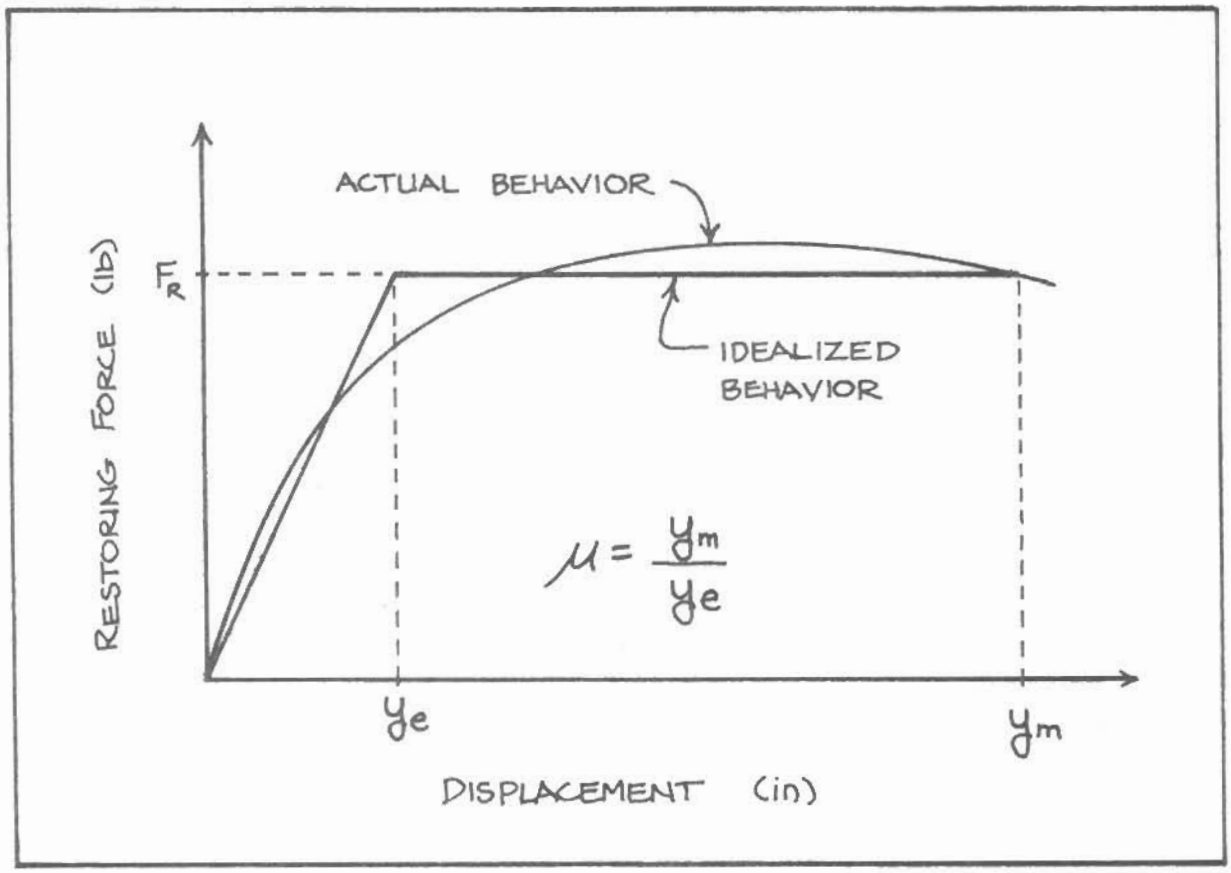

FIGURE 3-8: The restoring force as a function of displacement for a concrete wall, and the definition of the ductility ratio, μ .

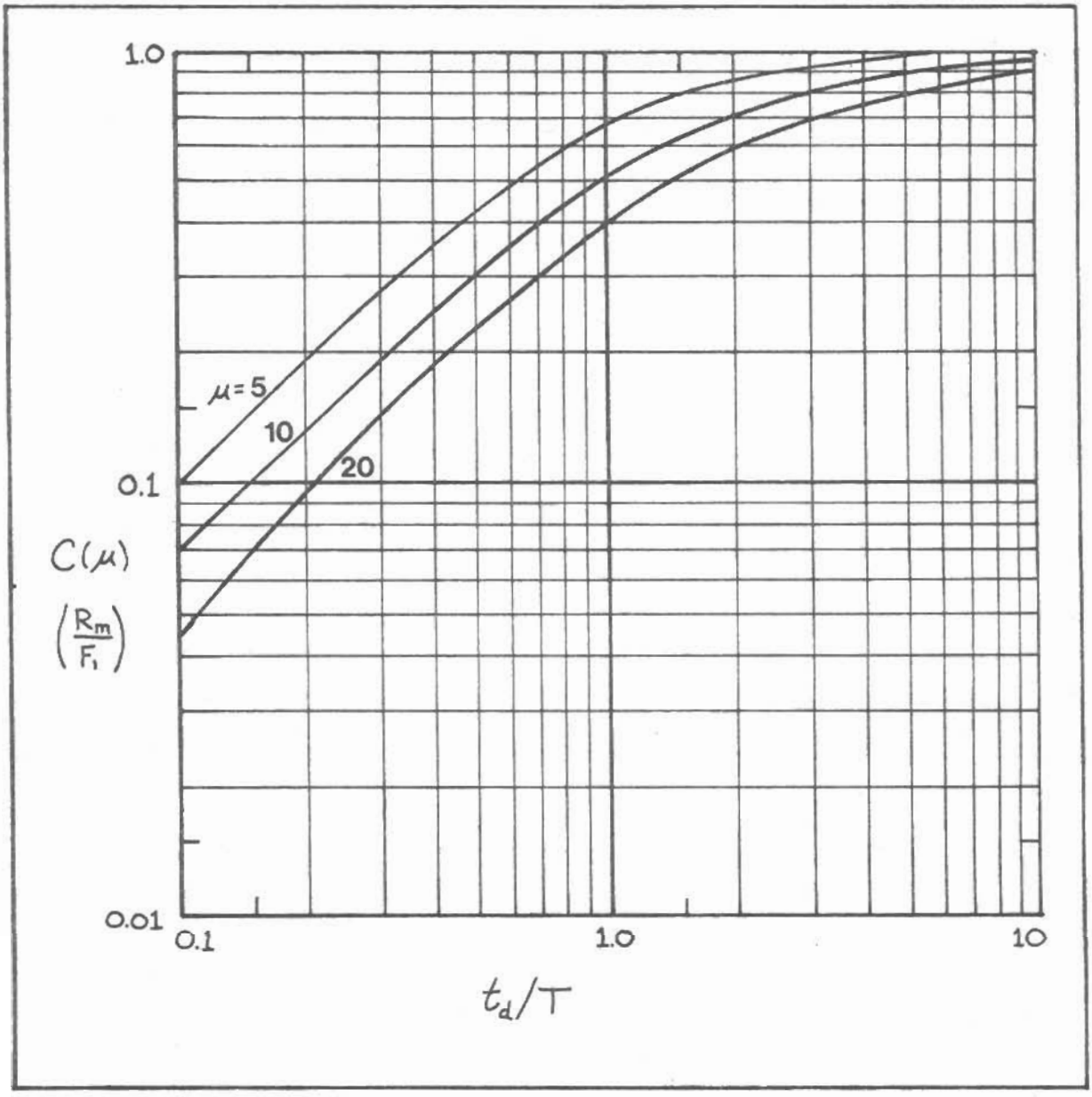

FIGURE 3-9: The maximum response of a wall slab subjected to a triangular loading pulse, as a function of (t_d/T) and the ductility ratio.

P_m	P_r	Q_m	r (ft)	U (ft/s)	I_p^+ (psi-s)	t_p^+ (s)	t_q^+ (s)	t_s (s)	P_s (psi)	P_1 (psi)	P_2 (psi)	t_{d_1} (s)	t_{d_2} (s)	I_r (psi-s)
10	25	2.2	10,300	1,400	7	1.9	2.6	0.14	9.6	14.	11	0.14	1.7	9.8
15	42	4.8	8,200	1,500	7.8	1.6	2.4	0.13	15	26	16	0.13	1.4	12.8
30	100	17	5,900	1,900	10	1.2	2.8	0.11	32	65	35	0.11	1.0	19
50	200	41	4,600	2,200	13	.98	2.9	0.088	58					26
100	500	120	3,400	2,900	18	.90	2.7	.066	122					40
200	1,200	330	2,600	4,000	27	.94	2.6	.049						61
500	3,700	1,000	1,900	6,200	42	1.1	2.5	.032						100
1000	8,600	2,300	1,500	8,700	56	1.2	2.4	.023	660					160
2000	2×10^4	4,800	1,200	12,000	74	1.3	2.4	.016						240
5000	6×10^4	1.2×10^4	880	19,000	103	1.4	2.4	.010						420
10^4	1.4×10^5	2.5×10^4	700	27,000	130	1.5	2.4	.0072	3500					640

TABLE 3-2.

Using the data in Table 3-2 and solving Equation 3-13, we find the results for the simple supported wall which are shown in Figure 3-10.

Fixed Slab: Virtually the same analysis can be applied to a slab which is fixed on all sides. From reference (13) we have

$$R_m = (12(M_{Pfa} + M_{Psa}) + 9.4(M_{Pfb} + M_{Psb}))/a \qquad (3\text{-}14)$$

To simplify the analysis, we will assume that the bending strength of the slab is uniform around the perimeter, so that $M_{Pfa} = M_{Psa}$ and $M_{Pfb} = M_{Psb}$. If this is true, then the maximum resistance will be twice the value of R_m for a simple-supported slab, so that $R_m = 19$ psi.

The only other parameter which changes for the fixed slab case is the spring constant, k , which is now given by

$$k = \frac{460\ EI_a}{a^2} \qquad (3\text{-}15)$$

Substituting the appropriate values into Equations 3-15 and 3-9, we find that $T = 0.48$ s. Once again, we solve Equation to find the resulting curve of the ductility ratio vs. the maximum overpressure, which is plotted in Figure 3-10.

Results for Flat Slab Analysis: The "equivalent flat slab" lies somewhere between a fixed slab and a simple-supported slab, and the approximation assumed here is shown in Figure 3-10. It is generally believed that the containment wall will fail at about $\mu = 10$, and that it will certainly fail before $\mu = 20$.[15] From Figure 3-10, we see that $\mu = 10$ when $P_m = 16$ psi, and $\mu = 20$ when $P_m = 22$ psi. From this analysis we can infer that the lower bound for containment failure is $P_m = 16$ psi.

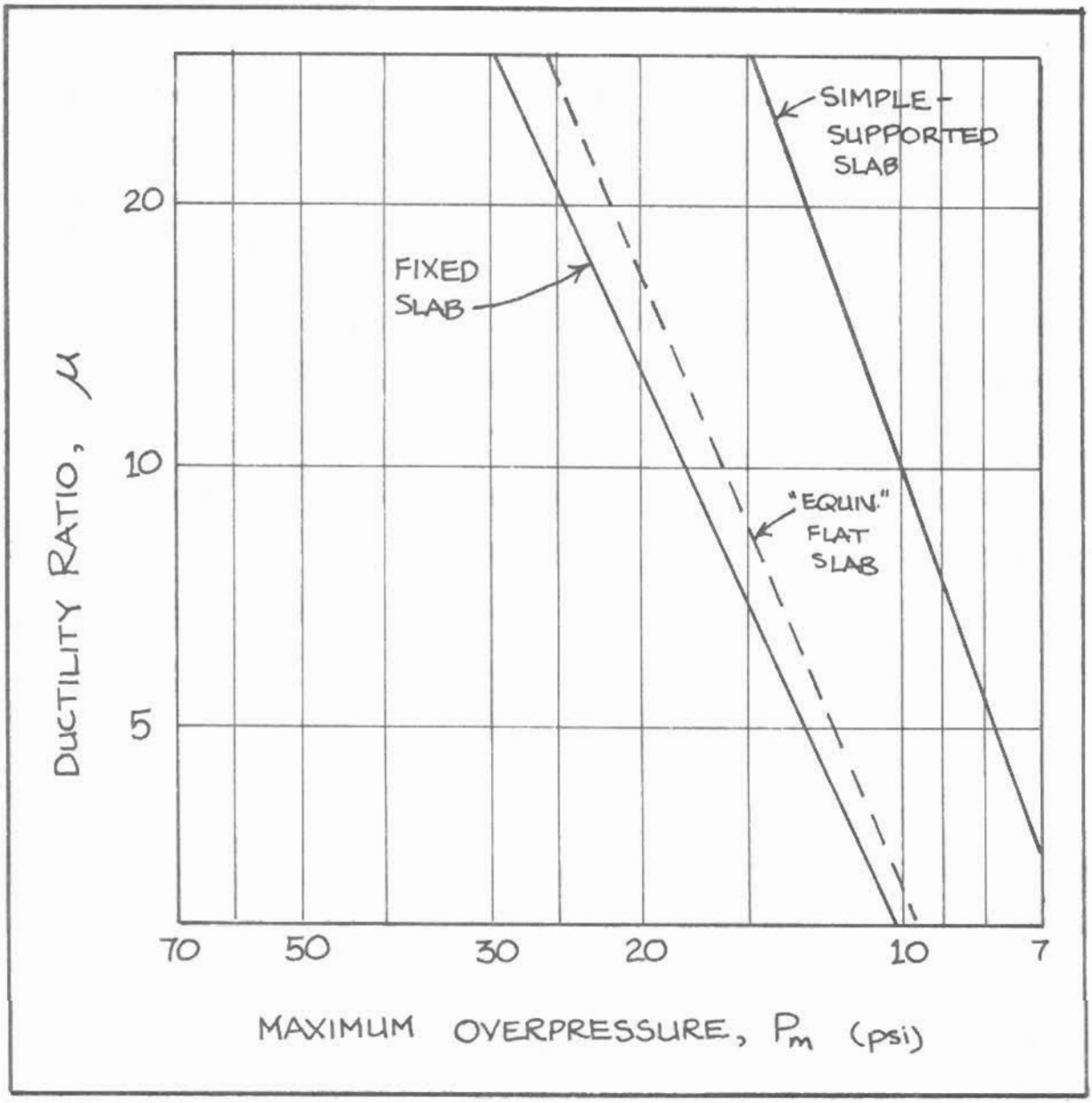

FIGURE 3-10: The ductility ratio that results from a maximum overpressure P_m on a simple-supported and fixed slab. The "equivalent flat slab" lies between these two, as indicated.

Spherical Shell

The top part of the containment structure is a hemisphere, with a radius of 65 feet, and a shell thickness of 30 inches. The analysis of this dome is quite different from the preceding analysis of flat slabs, mainly because the dome resists flexure very well and because the natural periods of domes are extremely short, given approximately by $T = r_d/2500$ s, which gives a period of 0.026 s for the dome under consideration. Notice that this period is much shorter than the times characteristic of the blast wave, and that the loading remains at relatively high levels for long periods of time. For these reasons it is sufficient to consider the pressure as if it were applied statically. If the ultimate strength is then set equal to the internal forces corresponding to the maximum applied pressures, the following expression results:[16]

$$\tfrac{1}{2}P_m r_d + 3P_r r_d/4 = D_c(0.85\sigma'_c + 1.8f_s\sigma_s) \qquad (3\text{-}16)$$

Substituting the appropriate values from Tables 3-1 and 3-2 we find that this relation is satisfied when $P_m = 57$ psi.

From the previous discussion, we have seen that the containment will be breached when

$$15 < P_m < 60 \text{ psi}$$

corresponding to: $4{,}400 < r < 8{,}200$ ft

However, just from reading the literature on the effects of blast on structures in the Nevada test sites and the Japan experiences we could have guessed the above figures. Glasstone

reports that the walls of a multistory reinforced concrete building with no windows and of blast resistant design will be breached at about P_m = 20 psi.[17]

It is unfortunate that no serious attempts have been made to determine the peak overpressure that would breach the containment structure of a nuclear reactor. Geiger has made some preliminary estimates based on a flat wall analysis similar to that above, and his results appear in Figure 3-11.[18] Notice that for reflected impulses that are characteristic of a one-megaton nuclear blast, the ductility ratio is relatively insensitive to variations in the reflected impulse, and depends mostly on the peak overpressure. Also notice that his predictions are more severe than those given here; for μ = 10, P_m = 8 psi, and for μ = 20, P_m = 13 psi.

Another important consideration is that the reactor building is not a lone structure - in fact, it is usually surrounded by many other structures which will reflect and diffract the incident wave. This could have the effect of shielding the containment, but it has been shown in one study that for certain reactor configurations the peak reflected pressure on the containment is <u>increased</u> by a factor of 1.7[19] It is difficult to state what effect this will have on the containment, except to say that if the above calculations seemed a bit conservative (that is, overestimate the hazard), then this considerstion certainly nullifies this conservatism. The additional complication introduced at this point become much too uncertain and complex to deal with easily.

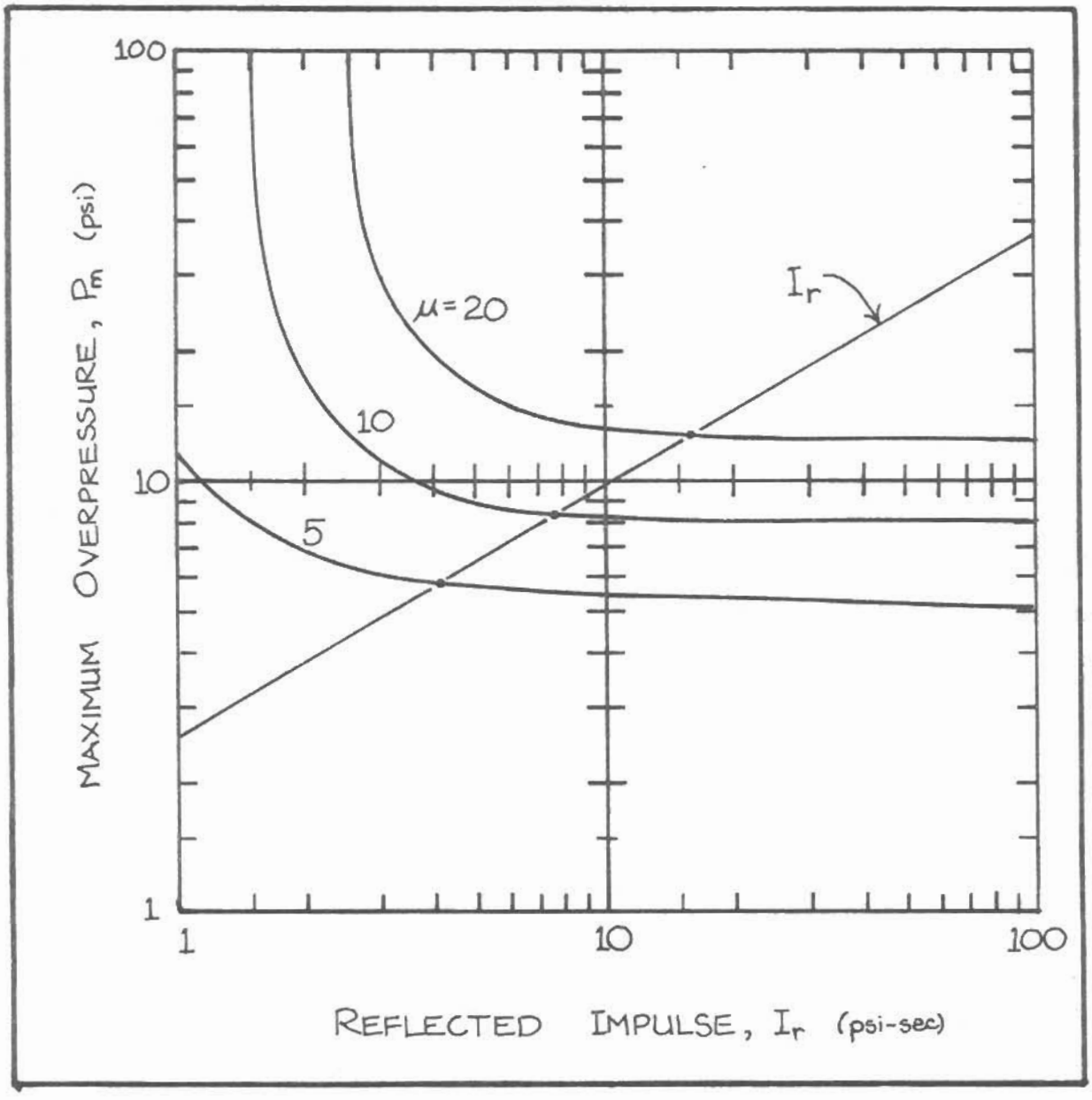

FIGURE 3-11: The degree of plastification (ductility ratio) that results when a blast wave of maximum overpressure P_m and reflected impulse I_r is applied to the reactor containment. The straight line gives $I_r(P_m)$ for a one-megaton weapon. (After Geiger)

The nature of the problem is not probablistic; for a given blast one can in principle solve the equations of motion and the containment will or will not fail. But when one is dealing with such a wide range of estimates with considerable uncertainty, it helps to assign a "probability" that each estimate is correct. It is always difficult to make such decisions, but if progress is to be made, assumptions must also be made. For the purposes of this analysis we will say that we can be 95% sure that the containment will fail if $P_m > 60$ psi, 50% sure if $P_m \geq 20$ to 30 psi, and 5% sure if $P_m < 5$ psi. The results are summarized in Table 3-3.

The preceding discussion addressed the minimum overpressure levels that would cause damage to the containment building. It is also wise to consider the levels that would cause the maximum release of radioactivity possible from the reactor. This will occur when the containment structure is completely destroyed, and the reactor vessel itself is severely breached, allowing the reactor core to be fragmented and swept up into the radioactive cloud of the weapon.

This is a tremendously complex question, and it cannot be solved theoretically. Little or nothing is known about the behavior of structures under such intense pressure pulses. Fortunately, one experimental work has been done on this problem, by constructing a 1/100 scale model reactor vessel, containment wall and biological shield, and subjecting them to high impulses from a chemical explosive. The ability of this experiment to predict the distance at which the reactor vessel is ruptured depends on two assumptions: that the strength of the walls is

TABLE 3-3

u	Simple Supported	Fixed	Equiv. Flat Slab	Geiger	Spherical Shell	Probability of Failure
5	8	13	12	6	--	5%
10	10	18	16	8	--	50%
20	13	25	22	13	57	100%

Summary of the calculated effects of air blast on the reactor containment structure.

small compared with the force of the air blast, and that damage is only inflicted by air blast and by the moving contents of the reactor containment structure. Although the first assumption is a very good one, the latter assumption neglects the effects of nuclear and thermal radiations on the reactor materials, and the effects of cratering and ejecta in damaging the vessel. This is discussed in greater detail in Chapter 6.

In this experiment, the authors report that an impulse of about 200 psi-sec is needed to rupture to pressure vessel.[20] There is no test data for impulses above 40 psi-sec from weapons tests, and so we will have to rely on theoretical considerations and approximations to extend the test data into this range. Equation 3-6 predicts an impulse of 200 psi-sec at a distance of 800 feet from the containment wall, while other published material gives values of 420, 460 and 620 feet.[21,22,23]

CHAPTER 4

CRATERING

When a megaton weapon detonates at ground level, about 15% of the weapon's energy is transmitted into the ground, appearing mostly in the kinetic energy of the soil.[1] Some of the soil is vaporized and travels upward with the weapon debris. A greater amount of soil is pulverized by the multi-megabar shock wave; most of this is sucked into the radioactive cloud by strong updrafts. Roughly an equal amount of soil is fragmented and ejected hundreds or thousands of feet from the point of burst. Lastly, the air blast wave, direct ground shock and crater - induced ground shock move the soil in a manner similar to that of an earthquake miles from the point of detonation. The first three mechanisms, vaporization, pulverization and fragmentation, lead to the formation of a crater and the expulsion of ejecta, which are discussed next. Ground shock will be the subject of the next chapter.

A typical crater formed by a surface burst is shown in Figure 4-1. The "true" crater is measured to the point at which a definite shear has occured in the medium. However, fragmented soil often falls back into the crater, leaving the depression that one actually sees called the "apparent crater". It is the apparent crater which has been measured in the various weapon tests.

Glasstone gives approximate relationships for predicting the size of the crater for four different soil types.[2] The relationships yield the following crater dimensions:

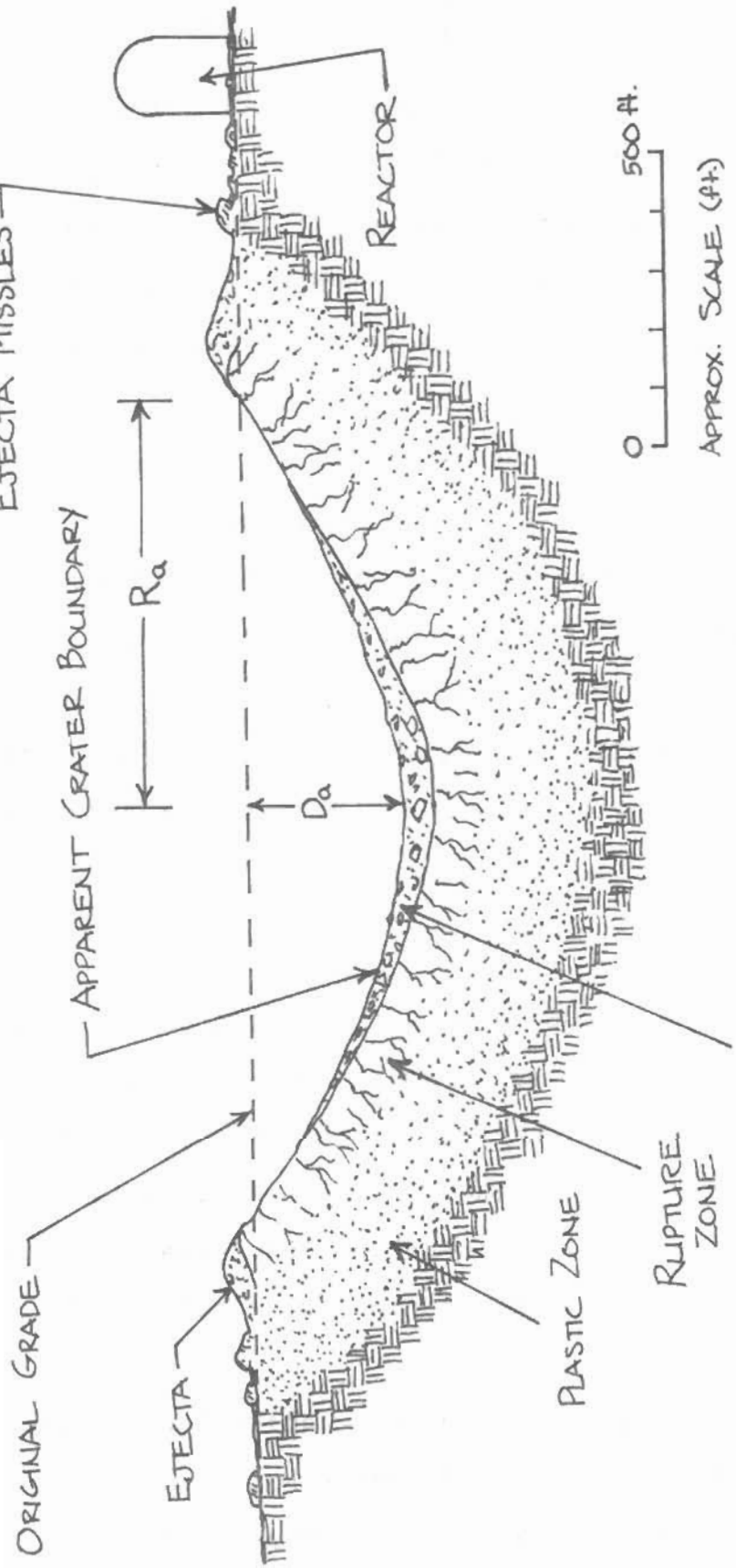

FIGURE 4-1 - CROSS SECTION OF A CRATER FORMED BY A ONE-MEGATON NUCLEAR DETONATION IN WET SOIL.

SOIL TYPE	R_a	D_a	V_a
Wet soil or wet soft rock	660 ft.	250 ft.	1.7×10^8 ft^3
Dry soil or dry soft rock	490	220	8.4×10^7
Wet hard rock	460	220	7.6×10^7
Dry hard rock	390	180	4.2×10^7

TABLE 4-1

Instead of giving crater dimensions, Crawford gives cratering efficiencies for five different soil types.[3] The relations he gives for determining the radius and depth from the volume are not useful here, because they rely totally on the geology of the Pacific atoll islands. These craters have been shown to bottom out upon reaching a dense soil strata immediately beneath the surface, which doubles the radii and halves the depths given above by Glasstone. However, a more reasonable estimate of the crater dimensions can be made by assuming the crater to be roughly a paraboloid, and by keeping the radius to depth ratio the same as in Glasstone:

SOIL TYPE	R_a	D_a	V_a
Wet soil	700 ft	260 ft	2×10^8 ft^3
Wet soft rock	550	210	10^8
Dry soil	490	190	7×10^7
Dry soft rock	440	170	5×10^7
Hard rock	370	140	3×10^7

TABLE 4-2

The figures from these two sources compare very well, and from this information we can construct estimates for six soil types:

TABLE 4-3

SOIL TYPE	R_a	D_a	V_a
Wet soil	680 ft	260 ft	1.9×10^8 ft^3
Wet soft rock	600	230	1.4×10^8
Dry soil	490	210	7.7×10^7
Dry soft rock	460	200	6.7×10^7
Wet hard rock	420	180	4.8×10^7
Dry hard rock	380	160	3.6×10^7

These are the figures that will be used throughout the text. Notice that they are for the case of a surface burst only, or bursts which occur a few feet above or below the ground. If the burst occurs below 300 ft, the dimensions will about double; the dimensions will reach a maximum when the depth of burst is roughly 1,000 ft, when they will be triple the above values. Similarly, if the weapon is detonated a hundred feet above the surface the crater dimensions will be drastically reduced, and above several hundred feet no crater will be produced.

Also, these figures assume a uniform geology of the soil type mentioned, while most sites have layered geologies. Since most reactors are built near large bodies of water, the water table will be relatively high. If V_1 is the volume of the crater in the surface material alone, and V_2 is the volume of the crater in the sub-surface material alone which lies at a depth d, then the volume resulting from a blast in the layered geology is:[4]

$$\frac{(V-V_2)}{(V_1-V_2)} = 1 - \exp\left[-5.4d/V^{1/3}\right] \qquad (4\text{-}1)$$

TARGETING IMPLICATIONS:

It is physically impossible for a structure to survive in the cratered region or the plastic zone surrounding the crater. We can therefore assume that the reactor will be reduced to rubble if the weapon is detonated $1.25R_a$ from the reactor, which corresponds to the lip of the crater. For the geologies considered here, this is between 480 and 850 feet from the point of burst.

However, the above analysis does not indicate at what distance the reactor will be vaporized, pulverized, or fragmented. This is very important, because it will determine to a large extent whether the reactor debris will be carried into the radioactive cloud, or whether the reactor will be fragmented and appear as ejecta. In the next section we find that the ejecta outside the crater account for about 40% of the crater volume for soil or soft rock geologies, and 80% for hard rock.

Considering first the soft rock or soil geologies, which are more typical of reactor sites, this leaves 60% of the apparent volume of the crater unaccounted for. Some of this material has been compressed into the surrounding soil, while most has been pulverized or vaporized and lifted into the radioactive cloud. Unfortunately, there appear to be no published estimates of the relative importance of these two

(Glasstone estimates only 1-2% is vaporized)[5]
actions, and it seems unlikely that reliable calculations can be made. It is assumed here that compression accounts for little of the remaining 60% for the following reasons: the fallback which lies in the apparent crater is less dense than the undisturbed soil, therefore raising somewhat the estimates of the true volume of soil excavated, and assuming a relatively homogeneous geology, it seems unlikely that a great fraction of the soil could be compacted because the surrounding soil would transmitt the energy over great distances. If the ten foot thick layer surrounding the crater was compressed so that its density increased 10%, this would only account for 0.6% of the apparent volume of the crater. For these reasons, it is reasonable to assume that about 50% of the soil is carried aloft in the cloud, to be mixed with the weapon debris and return as fallout. If the weapon is detonated close enough to the reactor, the reactor will be part of the soil that is carried aloft. To demonstrate the feasibility of this occurring, the total volume of the containment is about 2.5×10^6 ft^3, of which only about 9×10^5 ft^3 is solid material. Comparing this to the 3×10^7 to 10^8 ft^3 that would be carried aloft, we can see that the reactor debris would only account for 1 - 3% of the total debris, in the case of soil or soft rock. If the blast occured in hard rock, reactor debris would account for 10 - 15% of the total. In any case, it is well within the realm of possibility.

It seems natural to assume that the soil closest to the detonation will be the soil that is lifted into the atmosphere. If we construct a paraboloid which is symmetrical with the

crater and contains 50% of the volume, the radius will be about $0.8R_a$. At this radius, then, the reactor can be assumed to join the radioactive debris in the atmosphere; this occurs at about 220 feet for dry hard rock and 540 feet for wet soil.

This does not mean to imply that the cloud will only contain debris located initially $0.8R_a$ from the point of burst. In fact, debris will certainly be swept up over at least the radius of the stem of the cloud, which is 4,000 to 5,000 ft. in this case.[6] This analysis only implies that of the soil excavated by the crater, it is reasonable to conclude that the soil lying $0.8R_a$ from the point of burst will be pulverized and lifted to high altitudes. Small objects, dust, or volitle fission products released during the destruction of the reactor will be sucked into the radioactive cloud over a radius corresponding to the stem of the cloud, and probably greater.

EJECTA

The fragmented pieces of soil or rock thrown beyond the radius of the crater are called "ejecta missiles". (See Figure 4-1) The distance to which missiles are ejected is limited by gravity, air resistance, and the finite initial velocity of the missles. Ejecta from nuclear and conventional cratering events and from meteor impacts have been studied extensively, and it is possible to predict the average number of impacts expected on a given area at a certain distance. For the purposes of determining the threat to the reactor, we wish to know the probability of a missile striking the reactor with a momentum

greater than that that would breach the containment structure, P_b .

To compute this, we must first know what mass would have an impact velocity such that $mv = P_o$. This can be done with the formulas provided by Crawford:[7]

$$v_i = 5.673 \left(\frac{r}{\sin 2\theta}\right)^{.5} e^{-r/r_o} \text{ (ft/s)} \quad r < r_o/2 \qquad (4\text{-}2)$$

$$v_i = 23.08 \left(\frac{a\gamma}{C_d}\right)^{.5} \text{ (ft/s)} \qquad r > r_o/2 \qquad (4\text{-}3)$$

where

$r_o = 90\gamma a \sin\left(\frac{2\theta}{C_d}\right)$ ft γ = density of missile, (lb/ft^3)

a = missile diameter (ft) C_d = drag co-efficient

θ = ejection angle (from horizontal)

v_i = impact velocity (ft/s)

For the ranges and diameters considered here, equations 4-2 and 4-3 will differ little. Because equation 4-3 represents the limiting value or "terminal velocity", and because it is much easier to work with, only equation 4-3 will be used. The results will therefore be slightly conservative for short ranges, where the velocity would be less.

Crawford suggests nominal values of $\theta = 45^\circ$ and $C_d = 0.6$. Substituting these values, and noting that the mass $m_o = \frac{\pi}{6}\gamma a^3$, we have:

$$m_o = 0.0497 \left(\frac{P_o}{\gamma^{1/3}}\right)^{6/7} \text{ lbs.} \qquad (4\text{-}4)$$

Now we may ask the question, what is the probability that a missile with mass greater than m_o will impact a given area. To answer this, we must know the size distribution of the ejecta. If $f(a)$ is the distribution of ejecta according to the diameter a of the missile, then the total mass of missiles with diameter greater than a_o, $M(a_o)$, is given by:[8]

$$M(a_o) = M_E \frac{\int_{a_o}^{a_m} \frac{\pi}{6} \gamma a^3 f(a)\,da}{\int_{o}^{a_m} \frac{\pi}{6} \gamma a^3 f(a)\,da} \quad \text{lbs.} \qquad (4\text{-}5)$$

where M_e is the total mass of the ejecta. If $\bar{m}$ is defined to be the average mass of a missile with diameter between a_o and a_m, then:

$$\bar{m} = \frac{\int_{a_o}^{a_m} \frac{\pi}{6} \gamma a^3 f(a)\,da}{\int_{a_o}^{a_m} f(a)\,da} \quad \text{lbs} \qquad (4\text{-}6)$$

Then the average number of missiles, $\bar{n}$, with diameter greater than a_o is:

$$\bar{\eta} = \frac{M(a_o)}{\bar{m}} = \frac{M_E \int_{a_o}^{a_m} f(a)\,da}{\int_{o}^{a_m} \frac{\pi}{6} \gamma a^3 f(a)\,da} \qquad (4\text{-}7)$$

Experimental evidence suggests that $f(a) = a^{-3.5}$, and so equation 4-7 becomes:[9,10]

$$\bar{\eta} = \frac{M_E \int_{a_o}^{a_m} a^{-3.5}\,da}{\frac{\pi}{6}\gamma \int_{o}^{a_m} a^{-.5}\,da}$$

$$\bar{n} = -\frac{M_e\left[a_m^{-2.5} - a_o^{-2.5}\right]}{2.5\,\frac{\pi}{3}\,\gamma\, a_m^{.5}} \qquad (4\text{-}8)$$

The expected number of impacts, $\bar{I}$, is the average number greater than a_o, $\bar{n}$, times the fraction of the ejecta reaching the radius r, $\bar{\delta}/M_e$:

$$\bar{I} = \bar{n}\,\frac{\bar{\delta}}{M_e} = -\frac{3\,\bar{\delta}\left[a_m^{-2.5} - a_o^{-2.5}\right]}{2.5\,\pi\,\gamma\, a_m^{.5}} \quad \text{impacts/ft}^2 \qquad (4\text{-}9)$$

where $\bar{\delta}$ is the areal density of ejecta, in lb/ft^2. Equation 4-9 is identical to the formula appearing in Crawford,[11] and so there appears to be experimental support for its use. Converting from diameters to masses:

$$\bar{I} = -\frac{\bar{\delta}}{5}\,\frac{\left(1 - \left(\frac{m_m}{m_o}\right)^{5/6}\right)}{m_m} \quad \frac{\text{impacts}}{\text{ft}^2} \qquad (4\text{-}10)$$

All that is needed to complete the calculations are estimates of $m_m(r)$ and $\bar{\delta}$. Crawford gives a relation for $m_m(r)$:[12]

$$m_m(r) = \frac{\pi}{6}\,\gamma\, a_m(r)^3 = \frac{\pi}{6}\,\gamma\left[.504\,K\,\gamma^{-0.0667}\,V_a^{0.267}\,W^{-0.0127}\left(r/V_a^{1/3}\right)^{-0.548}\right]^3$$

For W = 1000 kt:

$$m_m(r) = 0.0515\,(F\gamma)^{0.8}\,V_a^{1.35}\,r^{-1.644} \quad \text{lb} \qquad (4\text{-}11)$$

where F = 1 for soil and soft rock, and F = 2 for hard rock.

The areal density of ejecta, $\bar{\delta}$, is estimated by many

sources. Crawford suggests:[13]

$$\bar{\delta} = \gamma F V_a^{1/3} \left[0.749 \exp(-2.30 r/V_a^{1/3}) + 0.0168 \exp(-0.423 r/V_a^{1/3})\right]$$

For $r/V_a^{1/3}$ greater than four, the first term becomes neglible, and so for the range of interest here:

$$\bar{\delta} = 0.0168 \gamma F V_a^{1/3} \exp\left[-0.423 r/V_a^{1/3}\right] \left(\frac{lb}{ft^2}\right) \quad (4\text{-}12)$$

Glasstone recommends:[14]

$$\bar{\delta} = 0.9 \gamma D_a \left(\frac{R_a}{r}\right)^{3.86} F^{0.4} \left(\frac{lb}{ft^2}\right) \quad (4\text{-}13)$$

Brode uses a formula fit to agree with high explosive (HE) tests:[15]

$$\bar{\delta} = \frac{0.7 R_a M_\epsilon}{2\pi r^3}\left(1 + \frac{2R_a}{r}\right) = \frac{.378 F \gamma V_a W^{-0.0477} R_a}{2\pi r^3}\left(1 + \frac{2R_a}{r}\right) \quad (4\text{-}14)$$

Using equations 4-10, 4-11, and 4-12, 4-13, or 4-14, we can predict the average number of impacts per square foot at any distance from the point of burst. The probability of at least one missile striking an area of A ft^2 is then:

$$P = 1 - e^{-\bar{I}A} \quad (4\text{-}15)$$

TARGETING IMPLICATIONS:

Reactor containments are routinely designed to withstand impacts from external as well as internal missiles. Examples of "design basis" for containments are impacts of a car traveling at 50 mph, a 450 lb bolted wood deck traveling at 500 mph, or a 100 lb siding sheet traveling at 600 mph.[16] All of these objects have a momentum of about 3×10^5 lb-ft/s, and the containment is designed to be structually sound after an impact of this magnitude. How large a momentum is needed to breach the containment? This is a difficult question to answer, and depends on the shape of the missile, the point of impact on the containment, and the hardness of the missile.

Simple estimates can be made, however. Suppose that the containment is designed to respond elastically to an impact of momentum 3×10^5 lb-ft/s; that is, the maximum resulting displacement is less than or equal to the elastic limit, and $\mu = 1$. (See Figure 3-8). Now suppose that we take $\mu \cong 10$ to correspond to a breach of the containment vessel. This would mean that 18 times as much work would be required of the wall than if the wall responded elastically. So if m_o and v_o are such that $m_o v_o = P_o = 3 \times 10^5$ lb-ft/s, then:

$$18 m_o v_o^2 = m_b v_b^2$$

where m_b and v_b are the mass and velocity of a missile which breaches the containment. Using the relationship $P = mv$ and equation 4-4, we have:

$$\left(\frac{P_b}{P_o}\right) = (18)^{7/8} = 12.5 \qquad (4\text{-}16)$$

So if $P_o = 3 \times 10^5$ lb-ft/s, $P_b = 4 \times 10^6$ lb-ft/s. However, it is doubtful that the containment is designed to respond perfectly elastically, and it is also quite possible that the containment will be breached at a lower ductility factor. For these reasons, P_b will be taken to be $10P_o$; $P_b = 3 \times 10^6$ lb-ft/s.

In trying to support this estimate of P_b we may choose to consider some theoretical calculations on the effects of moderate amounts of high explosive placed close to a wall. Mathematically at least, there is not a great deal of difference between the two; if the charge is placed close enough, the impulse on the wall may roughly match that of an impacting spherical missile. For example, if a 160 lb charge is placed less than one foot away from the wall, it will create about the same impulse on the wall as a missile with momentum 3×10^6 lb-ft/s. Kot gives calculations for maximum wall rotations for these situations; the above charge would create a maximum rotation of about 4 - 6°; 5° is considered to be the limit if structural integrity is to be maintained.[17] This agrees very well with the rough estimate made above. In any case, the containment will certainly be breached by a missile of $P_b = 7 \times 10^6$ lb-ft/s, for which $\mu = 20$ and the max. rotation is 14°.

Using the above equations, the probability of the reactor suffering an impact by a missile with a momentum greater than P has been computed, for $P = 3 \times 10^5$, 3×10^6, 7×10^6 lb-ft/s and for detonations in wet soil and dry hard rock. The results appear in Figures 4-2 and 4-3.

Notice that the curves of Brode and Glasstone greatly

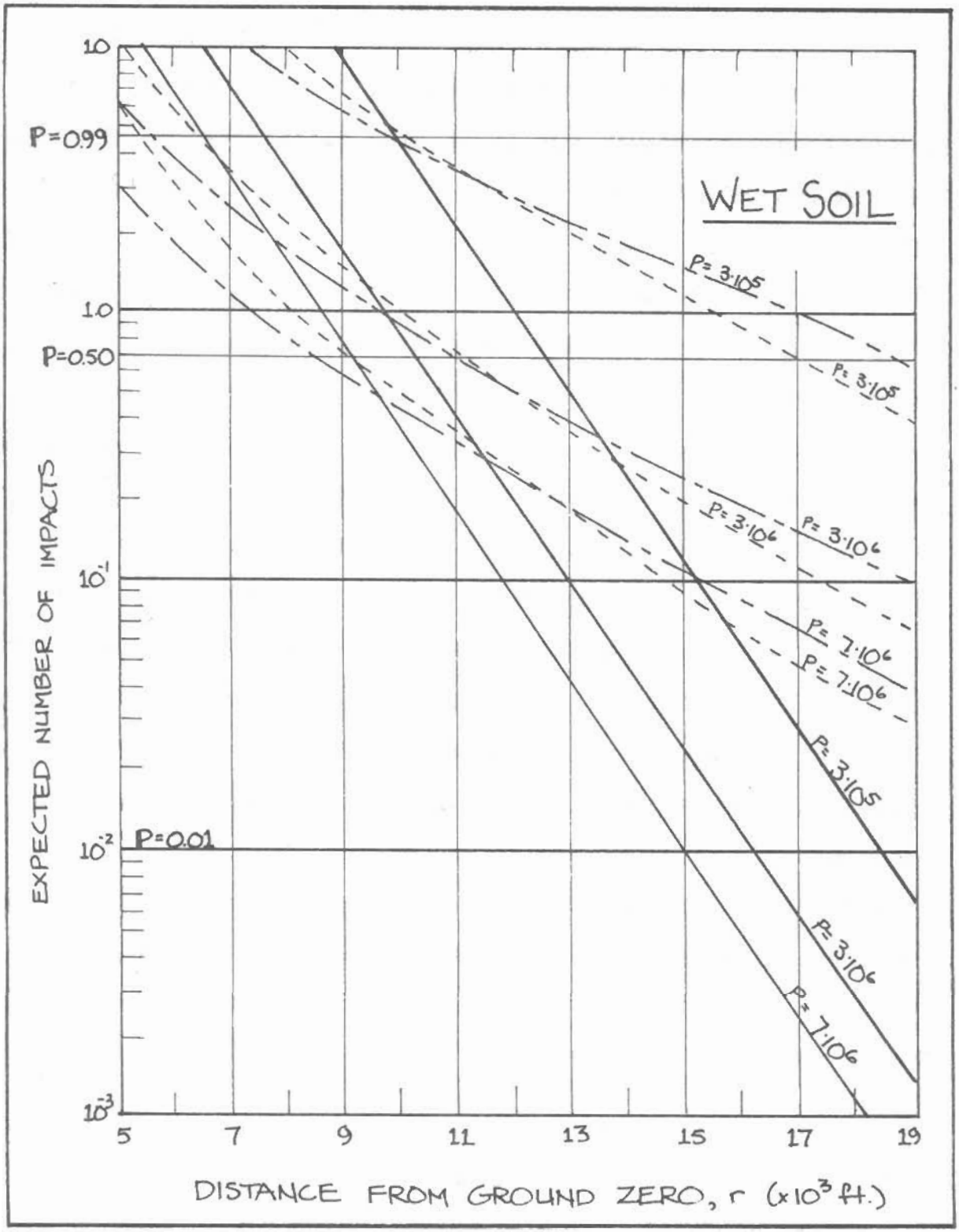

FIGURE 4-2: The expected number of missile impacts with momentum P on the reactor containment for wet soil. Solid lines are given by equation 4-12 (Crawford); dashed lines from equ. 4-13 (Glasstone); broken lines by equ. 4-14 (Brode).

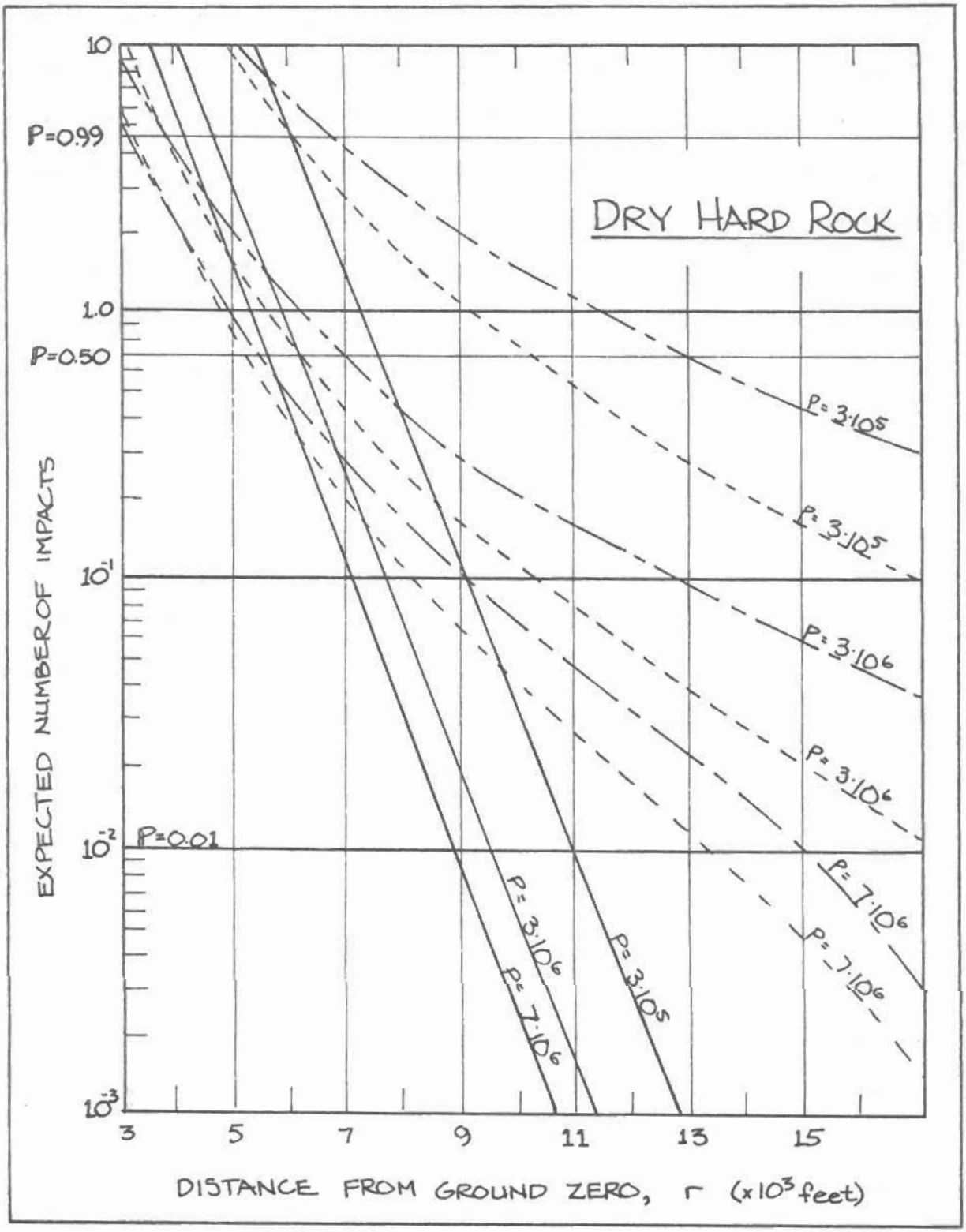

FIGURE 4-3: The expected number of missile impacts with momentum P on the reactor containment for dry hard rock. Solid lines are given by equ. 4-12 (Crawford); dashed lines by equ. 4-13 (Glasstone); broken lines by equ. 4-14 (Brode).

differ from the curves of Crawford at large distances. This is apparently caused by a lack of data at large ranges, and the curves were fit for the close-in data. No author gives estimates of the range of validity of these equations, although Crawford uses his equation in a sample calculation for r = 3400 ft. Because Crawford's equations are more internally consistent and seem more realistic, his equation for the areal density will be used at large distances. The final results appear below:

WET SOIL

	Probability of Occurrence		
P	99%	50%	1%
3×10^5	9,900 - 10,400	12,800	18,400 feet
3×10^6	5,600 - 7,400	10,100 - 10,800	16,000
7×10^6	4,500 - 6,600	8,300 - 9,200	15,000

HARD ROCK
DRY ~~SOIL~~

	Probability of Occurrence		
P	99%	50%	1%
3×10^5	6,000 - 6,800	7,600	11,000 feet
3×10^6	3,800 - 4,700	6,200 - 7,000	9,500
7×10^6	3,000 - 4,200	5,100 - 5,600	8,900

TABLE 4-4

In some ways these results are quite curious. Notice for example that, in wet soil, one can be almost certain of a complete breach ($\mathbb{P}$ = 99%; $P_b = 7 \times 10^6$) at a distance which corresponds to to a peak overpressure of 24-53 psi. In addition, one can be fairly sure that the containment will fail ($\mathbb{P}$ = 50%; $P_b = 3 \times 10^6$) for overpressures greater than about 10 psi; there is still a small chance of breaching the containment out to about 4 psi.

These calculations seem to contradict the statements of many authors on the construction of protective structures. All seem to imply that if a structure is designed to withstand the effects of blast, it will generally survive all other effects. The containment was shown in the last chapter to fail at 15-70 psi from blast effects, with a mean value of about 30 psi. The corresponding mean values for ejecta damage are 10 psi for wet soil, and about 25 psi for dry hard rock. This seems to imply that ejecta loads can be more damaging than blast loads.

Notice that the estimates of the areal density, the most important variable, are taken from three different sources, and that in most cases all three predict about the same range for $\mathbb{P}$ = 50%. Also notice that at longer ranges where this is not possible, the lowest value of the areal density was chosen. The results presented here should not be considered to be overly conservative. The ejecta arrive long after the blast wave and ground shock have affected the structure. If the structure is already considerably weakened by these effects, ($r < 15{,}000$ft), then even smaller ejecta masses can be considered to breach the containment structure.

CHAPTER 5

GROUND SHOCK

As mentioned in the last chapter, some 15% of the energy released from a one-megaton weapon finds its way into the soil. Some of this energy is involved in forming the crater, while the remainder results in ground motions which may be observed miles from the point of burst. In general, there are two sources of ground shock: the airblast wave and the direct coupling of the weapon's energy into the soil. For the cases under consideration here, the shock caused by air blast will be more important, because the air blast travels for thousands of feet at high peak overpressures, while the direct shock wave is attenuated rapidly with distance as it travels in the soil.

As described in Chapter 3, the air surrounding the point of burst is heated rapidly by the absorption of x-rays, forming a shock wave or air blast. This wave is characterized by an almost instantaneous rise to the peak overpressure, P_s , followed by a rapid exponetial decay. (See Figure 3-1) As the shock front moves away from the point of burst, the peak overpressure drops rapidly, and the velocity of the shock front, U , also becomes smaller.

At points close to the burst, the shock front velocity can be greater than the sesmic velocity of the soil, and so the ground motions produced by the air blast will lag behind the shock front itself. The ground shock is then said to be "super-seismic", because the air blast is traveling faster than the ground shock. Depending on the seismic velocity of the soil, the ground shock may always be super-seismic

(for seismic velocities less than the speed of sound), or the ground shock may only be super-seismic for ranges less than 1,000 ft. (for very high seismic velocities).

When the air blast shock front slows down to the point where the seismic velocity is greater than the shock velocity, the ground shock is said to be "outrunning", because the ground shock is traveling ahead of the shock front. In most of the cases examined here, the ground shock will be in the "outrunning" mode, which is the most difficult to analyze.

The most important quantity used to predict the damage done by ground shock is the peak acceleration that is induced in the soil. Unfortunately, ground shock is a very complex phenomenon and theoretical efforts to predict the peak accelerations are still in their infancy. We must therefore rely totally on empirical formulas which contain large uncertainties, resulting from the analysis of nuclear test data. The best source of this data is Sauer, which appears here in Figures 5-1 and 5-2.[1]

Still more useful are the empirical formulas given by Brode, because they are correlated to the characteristics of the soil in which the burst occurs:[2]

Super-seismic $$\ddot{y}_m \simeq \frac{340 P_m}{C_L} \pm 30\% \quad (g) \qquad (5\text{-}1)$$

Outrunning $$\ddot{y}_m \simeq \frac{2 \times 10^{11}}{C_L r^2} \begin{pmatrix} +\text{ factor } 4 \\ -\text{ factor } 2 \end{pmatrix} \quad (g's) \qquad (5\text{-}2)$$

$\ddot{y}_m$ = max vertical acceleration (g's) r = range (ft)
P_m = peak overpressure (psi)
C_L = seismic loading velocity $\approx \frac{3}{4} C_s$ (ft/s)
C_s = seismic velocity

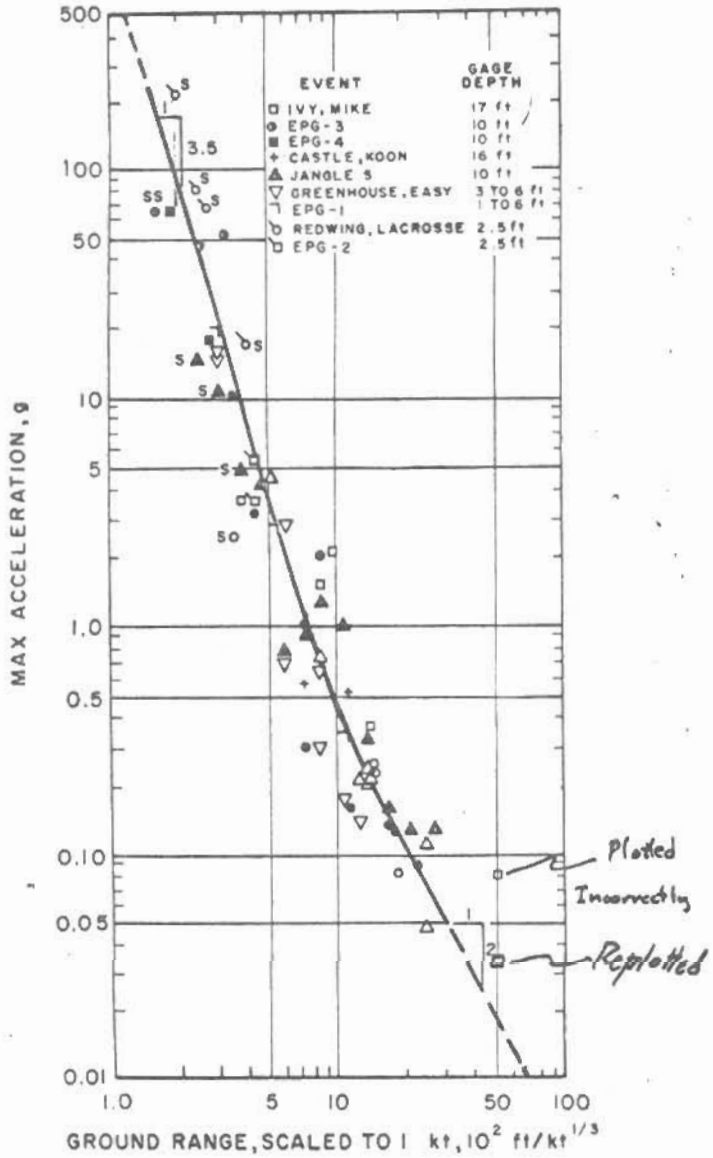

MAXIMUM VERTICAL ACCELERATION VS GROUND RANGE FOR OUTRUNNING GROUND MOTION, EPG (S INDICATES SUPERSEISMIC BLAST WAVE)

Figure 5-1 (Ref 1)

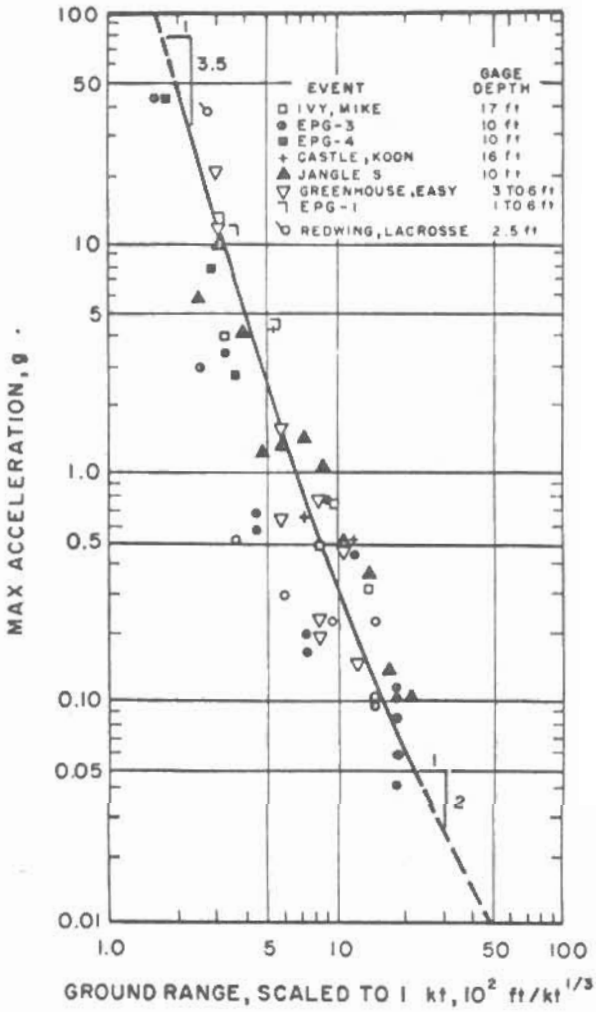

MAXIMUM HORIZONTAL ACCELERATION VS GROUND RANGE FOR OUTRUNNING GROUND MOTION, EPG

Figure 5-2 (Ref. 1)

The formulas are for vertical motions of the soil. For the super-seismic mode, the following theoretical approximation may be made for the peak horizontal acceleration, $\ddot{x}_m$:[3]

$$\ddot{x}_m \approx \tan[\arcsin(C_s/U)]\, \ddot{y}_m \quad (5\text{-}3)$$

Brode suggests that the horizontal motion will be quite comparable to the vertical motion in both modes.[4] A good comparison of Sauer's data shows that although the two motions are always of the same magnitude, the horizontal motions are always less - in some cases by a factor of two. It will be assumed here that the horizontal acceleration will be 0.5 to 1.0 times the vertical acceleration. All things considered, the formulas by Brode compare well with the data by Sauer, except for close-in ranges where Sauer predicts greater accelerations.

We will now apply these formulas to three soil types: dry soil, wet soil, and hard rock.

Dry Soil: First we must determine at what point the ground shock will make the transition from super-seismic to outrunning. This will occur when the shock velocity is equal to the seismic velocity; when $U = C_s$. From Equation 3-4, we have:

$$C_s = U = C_o\sqrt{1 + \frac{6P_m}{7P_o}} \qquad \text{if} \quad C_o = 1126 \text{ ft/s}, \quad P_o = 14.7 \text{ psi}$$

then

$$P_m = 17.15\left[\left(C_s/1126\right)^2 - 1\right] \quad (5\text{-}4)$$

The corresponding distance, r , can be found by solving equation 3-1, or by using Figure 3-2.

For dry soil we will examine two limiting sub-cases:

Soil Type	γ	C_s
dry clay	75 lb/ft^3	600 ft/s
dense dry sand	110	3300

Notice that for dry clay, the ground motion is always super-seismic, while for dense dry sand the transition occurs at 3,000 ft. (P_m = 130 psi). The ranges considered here will be greater than 3,400 ft. (P_m = 100 psi), and so the motion will be outrunning. The results are shown in Figure 5-3.

Wet Soil: For wet soil we examine the following sub-cases:

Soil Type	γ	C_s
wet clay	110 lb/ft^3	2500 ft/s
dense wet clay	135	6300

For wet clay, the transition from super-seismic to outrunning motion occurs at 3,900 ft. (P_m=67 psi), while for wet dense sand the distance is much closer than the ranges considered here (1,900 ft.; P_m=520 psi). The results for wet soil appear in Figure 5-4.

Hard Rock: The motion in hard rock is always outrunning for the moderate overpressures considered here. The results for the following sub-cases appear in Figure 5-5.

Soil Type	γ	C_s
granite	165 lb/ft^3	8000 ft/s
plutonic rock	170	25000

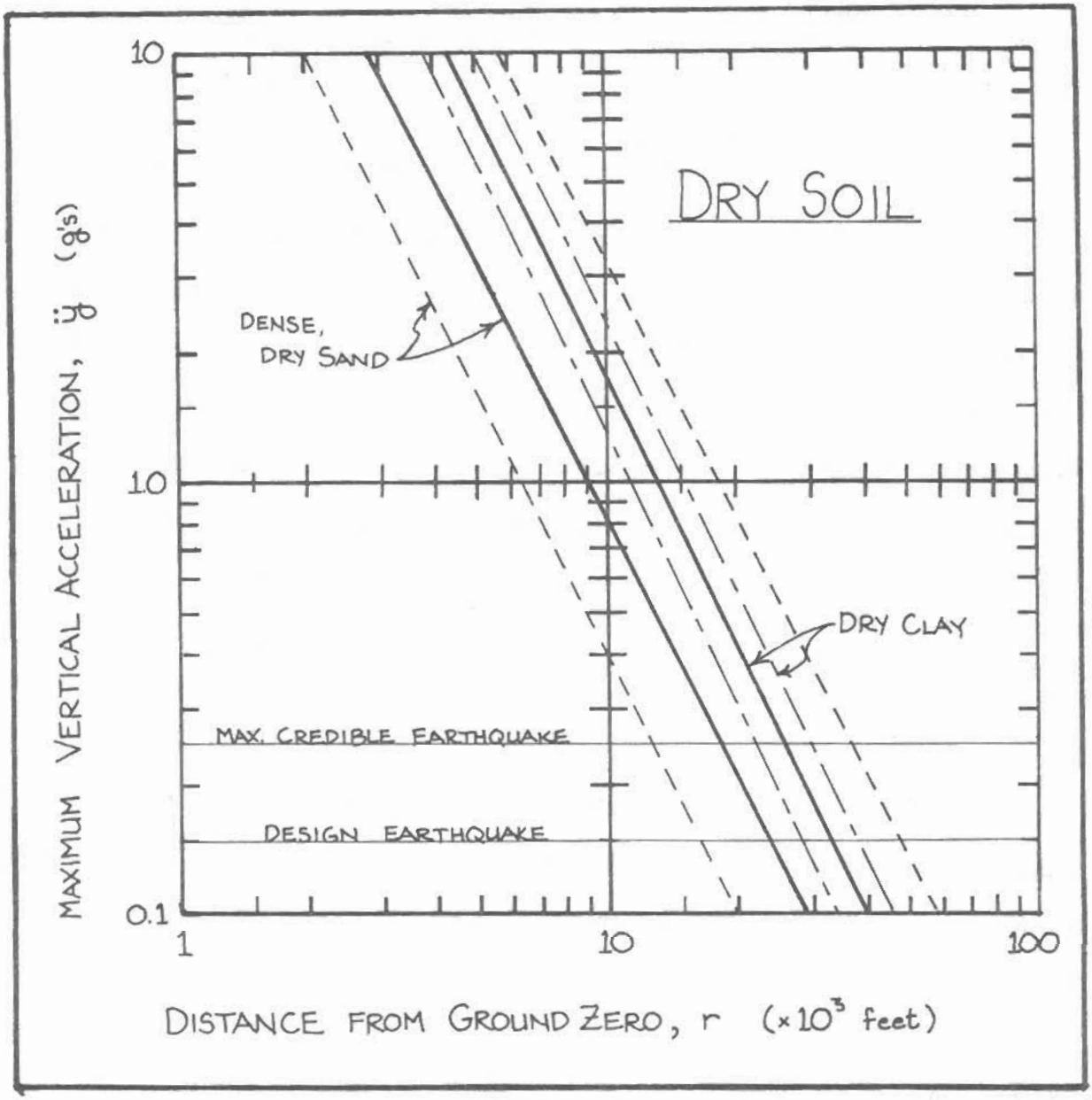

FIGURE 5-3: The maximum vertical acceleration resulting from the detonation of a one-megaton weapon in dry soil, as a function of distance.

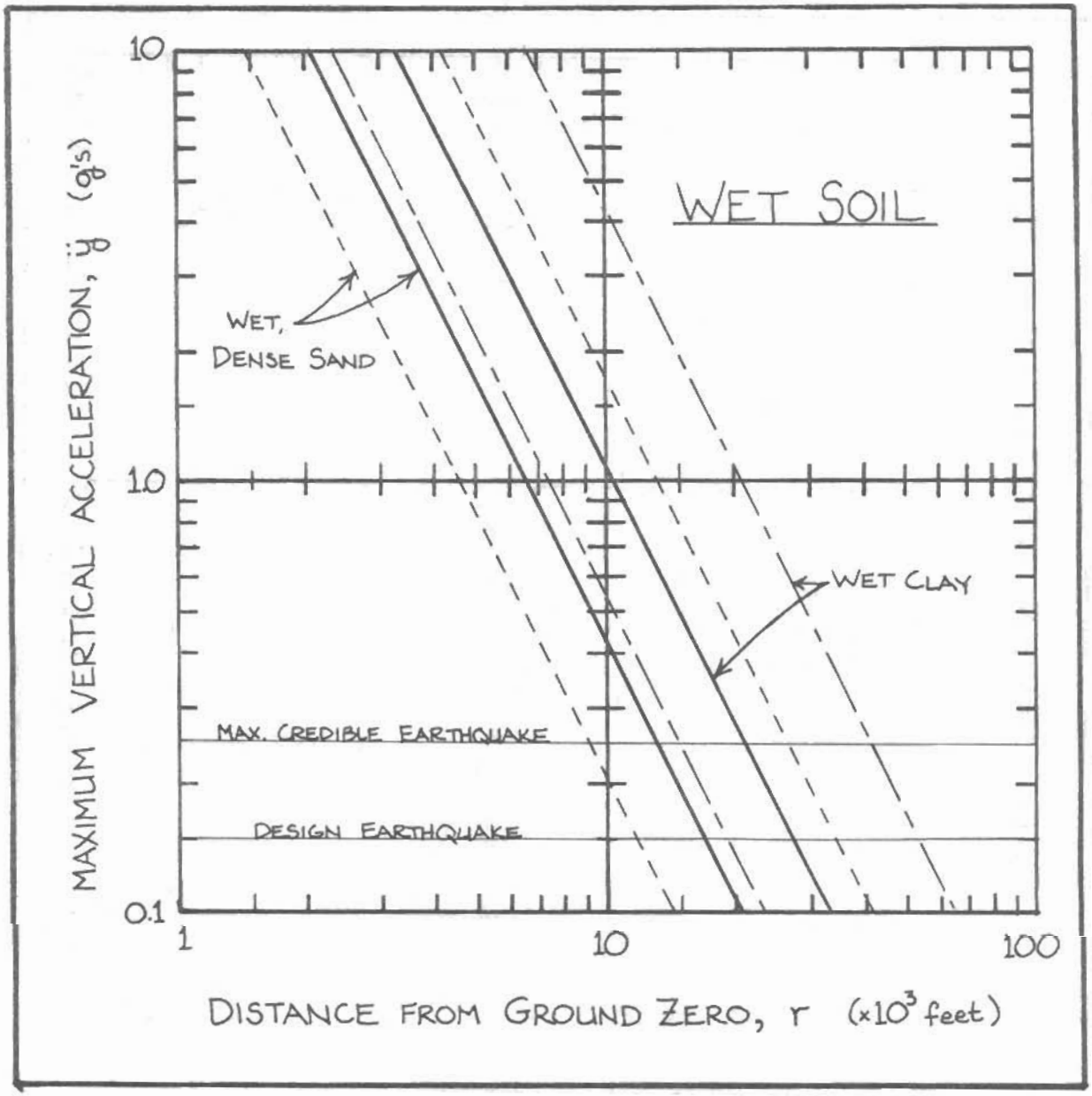

FIGURE 5-4: The maximum vertical acceleration resulting from the detonation of a one-megaton weapon in wet soil, as a function of distance.

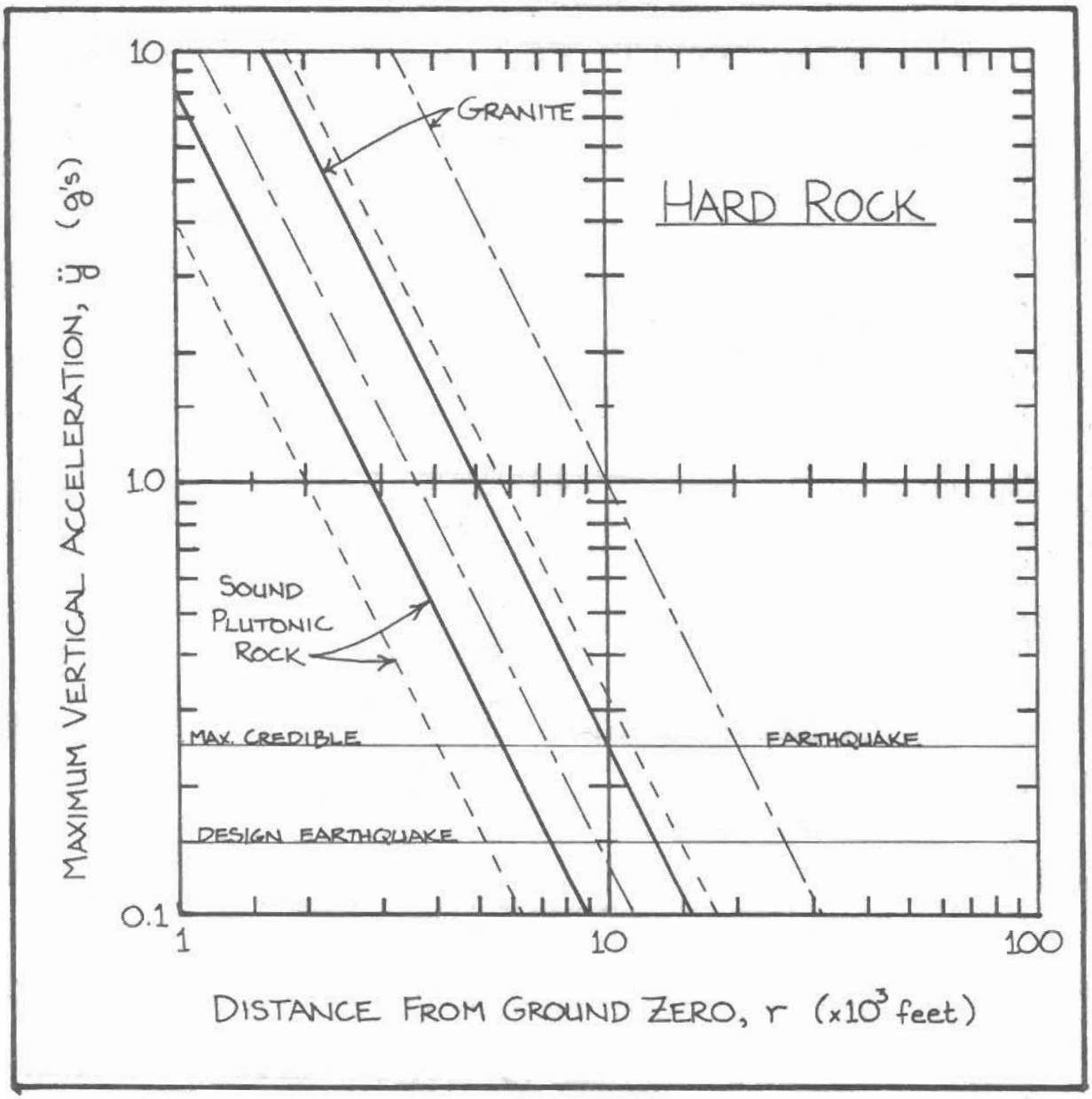

FIGURE 5-5: The maximum vertical acceleration resulting from the detonation of a one-megaton weapon in dry hard rock, as a function of distance.

TARGETING IMPLICATIONS

The ground shock produced by a nuclear weapon is very similar to that of an earthquake, and since reactor containments are routinely designed for earthquake loads we can use the calculations from the reactor safety reports directly to estimate the damage.

Figure 5-6 compares the maximum ground acceleration with the equivalent Richter Scale magnitudes, and gives a brief description of the damage expected from each. Almost all earthquakes observed fall into these categories.

A typical containment on the east coast is designed to withstand elastically a maximum horizontal acceleration of about 0.15g, which corresponds to a class VII earthquake. Also, the structure is analyzed to assure no loss of function for peak accelerations of 0.25g, corresponding to a class VIII earthquake.[5] The former (0.15g) is called the "design basis earthquake", and its magnitude is based on the largest earthquake previously observed on the site. The latter (0.25g) is called the "maximum credible earthquake", because it is based on the largest earthquake that could reasonably be expected to occur. From figure 5-6 it can be inferred that no structure is likely to survive a class X earthquake and retain structural integrity. For the purposes of this analysis, it is assumed here that the structure will certainly be breached when the maximum horizontal acceleration is greater than 1.0g. Applying the formulas presented in the last section, we obtain the following ranges for each of the above acceleration thresholds:

ABRIDGED MODIFIED MERCALLI INTENSITY SCALE

I	Not felt except by a very few under especially favourable circumstances.	
II	Felt only by a few persons at rest, especially on upper floors of buildings. Delicately suspended objects may swing.	
III	Felt quite noticeably indoors, especially on upper floors of buildings, but many people do not recognize it as an earthquake. Standing motor cars	may rock slightly. Vibration like passing of truck. Duration estimated.
IV	During the day felt indoors by many, outdoors by few. At night some awakened. Dishes, windows, doors disturbed; walls make creaking sound. Sen-	sation like heavy truck striking building. Standing motor cars rocked noticeably.
V	Felt by nearly everyone; many awakened. Some dishes, windows, etc., broken; a few instances of cracked plaster; unstable objects overturned.	Disturbance of trees, poles and other tall objects sometimes noticed. Pendulum clocks may stop.
VI	Felt by all; many frightened and run outdoors. Some heavy furniture moved; a few instances of fallen plaster or damaged chimneys. Damage slight.	
VII	Everybody runs outdoors. Damage **negligible** in buildings of good design and construction; **slight** to moderate in well-built ordinary structures;	**considerable** in poorly built or badly designed structures; some chimneys broken. Noticed by persons driving motor cars.
VIII	Damage **slight** in specially designed structures; **considerable** in ordinary substantial buildings with partial collapse; **great** in poorly built structures. Panel walls thrown out of frame structures.	Fall of chimneys, factory stacks, columns, monuments, walls. Heavy furniture overturned. Sand and mud ejected in small amounts. Changes in well water. Persons driving motor cars disturbed.
IX	Damage **considerable** in specially designed structures; well designed frame structures thrown out of plumb; **great** in substantial buildings, with	partial collapse. Buildings shifted off foundations. Ground cracked conspicuously. Underground pipes broken.
X	Some well-built wooden structures destroyed; most masonry and frame structures destroyed with foundations, ground badly cracked. Rails	bent. Landslides considerable from river banks and steep slopes. Shifted sand and mud. Water splashed (slopped) over banks.

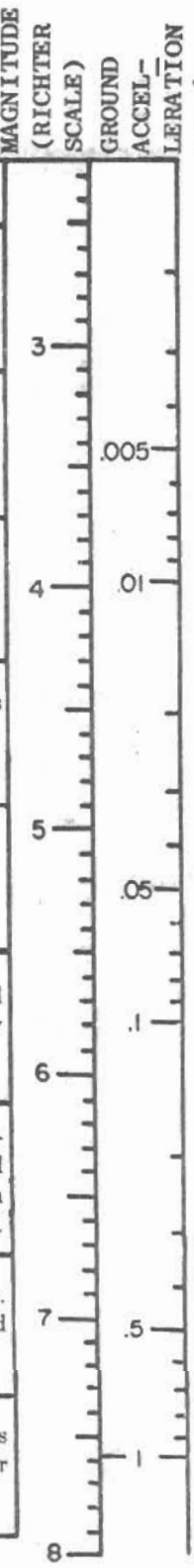

Modified Mercalli Intensity Scale after Wood and Neumann, 1931 (Intensities XI and XII not included).

Magnitude and acceleration values taken from Nuclear Reactors and Earthquakes, TID-7024, United States Atomic Energy Commission.

Fig. 5-6: Modified Mercalli Intensity Scale Approximate Relationship with Magnitude and Ground Acceleration

DISTANCE FROM POINT OF BURST (ft)

	Dry Soil	Wet Soil	Hard Rock
0.15	23,000 - 32,000	17,000 - 27,000	7,400 - 13,000 ft.
0.25	18,000 - 25,000	13,000 - 21,000	5,700 - 10,000
1.0	9,000 - 13,000	6,400 - 10,000	2,900 - 5,000

Just as in the last chapter on ejecta, these results appear to contradict the statement seen in many texts, that if a structure is designed to resist blast effects it will, in general, resist all other effects. Notice that in dry soil one can be certain of breaching the containment out to a distance which corresponds to a peak overpressure of 6.6 - 13 psi, which is a considerable distance beyond the air blast hazard. Even for wet soil (11-25 psi) and hard rock (42-160 psi), the ground shock hazard cannot be ignored. It is not clear at this time whether the apparent contradiction arises because of faults in the above analysis, or because the "conventional wisdom" that blast is the dominant effect is incorrect in this case.

In addition, in the final analysis it will be wise to consider the fact that the ground shock and the air blast will act on the structure simultaneously, causing failure of the containment at greater ranges than predicted above.

CHAPTER 6

SYNERGISM

Until now, we have discussed the different effects of nuclear weapons as if they were independent, unrelated events. This was done merely for convenience, so that we could understand the effects of highly different phenomena on the reactor structures. However, if we are to gain a true understanding of the response of the structure to the effects of a nuclear detonation, we must examine the combined destructive effects for thermal radiation, air blast, cratering, ejecta, and ground shock.

It can be easily seen that these are interrelated: the thermal radiation and air blast form the crater; the crater causes the ejecta to fly in all directions, and creates direct ground shock; the air blast causes induced ground shock. At any point a distance r from the reactor, these effects will be experienced at different times, depending on the yield of the weapon and the type of soil. Table 6-1 shows this time sequence of events for r = 4,600 ft.

The response of the structure is also dependent on the nature of this time sequence. First, nuclear and thermal radiations will be absorbed by the concrete shell, perhaps weakening it. Then ground motions begin to sway the structure, and continue until the blast wave arrives. After these have subsided, large masses of ejecta rain down on the containment, and finally the stem winds carry off any loose pieces. Although the structure may be able to resist any one of these effects independently, it may not be able to withstand the combined effects.

In principle, it is possible to solve this problem exactly

TIME	SOIL TYPE		
	WET	DRY	ROCK
0 s	DETONATION 4,600 ft. FROM CONTAINMENT SHELL		
<1ms	$3 \cdot 10^{13}$ n/cm² neutrons (72,000 rads) 10^5 r γ-rays		
0.2-1.0	GROUND SHOCK BEGINS. MAX. VERTICAL ACCELATIONS:		
	1-10 g	2-11 g	.25-2.5 g
0-1.0	THERMAL RADIENCE REACHES A MAX. TOTAL BEFORE 1.0s IS 164 cal/cm²		
1.0	AIR BLAST ARRIVES. PEAK OVERPRESSURE = 50 psi, PEAK REFLECTED PRESSURE = 200 psi MAX. WIND SPEED > 900 mph		
2.0	POSITIVE OVERPRESSURE PHASE OVER		
5-20 s	EJECTA ARRIVES. AVERAGE NUMBER OF MISSLE IMPACTS:		
	$\frac{P}{3 \cdot 10^6}$ 8-30	5-15	2-5
	$7 \cdot 10^6$ 5-15	3-11	1-6
10s	TOTAL RADIANCE = 660 cal/cm²		
30s	STEM WINDS BEGIN, REACH MAX OF 500 mph		
600s	STEM WINDS OVER.		

TABLE 6-1: TIME SEQUENCE OF EVENTS 4,600 FT FROM THE DETONATION OF A ONE-MEGATON WEAPON ON THE GROUND.

by applying the laws of mechanics to every particle in the system, and then subjecting them to the time varying forces created by the air blast, ground shock and ejecta. But as we have seen in previous chapters, this is not an easy matter, and even very approximate solutions are hard to obtain. Complex computer programs have been devised to solve very specialized parts of this problem, and such programs are often used to analyze the response of structures to earthquakes. Because of its complexity, this method has not been adopted, although such a method should be applied in the future.

Of all the weapon effects described here, only one, ejecta, deals explicitly with probabilities. In all other cases one can in principle predict the effects with great precision. But in the approximate methods applied in this report, the uncertainties in the predictions were typically very large, and so I assigned arbitrary "probabilities" that the result is correct. This probability is not the chance of the event actually occuring, it is the probability of a response to the event.

For example, although peak overpressure levels from air blast are well known, the response of the structure is not. From approximate calculations, we can be almost certain that the structure will not fail at peak overpressures below 5 psi, and that it will fail at overpressures greater than 60 psi. I therefore assigned a quite arbitrary probability of 0.99 to 60 psi, and 0.01 to 5 psi, with a mean value of 20-30 psi.

In the case of ground shock predictions, we applied equations 5-1 & 2 which predicted mean values, with an upper limit (in most

cases) of 4 times the mean value and a lower limit of $\frac{1}{8}$ the mean value. From examining the data of Sauer (Figure 5-1), we can see that 15% of the observations lie below the lower limit, while less than 5% lie above the upper limit. For these reasons, we can assign a "probability" of 0.85 to the lower limit, 0.50 to the mean value, and 0.05 to the upper limit.

Using these values, we can compute the probability that the containment structure will fail for any one of these destructive events, assuming that the events are independent, and that each could individually breach the containment:

$$P_1(r) = \left(1 - \prod_{n=1}^{N} (1 - P_n(r) \right) \qquad (6\text{-}1)$$

This does not in any way include the combined effects of these events. If there are lesser effects of the above type which will result in a breach if any two occur, then the probability that the containment will fail from combined effects is:

$$P_c(r) = \left(1 - \prod_{\substack{l,m \\ l \neq m}} (1 - P_l(r)P_m(r) \right) \qquad (6\text{-}2)$$

The total probability is therefore:

$$P(r) = 1 - P_1(r)P_c(r) \qquad (6\text{-}3)$$

For the problem at hand, the P_n's refer to an ejecta missile momentum greater than 7×10^6 lb-f/s, a maximum vertical ground acceleration greater than 1.0 g , and any level of air blast. For the P_l's and P_m's , it is assumed that a combination of o.50 g ground acceleration, 3×10^6 lb-ft/s missile momentum, and a peak overpressure greater than 5 psi will result in a breach, as

the combined effect of 0.50 g or 3×10^6 lb-ft/s with a peak overpressure greater than 25 psi. Also included is a 50% chance that the containment will fail from .50 g or 3×10^6 lb-ft/s alone. Equations 6-1,2, and 3 have been applied to these probabilities, and the results appear in Table 6-2.

The distance at which volatile fission products which are released promptly from the devastated reactor can be entrained in the radioactive cloud of the weapon is even more uncertain. The structures will almost certainly be destroyed at about 3,000 - 4,000 feet from the detonation (prompt loss of coolant). For fission products to be easily entrained in the cloud, the reactor must be located within the stem. From photographs of nuclear bursts, the stem is found to be approximately 1/10 to 1/5 of the radius of the cloud. The cloud radius is about 6 miles, so the stem radius is about 3,000 to 6,000 feet. It is therefore safe to conclude that entrainment of volatile fission products will be complete at ranges closer than 3,000 feet.

The distance at which the total reactor core is entrained is also difficult to ascertain. It was concluded in Chapter 4 that if the reactor was within 220 to 540 feet from the burst, it would be entrained. In Chapter 3, we discussed an experimental work which indicated a range between 420 and 800 feet. In the first case, only cratering was considered, and in the second case, only air blast was considered. Because of the complexities at these close ranges, it is impossible to study the combined effects

INDEPENDENT EVENTS ONLY

Probability of Breach	Wet Soil	Dry Soil	Dry Hard Rock
99%	5,500-7,700	6,000-10,000	4,600-5,200
50%	9,500-12,000	9,800-13,000	7,000-8,400
1%	19,000-27,000	19,000-28,000	18,000

COMBINED AND INDEPENDENT EVENTS

Probability of Breach	Wet Soil	Dry Soil	Dry Hard Rock
99%	8,100-10,000	8,200-13,000	5,200-6,500
50%	13,000-16,000	15,000-18,000	8,000-9,500
1%	22,000-28,000	23,000-32,000	20,000

TABLE 6-2: The distance in feet at which there is a certain probability of breaching the reactor containment structure, with and without including combined effects.

of the intense nuclear and thermal radiations, the hot fireball, cratering and air blast. However, the resulting radius must be greater than that indicated for the individual effects. All things considered, a distance of 500 to 1000 feet is recommended.

CHAPTER 7

DAMAGE FROM ENHANCED FALLOUT

The most damaging effects of an attack on a nuclear reactor occur when the radioactive materials of the reactor core or spent fuel are entrained in the radioactive cloud of the weapon. The material from the reactor will then join with the weapon debris, and rise up to twelve miles. The cloud will then travel downwind and the radioactive debris will fall to the earth, contaminating large areas of land.

If the entire reactor core is pulverized and lifted into the cloud, the resulting fallout will be much richer in long-lived fission products than the fallout from a weapon alone. For the isotope Cesium-137, for example, this increase will be on the order of a factor of 50. Hence, even though the radioactivity from the weapon alone is initially much stronger, at longer times after the detonation the debris from the reactor will greatly increase this level of radioactivity. This will increase the time it takes for the dose-rate to drop to a safe level.

In order to predict the damage done by this enhanced fallout, we must be able to predict the resulting fallout distribution, the decay of the fallout, and the corresponding doses received. This is the subject of the following sections.

Distribution of Fallout from a Nuclear Weapon

When a nuclear weapon is detonated at ground level, it excavates a large crater, and sweeps up a great amount of debris into the surrounding air. Some of this material is carried to high altitudes in the radioactive cloud, where the dust and debris mix with the intensly radioactive weapon gases, which condense onto these dirt particles. As the cloud is carried along by the prevailing winds these particles fall back to the ground, causing radioactive contamination. This is called fallout, and this chapter attempts to predict the amount of land which is contaminated.

Various methods have been developed for predicting the distribution of radioactive contamination from a surface burst. In general, the prediction depends on the nature of the surrounding soil, the target materials, the wind velocity and direction, the wind shear, weapon yield, the fraction of the weapon yield due to fission, the details of the weapon construction, and the presence of precipitation.

The method adopted in this study is taken from The Effects of Nuclear Weapons, which predicts idealized contours which ignore most of the details of a specific situation, since they are not available, and represent an average fallout field based on weapon tests.[1] The model assumes assumes a small wind shear of 15^{o}, and an average wind velocity of 15 miles per hour, although predictions for wind velocities between 8 and 45 miles per hour can easily be obtained. The result of the model will be idealized elliptical iso-dose contours; that is, contours along which the dose will be

equal. Although in a real situation the wind velocity and direction may change considerably over the time in which the cloud is depositing fallout, the area of contamination will remain roughly equal to that predicted here for the idealized ellipses. This is fortunate, since the amount of land contaminated is in general more important in making damage predictions than the exact spatial distribution of the contaminants. An example of an idealized fallout pattern is shown in Figure A-1.

For any thermonuclear weapon of yield W, of which a fraction f is derived from fission, the resulting contour dimensions are given in the following table:[2]

R_1/f (rads/hr)	Downwind Distance, r (mi)	Max. Width, w (mi)	Area, A (mi^2)
3000	$0.95\ W^{.45}$	$0.0076W^{.86}$	$0.0057\ W^{1.31}$
1000	$1.8\ W^{.45}$	$0.036\ W^{.78}$	$0.051\ W^{1.21}$
300	$4.5\ W^{.45}$	$0.13\ W^{.66}$	$0.46\ W^{1.11}$
100	$8.9\ W^{.45}$	$0.38\ W^{.60}$	$2.7\ W^{1.05}$
30	$16\ W^{.45}$	$0.76\ W^{.56}$	$9.6\ W^{1.01}$
10	$24\ W^{.45}$	$1.4\ W^{.53}$	$26\ W^{.98}$
3	$30\ W^{.45}$	$2.2\ W^{.50}$	$52\ W^{.95}$
1	$40\ W^{.45}$	$3.3\ W^{.48}$	$103\ W^{.93}$

TABLE 7-1

The downwind distance, r , and the maximum width, w , of the iso-dose contours is shown in Figure 7-1, and the area A is computed by approximating the contours as ellipses with semi-major and semi-minor axis of $r/2$ and $w/2$, respectively.

The resulting area is then $A = \pi rw/4$.

R_1 is called the "unit-time dose-rate", and represents the dose-rate one hour after detonation. If one knows the decay function, or how fast the radioactivity decays with time for the event in question, then knowledge of R_1 allows one to compute the dose-rate at any later time.

As mentioned above, the values given in Table A-1 are for an average wind velocity of 15 miles/hour. The $\bar{v}_{effective}$ velocity means the average of all wind velocities from ground level to the top of the cloud. If the wind velocity is greater than this, the particles will travel farther downwind before returning to earth, which increases the maximum downwind distance, r . Similarly, the maximum width, w , will decrease slightly if the wind velocity is increased. It has been found by experimentation with computer codes that although the downwind distance may increase considerably, the change in the maximum width is small, and can be ignored. Therefore for wind velocities between 15 and 45 miles/hr, the following facter F should be multiplied by the values obtained from Table A-1:[3]

$$F = 1 + \frac{u - 15}{60} \qquad (7\text{-}1)$$

where u is the average wind velocity. For wind velocities less then 15 but greater than 8 miles/hour, the following factor should be used:

$$F = 1 + \frac{u - 15}{30} \qquad (7\text{-}2)$$

Table A-2 gives the values of F for a few values of the wind velocity.

TABLE 7-2

Wind Velocity u (mi/hr)	F
8	0.77
15	1.00
30	1.25
45	1.50

I have derived the following approximation which gives the area contaminated by a minimum unit-time dose rate R_1:

$$A = \left[\frac{3.98\times10^{4}(R_1/f)^{-0.598}}{(R_1/f)^{1.37} + 391}\right] F\, W^{\left[0.0346(R_1/f)^{0.317}+0.9\right]} \qquad (7\text{-}3)$$

For the weapon considered in this study, W=1000 kilotons, and f=0.5. Using these values, and assuming an effective wind velocity of 15 mi/hr, we obtain the curves given in Figures 7-2, 3, and 4, which plot R_1 as a function of r, w, and A, respectively.

Notice that for $R_1 \simeq 20$ rads/hr, the maximum width is very nearly 1/10 of the downwind distance, and so the expression for the area is approximately $A = \pi r^2/40$.

These fallout patterns are assumed to be independent of the target, and form the basis for all the fallout predictions in this text.

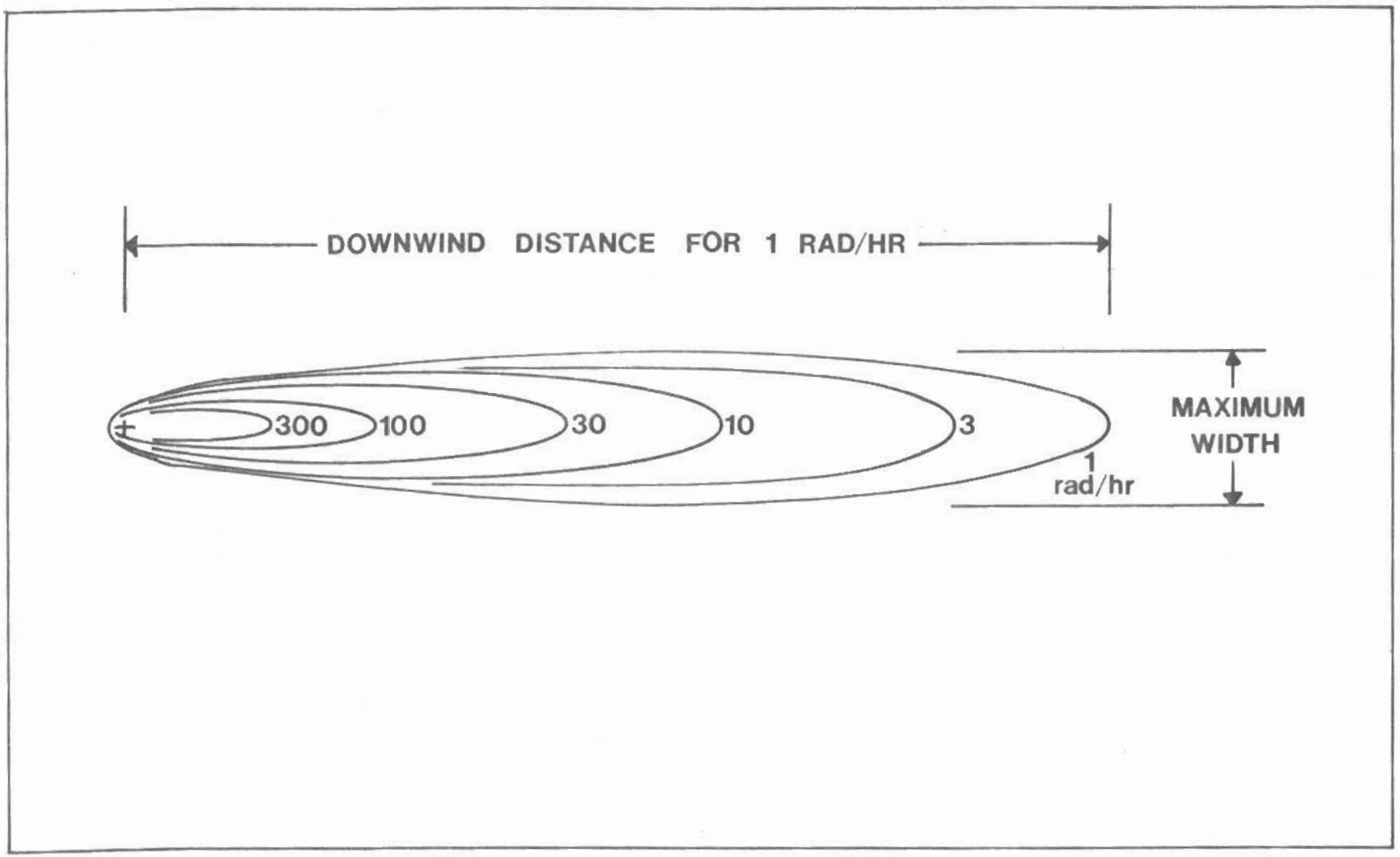

Figure 7-1. Illustration of idealized unit-time dose-rate pattern for early fallout from a surface burst. (The contour dimensions are indicated for a dose rate of 1 rad/hr.)

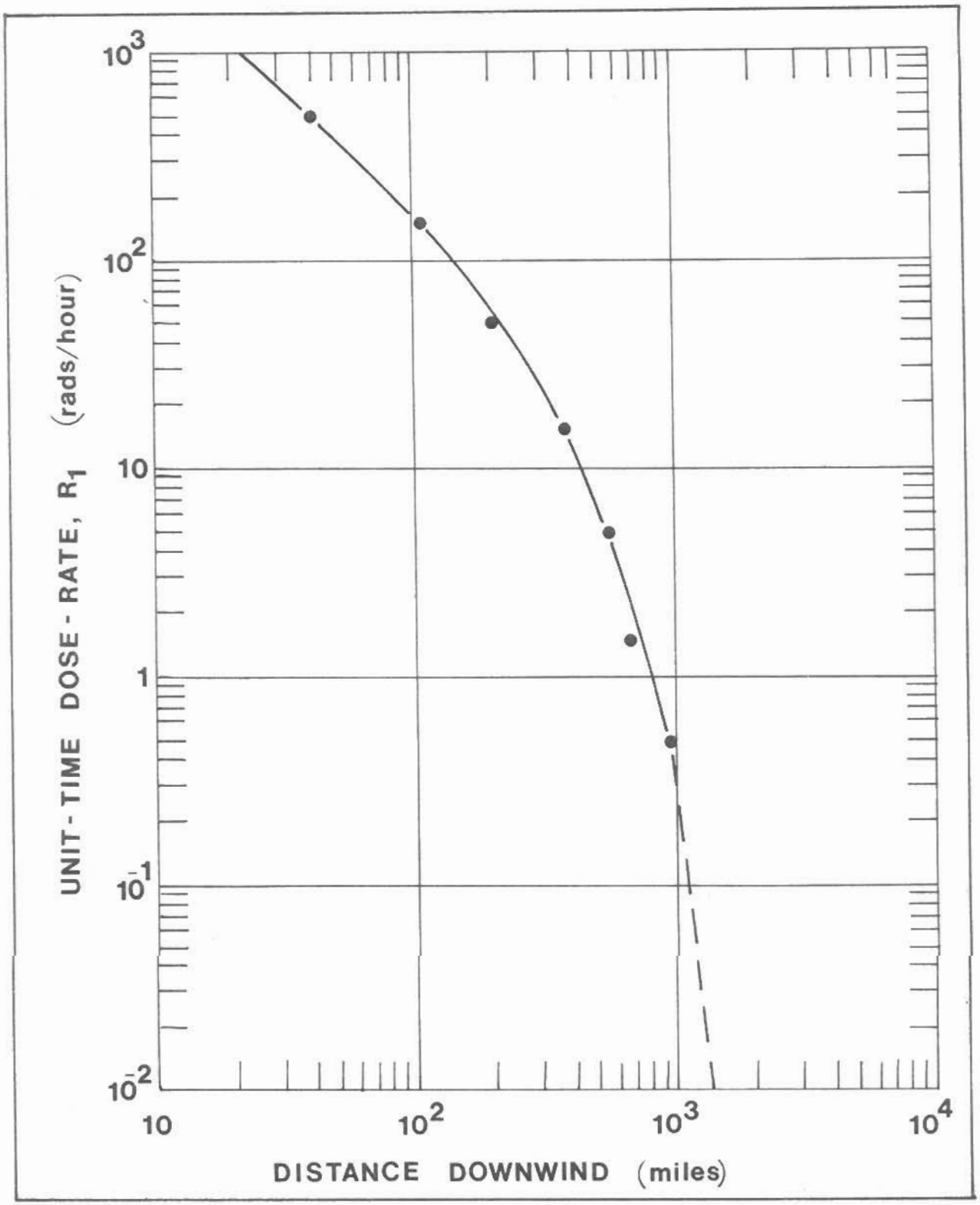

Figure 7-2. The maximum downwind distance for a given unit-time dose-rate, R_1. The points indicate calculated results given by the formulas on p. 90 and are listed in Table 7-1.

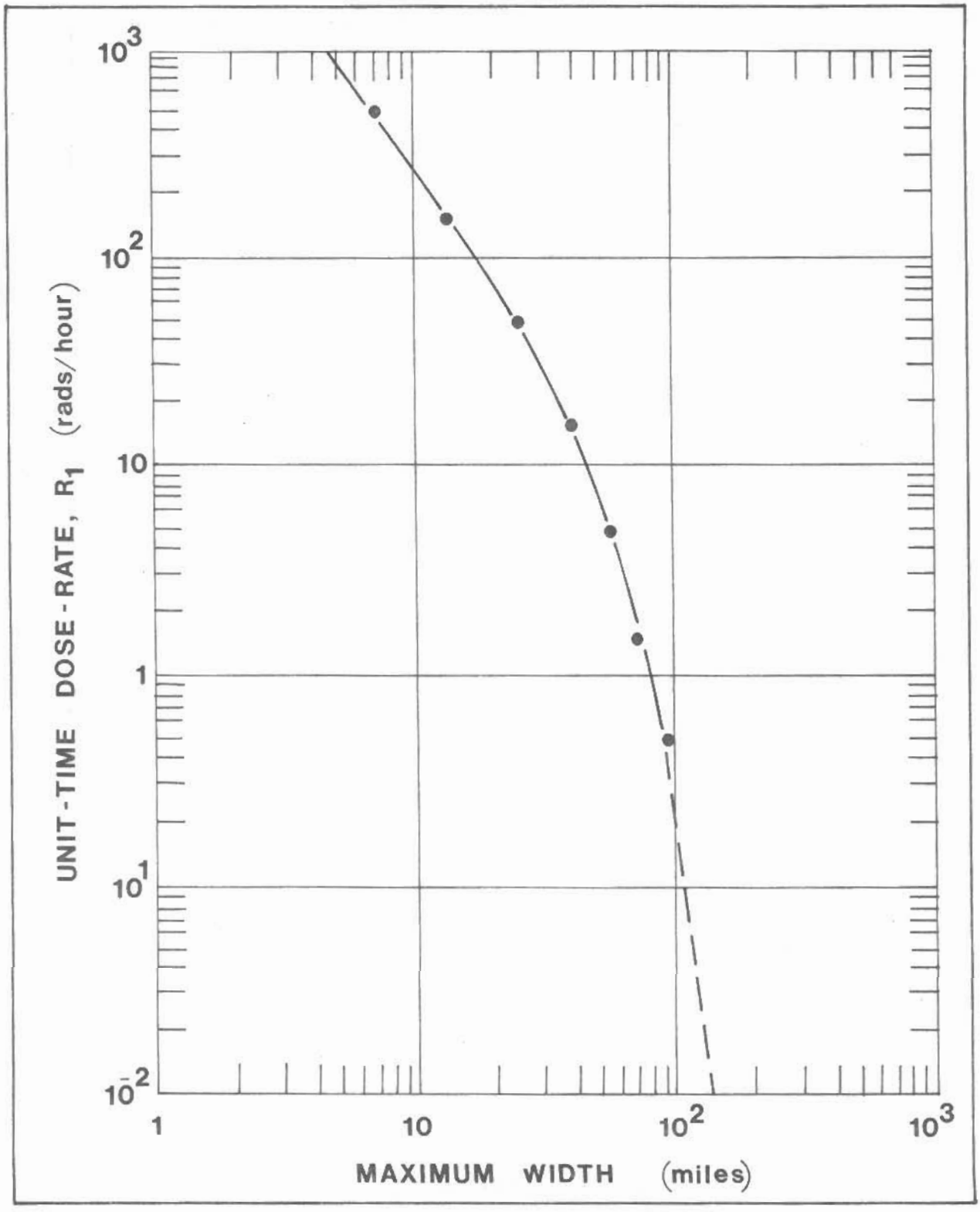

Figure 7-3. The maximum width for a given unit-time dose-rate, R_1. The points indicate calculated results given by the formulas on p. 90 and are listed in Table 7-1.

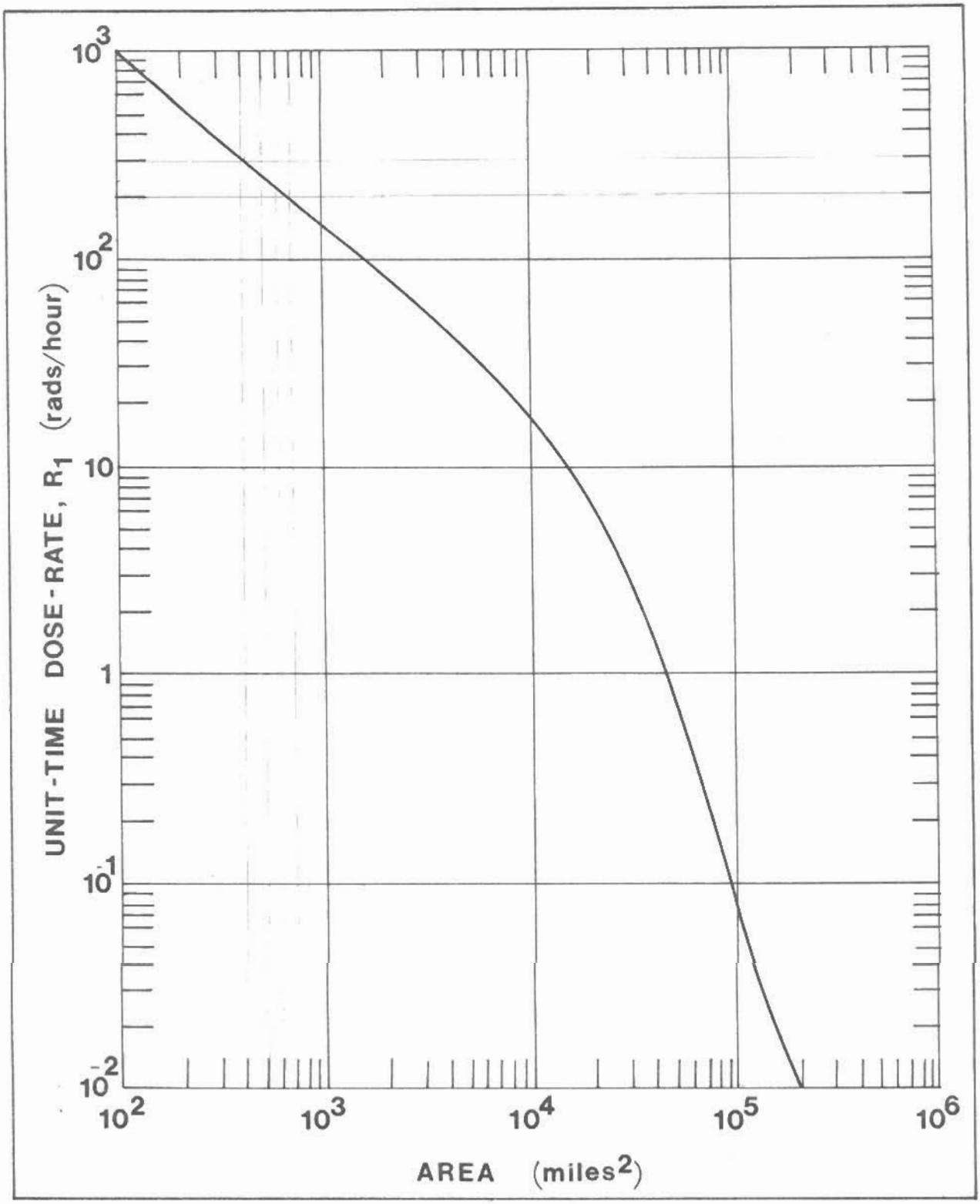

Figure 7-4. The area of the unit-time dose-rate contours, assuming that the contours are elliptical. The area is then $A = \pi rw/4$. Values for r and w are taken from Figures 7-2 and 7-3.

Decay of Fallout and Determination of the Dose

Although we may know the amount of land that is contaminated to a certain degree, in order to predict the damage that is done by this contamination we must determine the biological effect of some total dose of radiation over a given time period. It is well known that a dose of 400 rem over a period of about 96 hours will cause death in about 50% of the exposed population. If the dose is greater than 1000 rem, survival is nearly impossible, even with heroic medical care. At lower doses that are absorbed over the same or a much greater period of time, other effects may be observed: spontaneous abortions, birth defects, sterility, and latent cancer. An exposure of 50 rem will cause radiation sickness in about half of those exposed.[4] It is believed by some biologists that all doses of radiation are harmful and increase the chance of cancer, although the data are uncertain at this time.

We can determine the dose of radiation in a given time period if we know the dose-rate at some time after the event (for example, R_1), and if we know how the radioactivity decreases or decays with time.

There are two main processes which reduce the dose-rate as time increases. The most important of these is the radioactive decay of the atoms which compose the sample, or how long it takes, on the average, for these excited atoms to release energy (radiation) and become stable again. As more atoms go through this process, less remain in an excited state, and so the activity decreases. A measure of the time it takes for the atoms to decay is their

"half-life", $T_{\frac{1}{2}}$. Each radionuclide has a characteristic half-life, which is well determined and does not change with time. The radioactive decay function for a single type of radionuclide is therefore:

$$f_{r_i}(t) = a_{o_i} c_i \text{EXP}(-.693t/T_{\frac{1}{2}}) \qquad (7\text{-}4)$$

From this we see that when $t = T_{\frac{1}{2}}$, the decay function is just one-half its initial value, R_{o_i} . Half-lives of different radionuclei range from fractions of a second to several billion years. c_i is a constant which depends on the type of radionuclide, and converts from disintegrations/second to a dose. If we have N different radionuclei, then the total radioactive decay, $f_r(t)$, is given by the sum:

$$f_r(t) = \sum_{i=1}^{N} a_{o_i} c_i \text{EXP}(-\lambda_i t) \qquad (7\text{-}5)$$

where $\lambda_i = .693/T_{\frac{1}{2}}$ is called the "decay constant".

Another important factor in the reduction of the dose-rate with time is called "weathering", and refers to the effects of rain, wind, and snow on the dose received from radionuclides deposited on the soil. Although weathering does not change the emission of radiation from the nuclei, precipitation washes the particles below the surface of soil and partially shields a person from the dose he would receive if the particles were on the surface. It has been observed experimentally that the decay due to weathering, $f_w(t)$, can be approximated by the following expression:[5]

$$f_w(t) = 0.63\text{EXP}(-1.29\text{x}10^{-4}t) + 0.37\text{EXP}(-8.54\text{x}10^{-7}t) \qquad (7\text{-}6)$$

The total decay function, f(t) , will be the product of these two functions:

$$f(t) = \sum_{i=1}^{N} a_{o_1} c_1 \mathrm{EXP}(-\lambda_1 t)\ 0.63\mathrm{EXP}(-1.29\times10^{-4}t) + 0.37\mathrm{EXP}(-8.54\times10^{-7}t) \qquad (7\text{-}7)$$

Surface Burst

In the case of a surface burst, the above computations for $f_r(t)$ have already been carried out, and they appear in The Effects of Nuclear Weapons,[6] and we need only multiply this by the weathering decay function to determine the total decay function. These results appear in Figure 7-5.

To calculate the total dose received between any two times t_1 and t_2 , one integrates f(t), so that:

$$D(t_1, t_2) = R_1 \int_{t_1}^{t_2} f(t)dt = R_1(F(t_2) - F(t_1)) \qquad (7\text{-}8)$$

F(t) is the indefinite integral of f(t) . For the case of the surface burst, $f_1(t)$ has been integrated numerically, and the resulting plot of $F_1(t)$ appears in Figure 7-6.

Surface burst on a Reactor

If a surface burst occurs sufficiently close to a reactor, radioactive materials from the reactor site may be entrained in the radioactive cloud of the weapon, where they will be mixed with the weapon debris and dust and return to the earth as fallout.

It is assumed that the fallout distribution is independent of the target, and so the fallout patterns will be essentially the same as those predicted in the first part of this chapter, although the dose-rates may be higher because of the added radioactivity

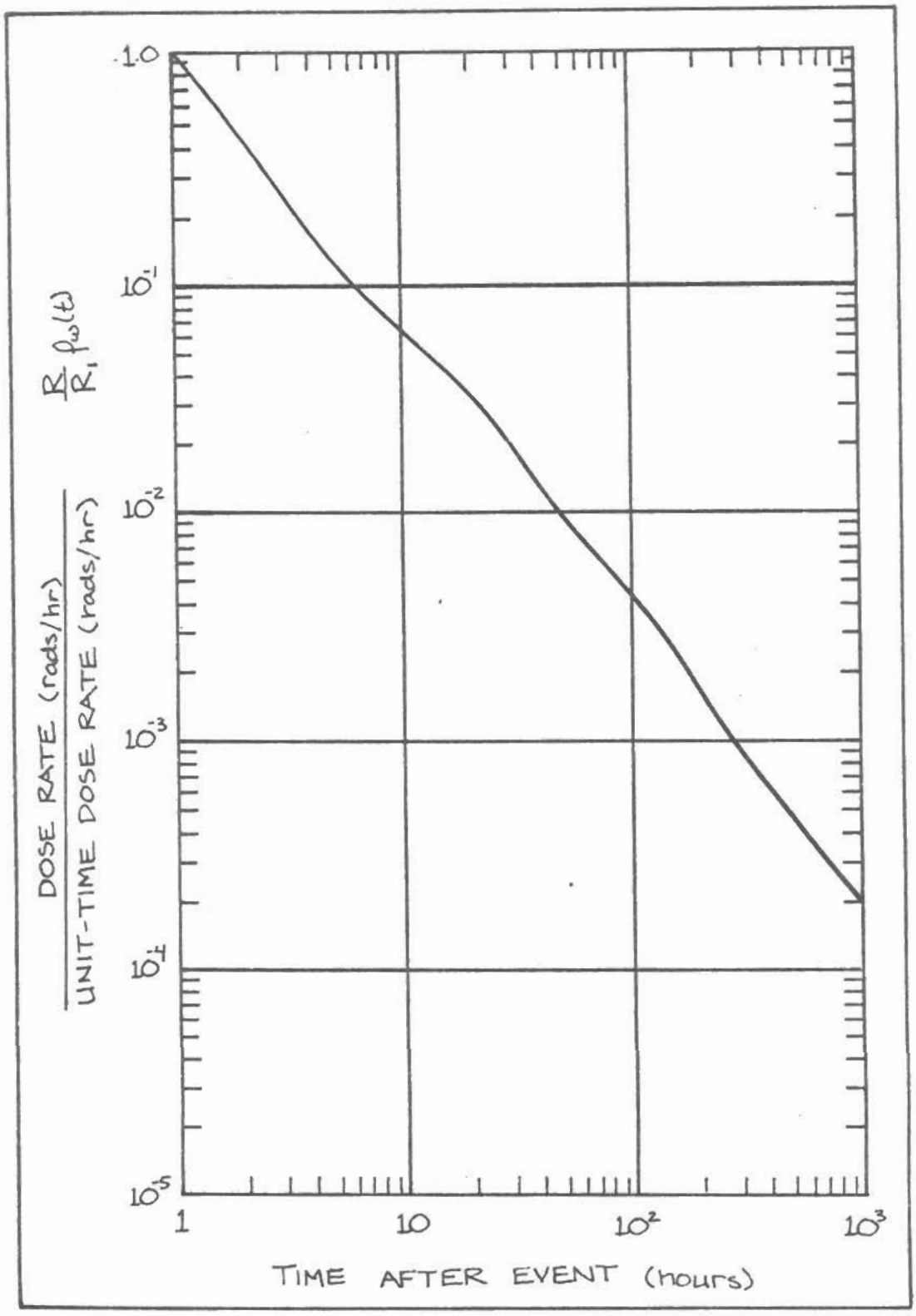

FIGURE 7-5a: The decay of the dose-rate with time of the debris of a surface burst, including the effects of weathering. At one hour, the total activity is 2.7×10^{11} curies.

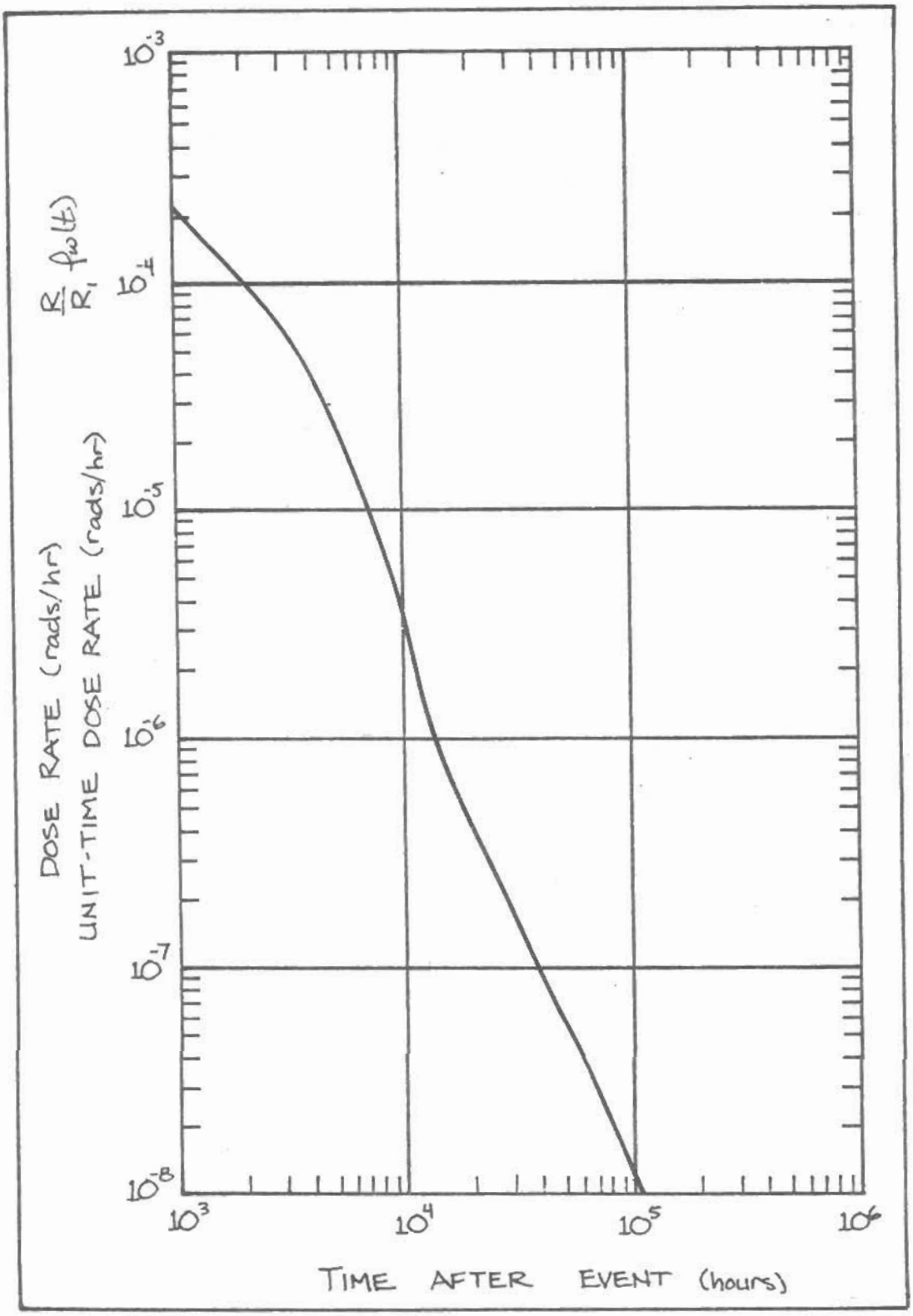

FIGURE 7-5b: The decay of the dose rate with time of the debris of a surface burst, including the effects of weathering. At one hour, the total activity is 2.7×10^{11} curies.

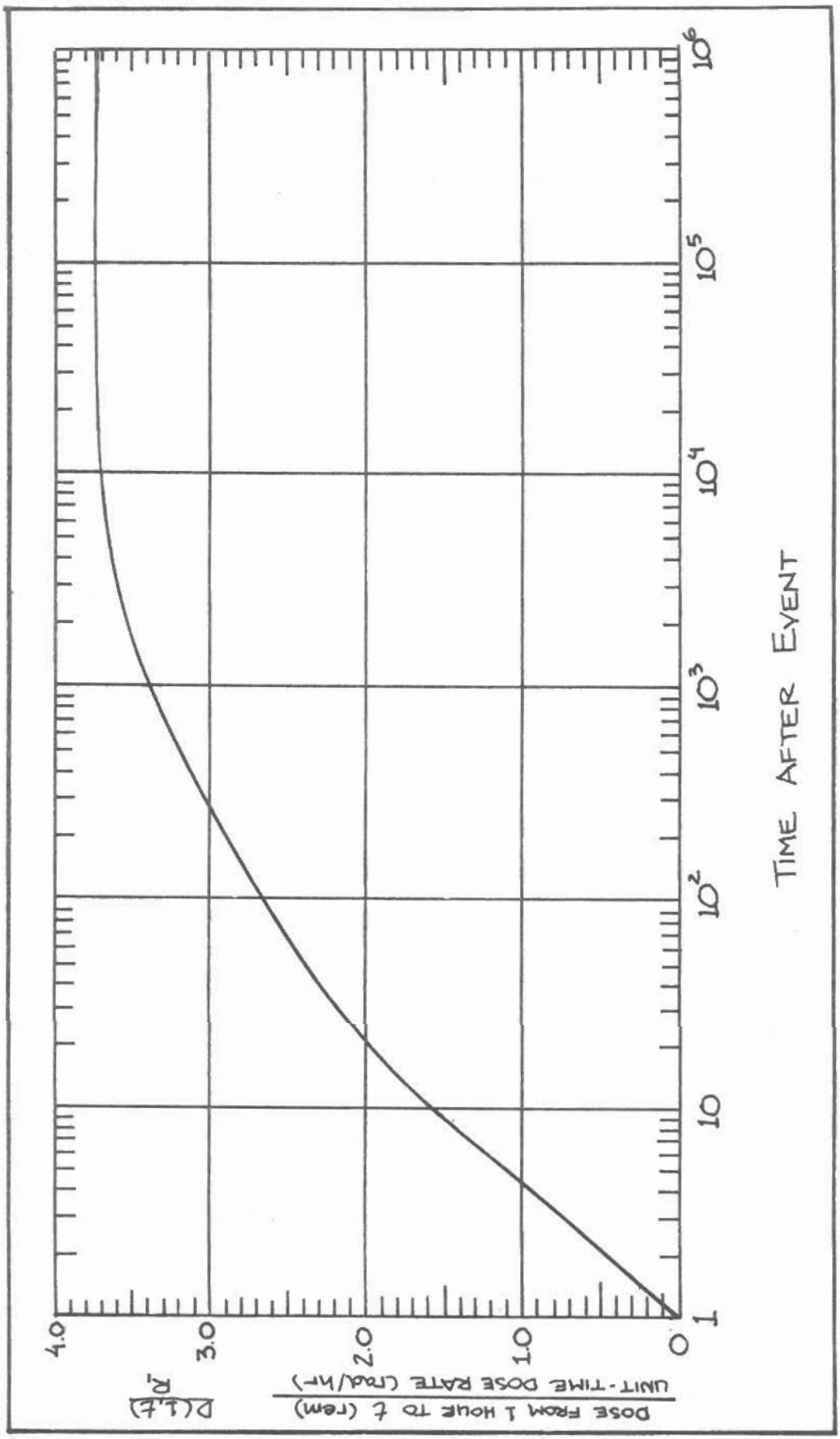

FIGURE 7-6: The integral of the function in Figures 7-5a and 7-5b from one hour to time t, $F_1(t)$.

from the reactor. After one hour, the debris from the detonation of a one-megaton weapon will have a total activity of about 2.7×10^{11} curies, while the entire reactor core has an activity of about 5×10^{9} curies, or over a factor of 50 lower.[7] For this reason the unit-time dose-rate (the dose-rate after one hour) predictions will differ very little in this case from the case of a surface burst alone.

There are two approaches used here to determine the decay function of the reactor core, $f_2(t)$. The easiest method utilizes the fact that the dose is approximately proportional to the amount of energy that is emitted, and therefore the dose-rate is proportional to the total power emitted by the core. This has been computed for various irradiation times, and times after irradiation, and these curves can be found in standard references.[8] When multiplied by $f_w(t)$, the result is $f_2(t)$; this is given in Figure 7-7, normalized to 1.0 at one hour.

Another method is to use equation 7-7, and with knowledge of the initial concentrations and decay constants of the various radionuclei, compute the radioactive decay. a_{o_i}, λ_i, and c_i where taken from the Reactor Safety Study.[9] The results are shown in Figure 7-7.

The two curves obtained in this way match fairly well, and are always within a factor of two of each other. The $f_2(t)$ used in this study is the average of these two functions, which is also displayed in Figure 7-7.

$F_2(t)$ has been obtained by integrating the average decay function, and this is plotted in Figure 7-8.

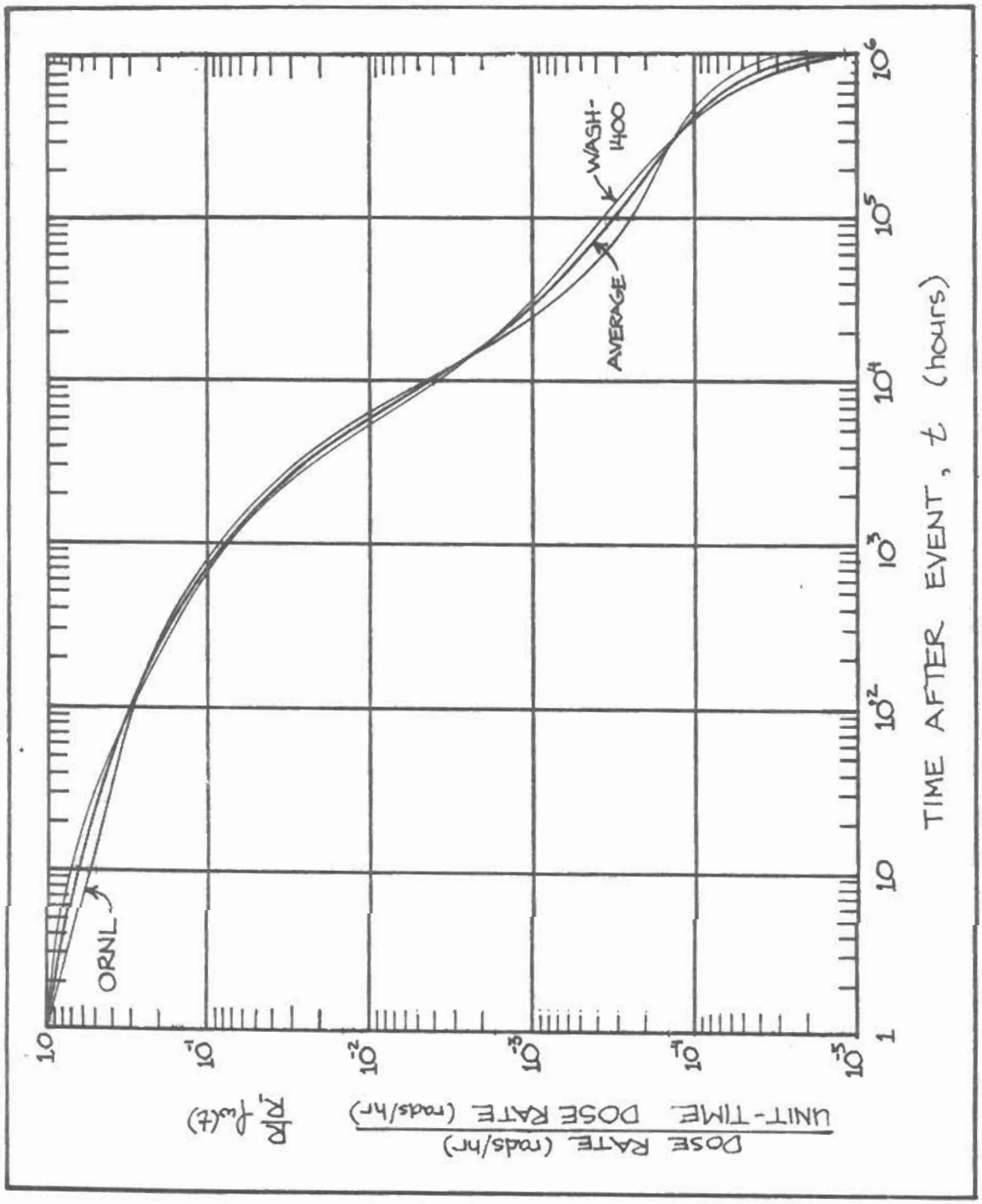

FIGURE 7-7: The decay of the dose rate with time of the three-region core of a one gigawatt (electric) nuclear reactor, as given by equation 7-7 (WASH-1400), and by the decay heat of the fission products (ORNL). Includes weathering.

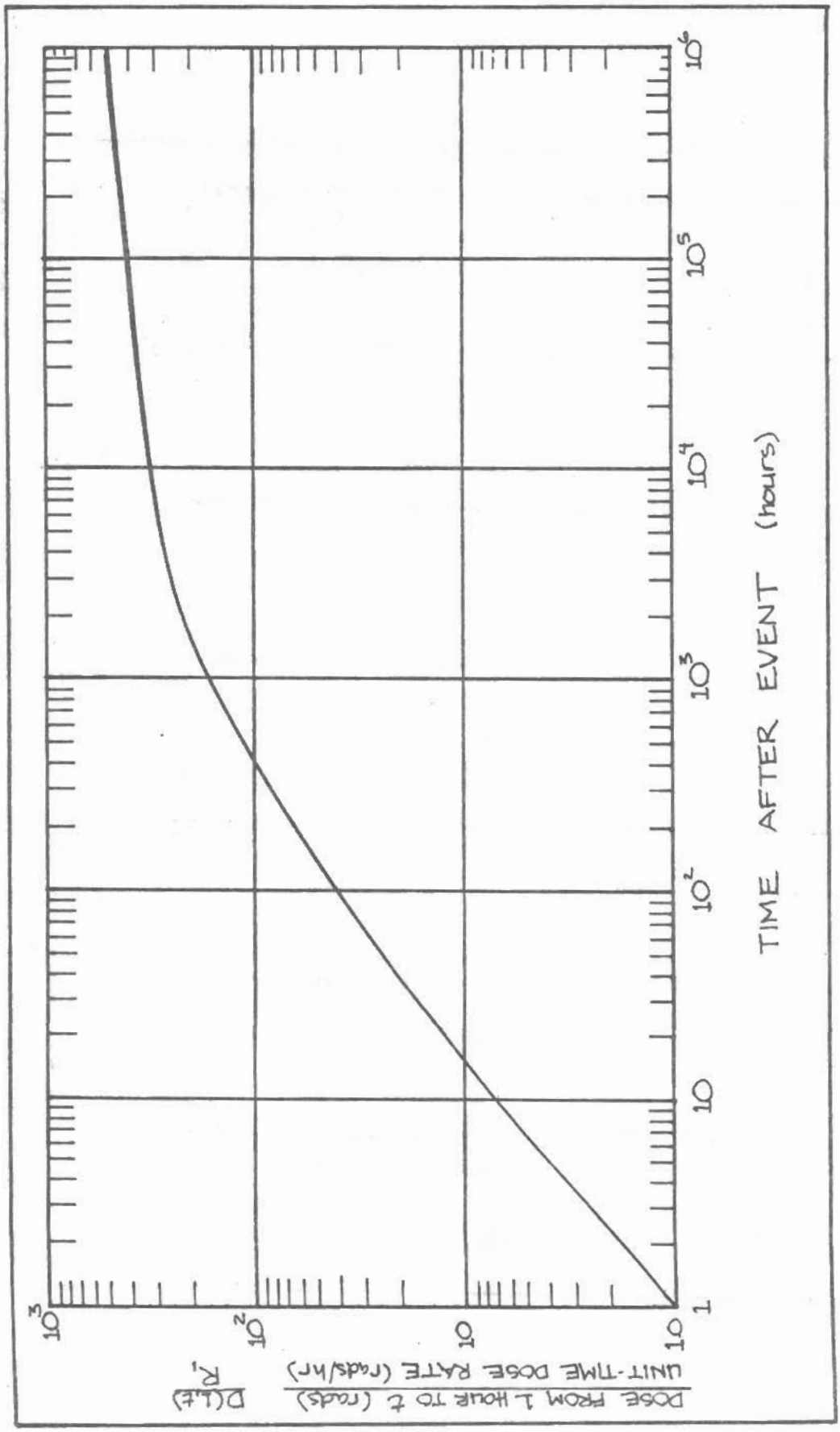

FIGURE 7-8: The integral of the (average) fuction in Figure 7-7 from one hour to time t, $F_2(t)$.

Spent Fuel

The containers which hold the spent fuel of the reactor are located close to the reactor site, and it is quite probable that if the reactor core is entrained in the cloud, that the spent fuel be also.

One-third of the reactor core is removed every year and replaced, and this spent fuel is stored in a concrete pool until the fuel decays to the point to which it can be reprocessed. The only difference between the decay function of the spent fuel and the reactor core is that the spent fuel has been irradiated for a full three years, while the three regions of the core have only been irradiated for 230, 470, and 700 days, respectively, at the time of the assumed attack. If t is the time after the event, and t' is the time the spent fuel has been stored in the pool, then $f_3(t+t')$ is the decay function of the spent fuel for the event.

At the present time, spent fuel pools only contain one-third of a core at a time, but this might quickly change if there continues to be little or no reprocessing in the United States. Plans are now being made to increase the capacity of present on-site storage to seven-thirds of a core of spent fuel in normal operation.

The decay function and the integrated function are shown in Figures 7-9 and 7-10.

Volatile Fission Product Release

There is a range in which a nuclear weapon will not entrain the reactor core in its radioactive cloud, but will devastate the

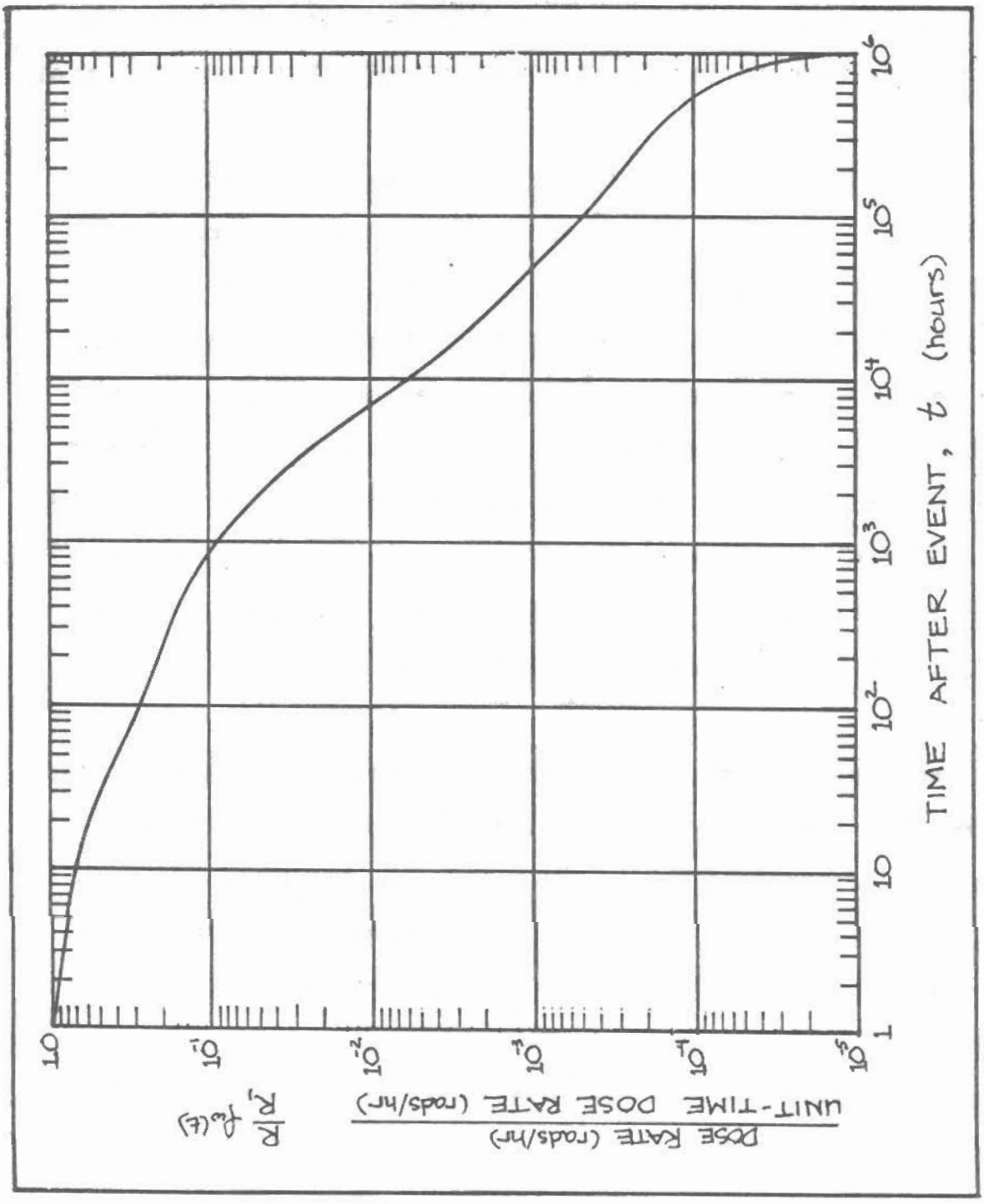

FIGURE 7-9: The decay function of the spent fuel with the time after irradiation, as given by the average of equation 7-7 and the decay heat of the fission products. The effects of weathering are included.

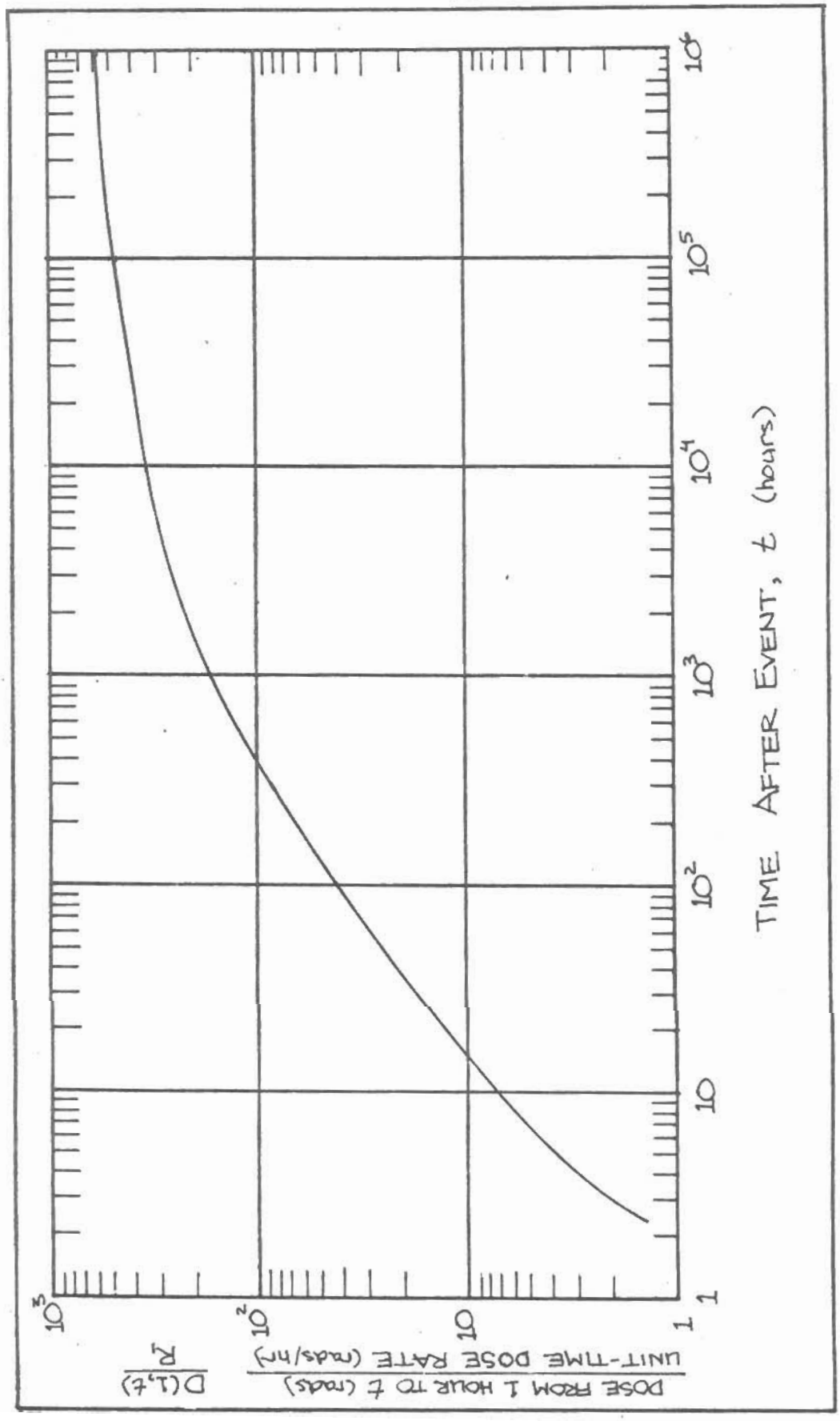

FIGURE 7-10: The integral of the function in Figure 7-9 from one hour to time t, $F_3(t)$.

reactor to such an extent that the volatile fission products will escape the reactor within minutes and rise into the radioactive cloud. These low-melting-point substances include iodine, cesium, tellurium and rubidium. The total decay function of these elements has been computed using equation 7-7, and the results appear in Figure 7-11. The integrated decay function, $F_4(t)$, appears in Figure 7-12.

Summary

The total decay functions for the following events are given by:

Surface burst: $f(t) = f_1(t)$

Surface burst on a reactor plus 1/3 core spent fuel: $f(t) = f_1(t) + f_2(t)/57 + f_3(t+4380)/172$

Surface burst on a reactor plus 7/3 core spent fuel: $f(t) = f_1(t) + f_2(t)/57 + \sum_{n=0}^{\infty} f_3(t+4380+8760n)/172$

Surface burst plus reactor volatiles: $f(t) = f_1(t) + f_4(t)/310$

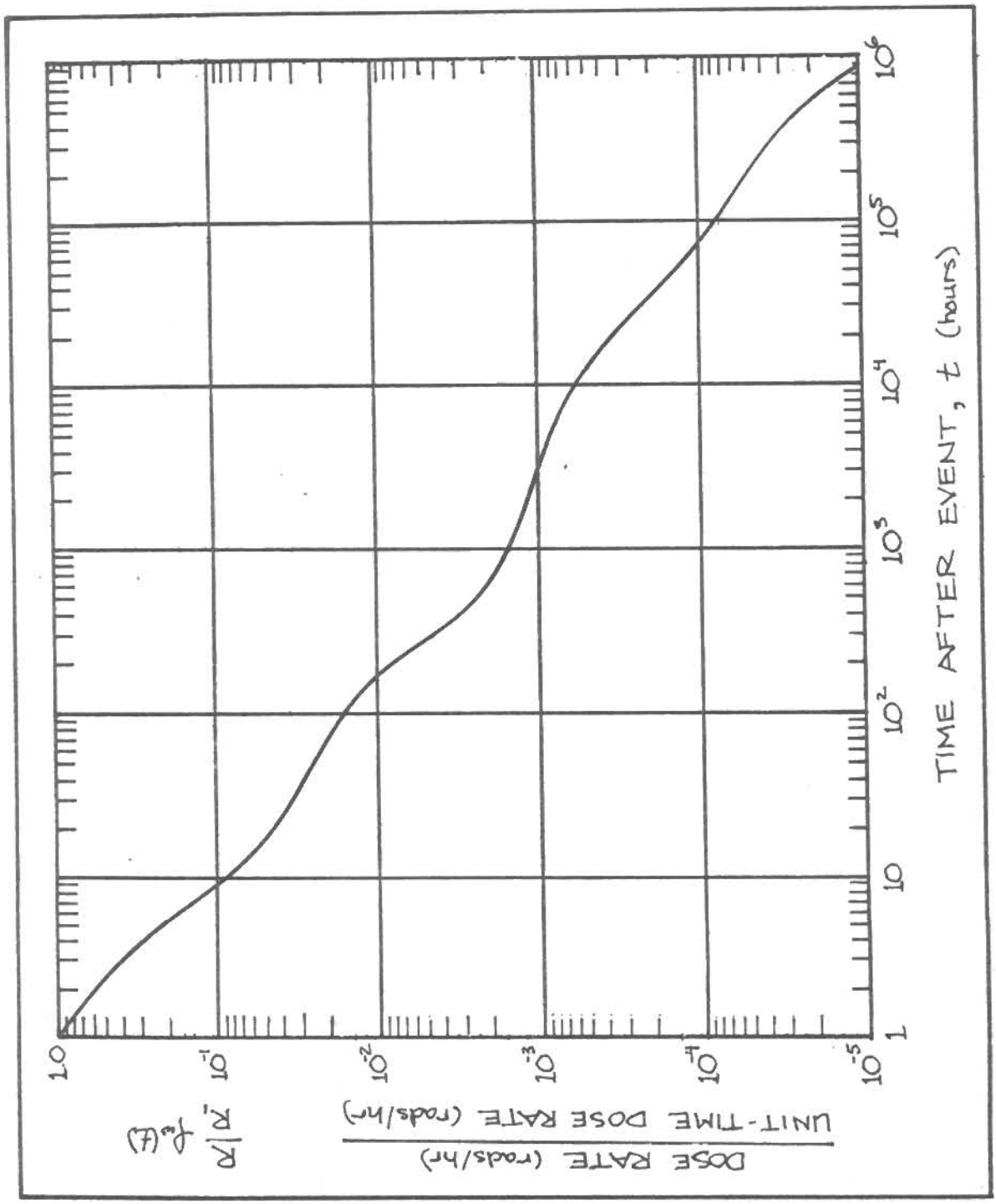

FIGURE 7-11: The decay of the dose rate with time as given by equation 7-7, for the volatile fission products in the reactor core. Weathering included.

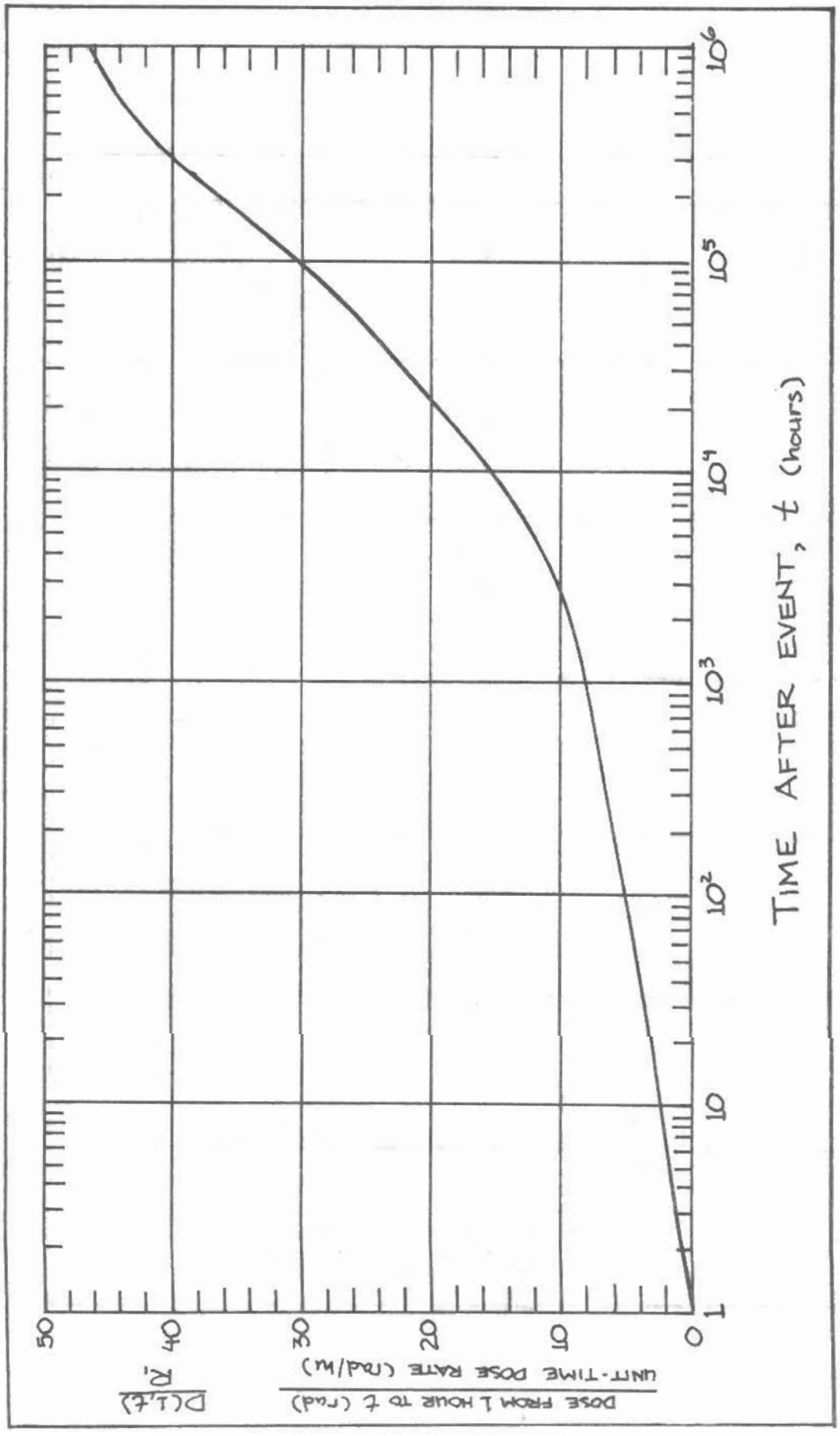

FIGURE 7-12: The integral of the function in Figure 7-11 from one hour to time t, $F_4(t)$.

Damage from Fallout

The most obvious measure of the damage caused by fallout is the number of people that would die from fallout in the first few days. This corresponds to the "lethal area", and it is assumed here that a population receiving over 400 rem in 96 hours will have no survivors. If $f(t)$ is the decay function for the event, then the lethal area will be defined by an $R_1(r)$ such that:

$$R_1(r) = \frac{400}{(F(96) - F(t_1))} \qquad (7\text{-}9)$$

where t_1 is the time it takes for the radioactive cloud to reach the point r downwind. t_1 is given approximately by:

$$t_1 = \frac{r - r_a}{u} \qquad (7\text{-}10)$$

Here r_a is the cloud radius (6 miles for 1 MT), and u is the wind velocity.[10] Because there is no analytic expression for $R_1(r)$ Equation 7-9 must be solved numerically.

Another measure of the damage to the population is the number of people that will suffer immediate radiation sickness. If it is assumed that the entire population will suffer radiation sickness where the dose is greater than 50 rem, then the corresponding area can be found by replacing the 400 in Equation 7-9 with 50 and solving for $R_1(r)$.

Still another measure of damage is the amount of land which will remain uninhabitable after the attack, or the "land denial". In order to compute this we must assume that there exists some maximum tolerable dose of radiation, and any area which receives

a dose greater than this will be uninhabitable. Several time periods have been used to measure this dose in previous studies, the most popular being one week, one year, and thirty years.[7] In this study, one year has been chosen as the time period because a thirty year period is not sensitive to changes which we normally would consider were important, and one week would ignore the long term risk. One year is a good natural measure of the time one inhabits an area.

In a post-attack situation, even if only one weapon were detonated it is likely that the minimum dose that would be considered harmful is 2 rem/yr. This is over ten times the maximum EPA exposure to the general public and over twenty times the natural backround dose, but it is less than the five rem/yr that uranium mine workers are exposed to. On the other extreme, it is highly unlikely that survivors would inhabit areas receiving more than 500 rem/yr, because this would cause a great many deaths among the population. Unless driven by hunger, people would probably not enter areas receiving more than 50 rem/yr, because this would cause radiation sickness and reduce life span considerably. For these reasons, I have calculated the land denied to the surviving population, A_d , for many values of the maximum acceptable dose in one year, D_o : D_o = 2, 10, 50, 100, 500 rem/yr.

The land denial is therefore determined by the following equation:

$$R_1(A_d) = \frac{D_o}{(F(t+8760) - F(t))} \qquad (7-11)$$

Results of Land Damage Analysis

Using the results of this chapter, we can now calculate the lethal area, the area in which prompt radiation sickness occurs, and the land denial for various D_o . These quanities have been computed for the following events, and the results appear in Figures 7-13 through 7-17 :

1) Surface burst
2) Surface burst in which volatile fission products from reactor are entrained in the cloud.
3) Surface burst on reactor in which core and 1/3 core spent fuel are entrained in cloud.
4) Surface burst on reactor in which core and 7/3 core spent fuel are entrained in the cloud.

Notice first of all, in Figure 7-13, how the dose in the first 96 hours following the arrival of the fallout. The data fall into two categories: the surface burst alone and the surface burst plus the reactor's volatile fission products, and the surface burst plus the reactor core and varying amounts of spent fuel. The attack on the reactor, if it can entrain the reactor core in the radioactive cloud, can increase the lethal area by 70% , and increase the area receiving radiation sickness by 50%.

However, if the attack only results in the immediate release of volatile fission products, these areas will increase by a negligible amount. A single weapon successfully detonated on a nuclear reactor can kill as many people by delayed radiation as two weapons detonated on other targets.

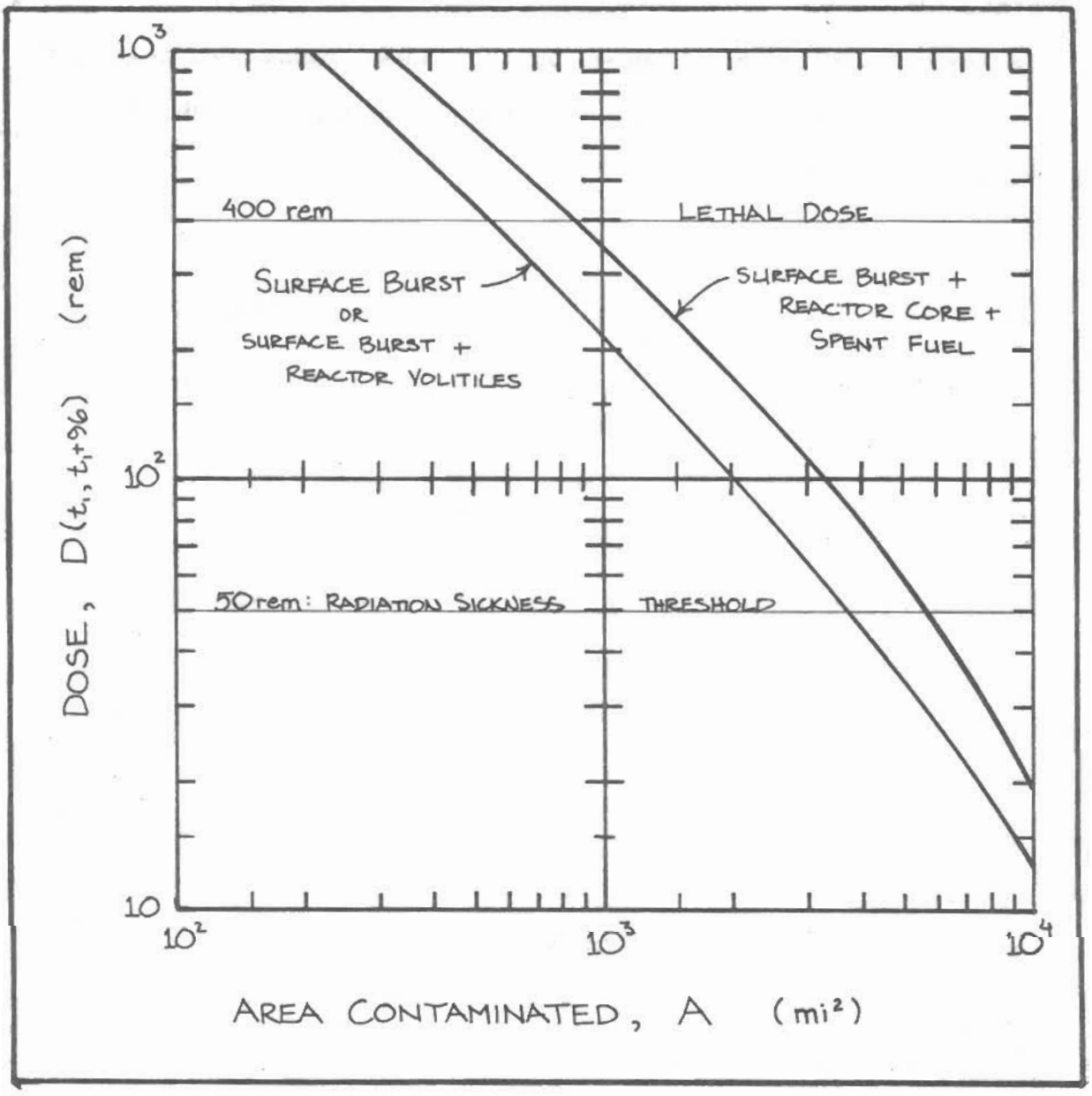

FIGURE 7-13: The area contaminated by a given dose in the first 96 hours following the event, for the cases examined here.

The results of the land denial analysis are more difficult to interpret, because they deal with a wide range of time perspectives and possible levels of damage to the surviving population. One method might be to simply compute the additional number of square miles that are rendered uninhabitable at a given time after the attack on the reactor. But even though 1,000 additional square miles of damage may seem significant, it more properly depends on what it is being compared to. For example, if only 20 square miles would have been uninhabitable if the reactor had not been attacked, then the additional 1,000 mi^2 will have a great impact; on the other hand, if 10,000 mi^2 would have been damaged anyway, then the additional damage is relatively unimportant. For these reasons, it is wise to also consider the factor by which the damage is increased.

Another measure of the damage from enhanced fallout is the total integrated land denial, from 100 hours to 10^6 hours. This is plotted in Figure 7-18 as a function of the maximum permissible dose per year, D_o .

A brief inspection of these figures shows that the attack can add tremendously to the long-term damage inflicted by a nuclear weapon, but only if the weapon is delivered accurately enough to entrain the reactor core in the radioactive cloud of the weapon. In this case, the damage is at least tripled, and renders many thousands of additional square miles uninhabitable. If the economic and social consequences of this additional loss of land outweigh the damages inflicted by an attack on other targets, then we can conclude that the reactor is vulnerable to attack.

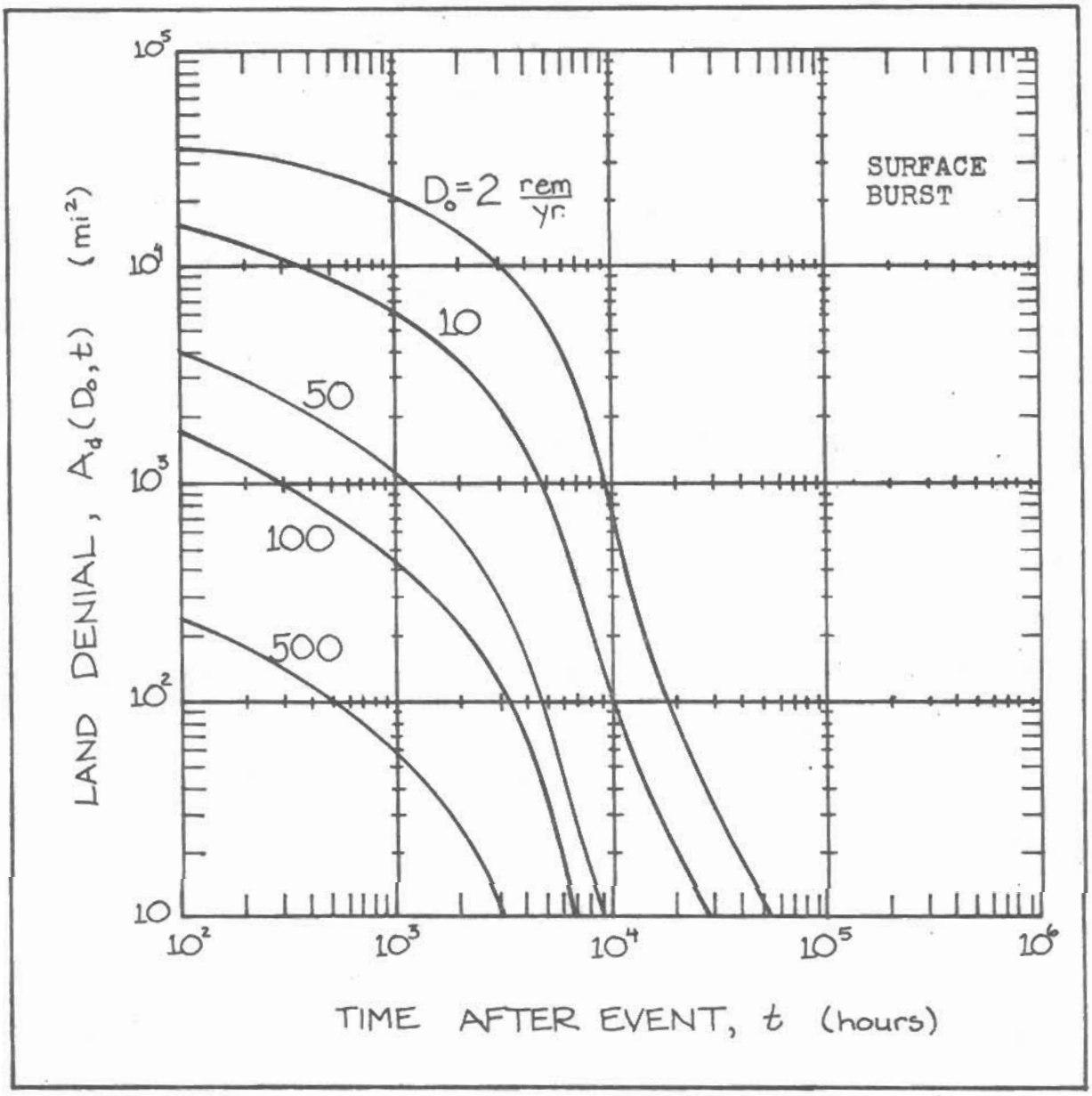

FIGURE 7-14: The land denial as a function of the time after the event for several values of the maximum acceptable dose, for a surface burst.

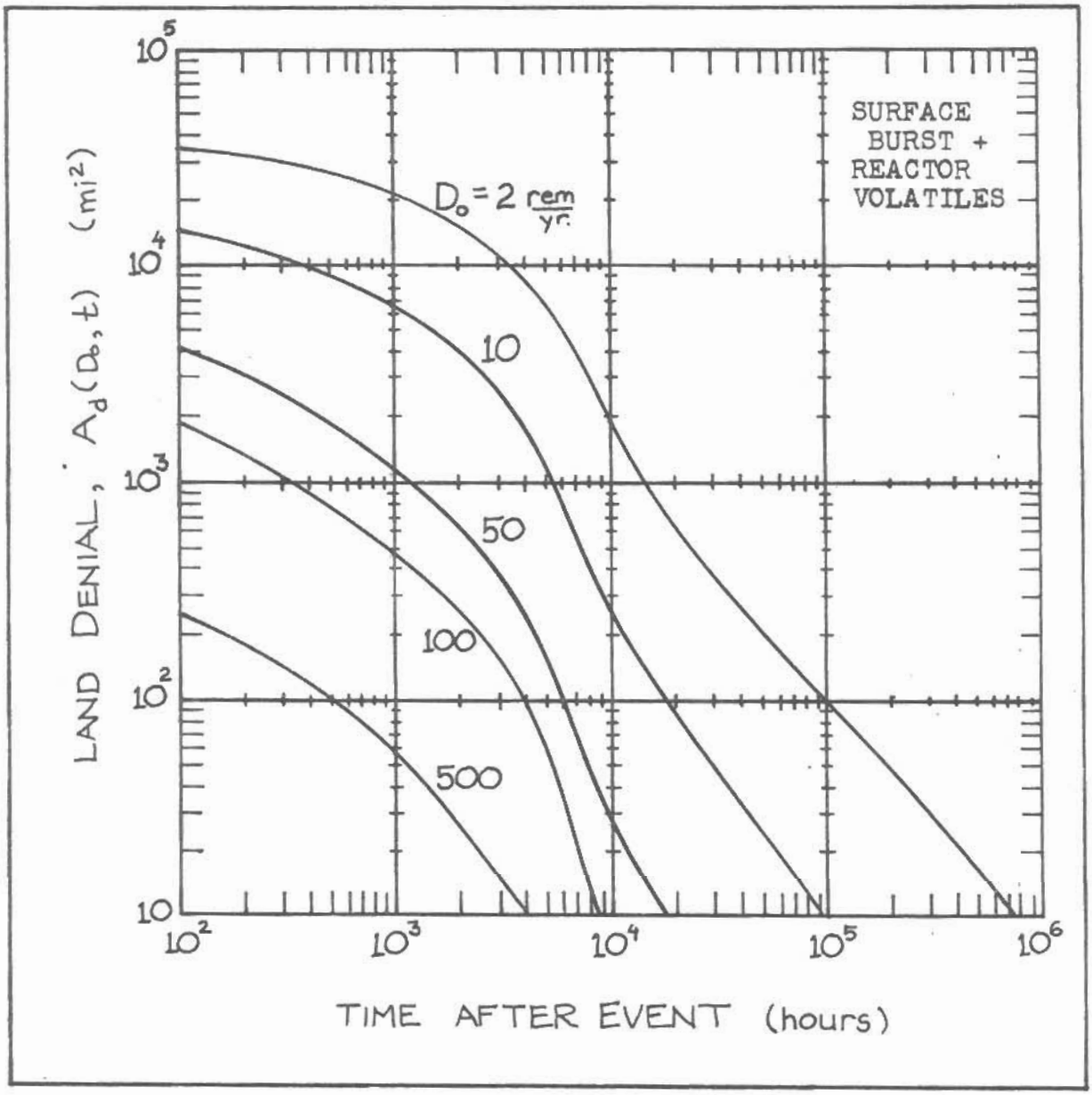

FIGURE 7-15: The land denial as a function of the time after the event for several values of the maximum acceptable dose, for a surface burst plus reactor volatiles.

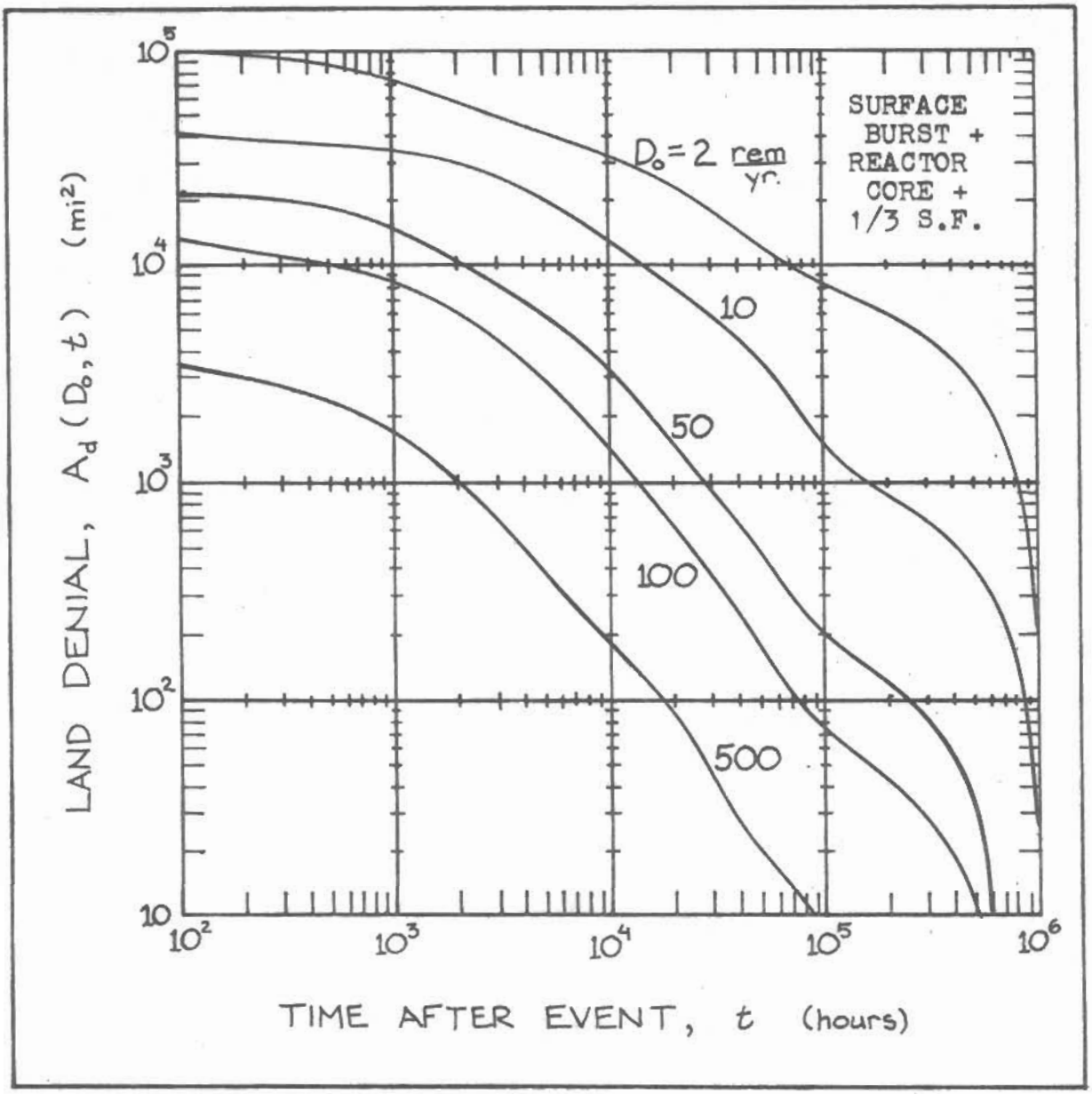

FIGURE 7-16: The land denial as a function of the time after the event for several values of the maximum acceptable dose, for a surface burst plus reactor core plus 1/3 core of spent fuel.

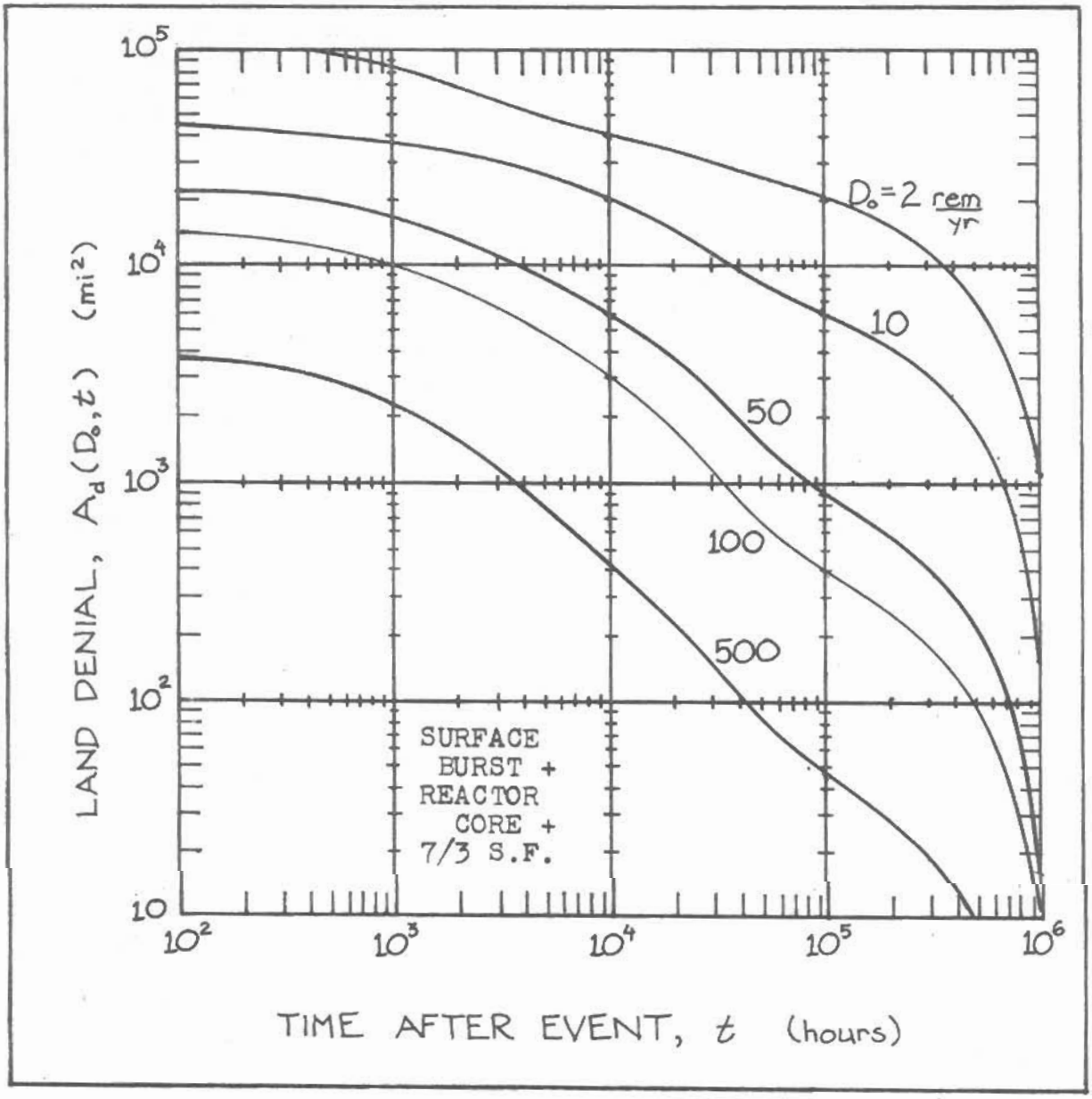

FIGURE 7-17: The land denial as a function of the time after the event for several values of the maximum acceptable dose, for a surface burst plus reactor core plus 7/3 core spent fuel.

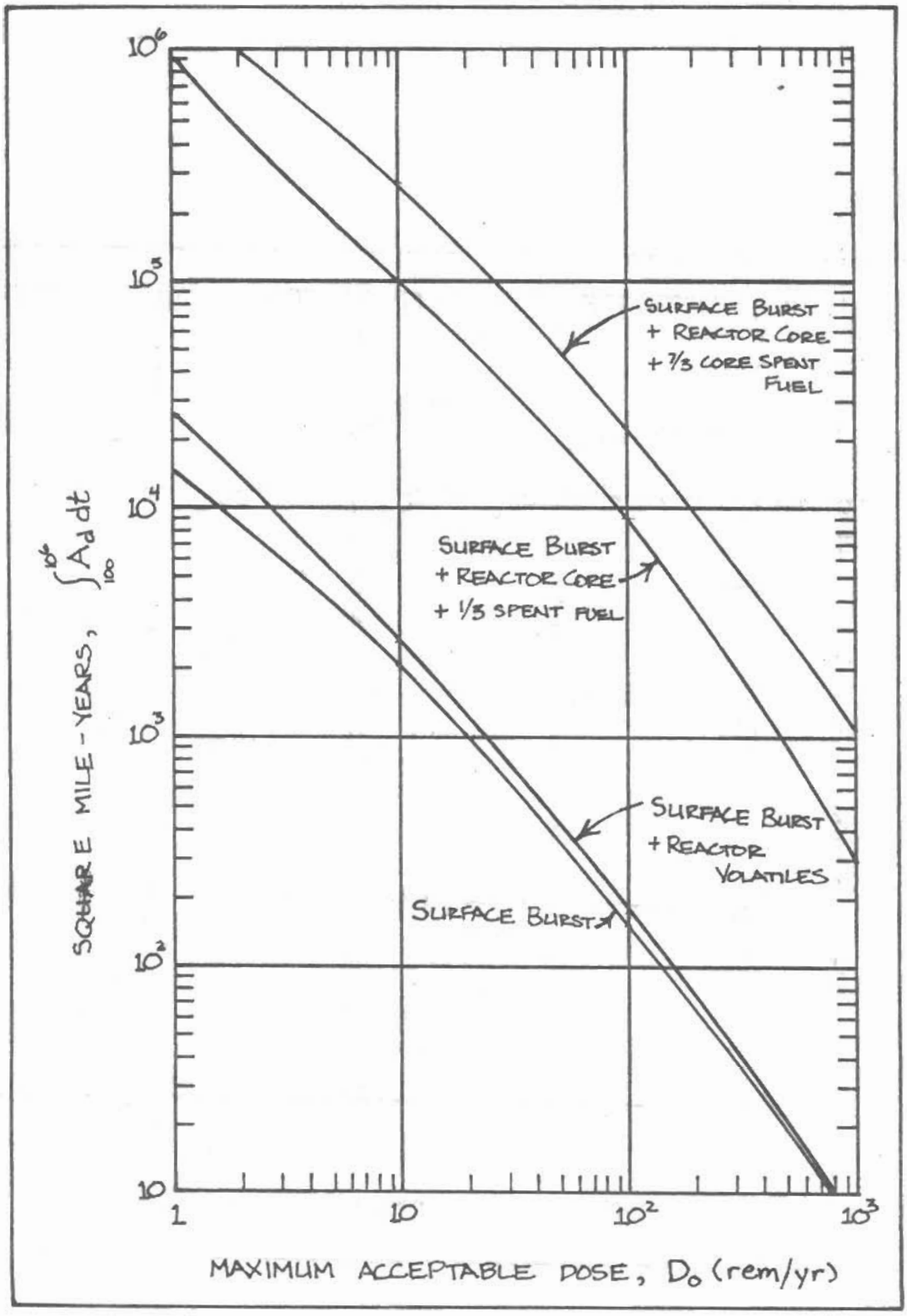

FIGURE 7-18: The integrated land denial as a function of the maximum acceptable dose for the events considered.

Contamination of Agricultural Products

Since one of the chief motives behind the desire of an attacker to contaminate widespread amounts of land is contamination of the food supply, it is necessary to estimate the amount of land whose produce will exceed a maximum allowable dose if ingested. Fortunately, most of these calculations have already been completed in connection with the Reactor Safety Study, and so I will simply apply these results to the cases considered here.

There are two ways in which foodstuffs can be pathways for the ingestion of contaminants. First, if a crop is being grown at the time of the attack, then contaminants will settle directly onto the plants, where some will remain until the plant is ingested. Secondly, if plants are grown on contaminated soil in subsequent seasons, the plants will absorb varying amounts of radionuclides from the soil through their roots. The first mode of exposure will be termed "direct deposition", and the second "root uptake"; because only a fraction of the contaminants in the soil are available for absorption, and because this fraction decreases with time, the dose by direct deposition represents a much greater health hazard than the dose by root uptake, if no steps to decontaminate the plants are taken. Also notice that in the case of direct deposition it is possible to wash off contaminants, but in the second case decontamination is not possible.

In general, the dose received from ingestion comes from two types of foods: those that were directly contaminated, then ingested, and those that come from animals who ate contaminated vegetation. Dairy products are the greatest food source which

falls into this second category.

Through a series of averaging techniques, the activity of ingested radionuclides has been correlated to the density of contaminants on the ground for these two types of foodstuffs. The conversion factor obtained in this way is called CF (curies/curie/meter^2), and this is shown in Table 7-3 for the most important contributing radionuclides.[11]

Also needed is the dose conversion factor from curies ingested to the whole body dose in rem, DC , and this is given in Table 7-4.[12] The total dose, D , from each radionuclide will then be the product of the density of the radionulide contamination, $d_1(r)$, CF_1 , and DC_1 . For the radionuclide mixture, the total dose will be the weighted sum of these products:

$$D = d(r)\sum_i a_i CF_i DC_i e^{-\lambda_i t} \quad \text{(rem)} \qquad (7\text{-}12)$$

where a_1 is the fraction of the ith nuclide in the mixture, and λ_1 describes any decay that takes place in the concentration with time (due to radioactive decay, weathering, etc.). The dose-rate after one hour from the reactor debris, R_{1r} , is:

$$R_{1r} = d(r)\sum_i a_i c_i \quad \text{(rem/hr)} \qquad (7\text{-}13)$$

where c_1 converts from curies/meter^2 to rem/hour.

But as mentioned earlier, the dose-rate caused by the weapon after one hour is much larger than the dose-rate caused by the reactor debris, and so to a very good approximation we may write:

$$D = R_1\left(\frac{R_{r1}}{R_1}\right)\sum_i CF_i DC_i e^{-\lambda_i t}/c_i \quad \text{(rem)} \qquad (7\text{-}14)$$

TABLE 7-3

Radionuclide	direct deposition via milk	direct deposition via other	root uptake via milk	root uptake via other
Sr-89	.402	.397	.00682	.0136
Sr-90	.588	.505	.669	1.34
Cs-134	4.22	8.44	.0547	.164
Cs-136	1.42	2.84	---	---
Cs-137	4.22	8.44	.0835	.251

The conversion factor CF (curies/curie/meter^2) for the dose from ingested radionuclides from contaminated vegatation.

TABLE 7-4

Radionuclide	DC (rem/curie ingested)
Sr-89	1910
Sr-90	6110
Cs-134	21200
Cs-136	8960
Cs-137	6080

The dose in the first year per curie of radionuclide ingested.

where (R_{1_r}/R_1) represents the ratio of the dose-rate received from the reactor debris to the dose-rate received from the weapon debris after one hour. If the maximum acceptable dose is D_o, then Equation 7-14 specifies an area which is defined by R_1:

$$R_1 = \frac{(R_1/R_{1r})\, D_o}{\sum_i CF_i DC_i e^{-\lambda_i t}/C_i} \quad \text{for an attack on a reactor} \qquad (7\text{-}15)$$

From this information we can also estimate the damage to farm produce from a surface burst alone. One kiloton of fission energy represents the fission of 1.45×10^{23} nuclei; in a one-megaton weapon which derives 50% of its energy from fission, 7.25×10^{25} fissions will take place. For every fission, about 0.035 atoms of Sr-90 will be formed and 0.055 atoms of Cs-137.[13] A one-megaton weapon therfore yields about 2.5×10^{24} atoms of Sr-90 and 4×10^{24} atoms of Cs-137.

At the time of the attack, the reactor will have produced 3.7×10^6 curies of Sr-90, and 4.7×10^6 curies of Cs-137.[14] If we simply multiply these amounts by the defintion of the curie (3.7×10^{10} disintegrations/second), and multiply by the half-life of these atoms, then we have the total number of atoms produced: 1.3×10^{26} atoms of Sr-90 and 1.7×10^{26} atoms of Cs-137. Just as the weapon is much more active initially, and the reactor debris can be neglected, so the reactor is much more rich in long-lived products, and the long-term contribution to the dose by the weapon can be neglected. This justifies using Equation 7-14.

Because the weapon contributes only about 1/50th of the Sr and Cs that the reactor contributes, the dose received from plants

contaminated by weapon fallout alone will be about 1/50th as great as indicated by Equation 7-15. Therefore:

$$50\left[R_1(r)\right]_{\substack{\text{weapon}\\\text{alone}}} = \left[R_1(r)\right]_{\substack{\text{weapon +}\\\text{reactor core}}}$$

By combining this information we can predict the unit-time dose-rate that will result in a dose D_o if the plants are eaten or used for grazing. This unit-time dose-rate then defines an area where the dose-rate exceeds D_o. Note that the dose from direct deposition can only take place in the first growing season, and the dose from root uptake, though much smaller, only takes place in subsequent seasons.

Figures 7-19, 20, & 21 predict the areas that will suffer damage from direct contamination. Figure 7-19 shows the areas that are damaged if the entire land area downwind is either all general purpose farmland or all dairy farmland, and no decontamination is attempted. Notice that an attack on a reactor results in a tremendous crop loss relative to a surface burst on another target. Decontamination of the crops by washing is possible at least in principle, and it appears that a decontamination factor of about 50 is possible after a thorough washing. Figure 7-20 shows the areas that yield unacceptable produce after decontamination.

It is very unlikely that the entire downwind area will be homogeneous farmland. Averages of land uses in the Eastern U.S. indicate that roughly ½ of all land is farmland, and that 1/3 of this is used for dairies.[15]

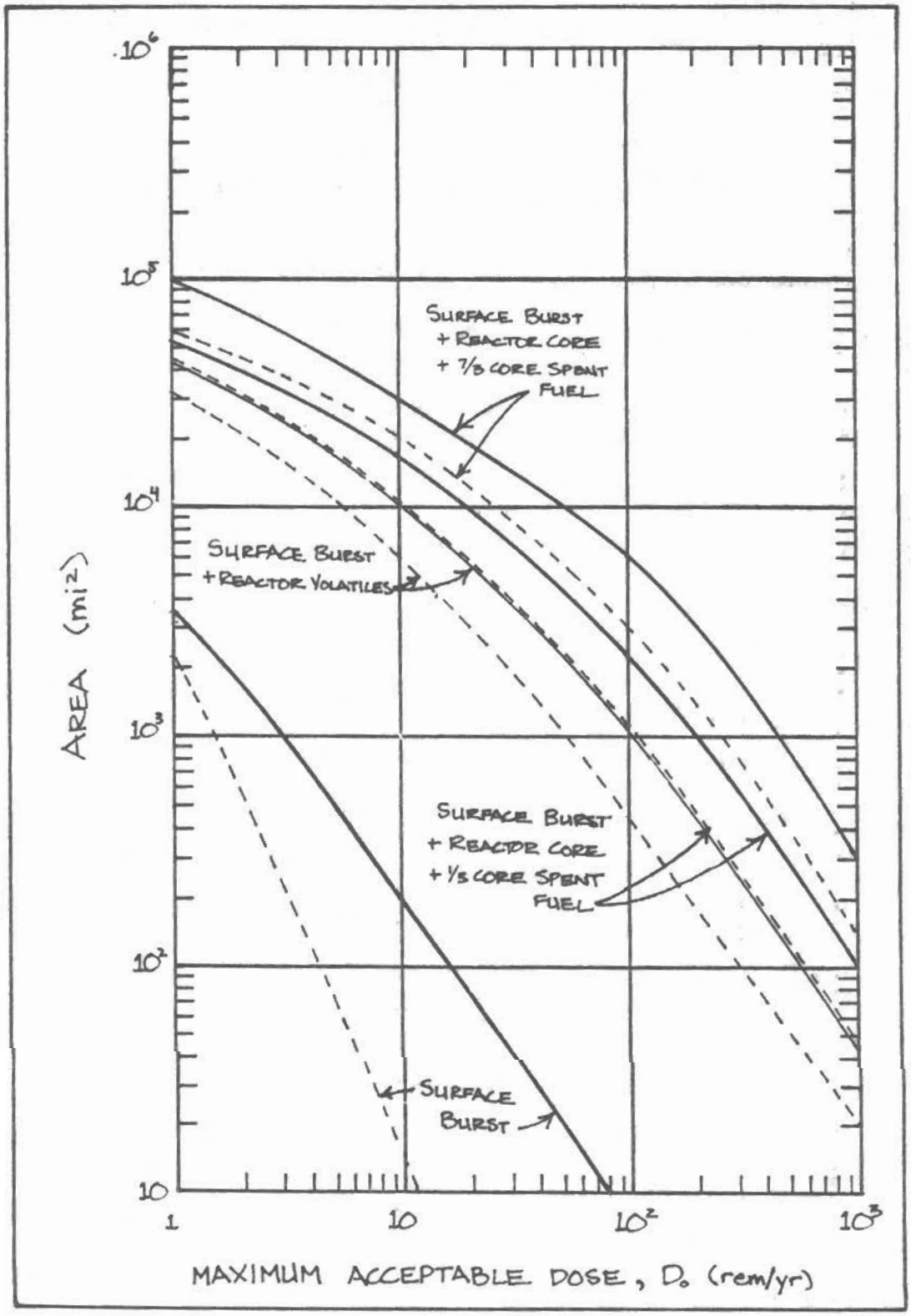

FIGURE 7-19: The area of agricultural land whose produce will produce a whole body dose greater than D_0 if eaten at normal rates. Solid lines refer to general purpose farmland; dashed lines to dairy farmland.

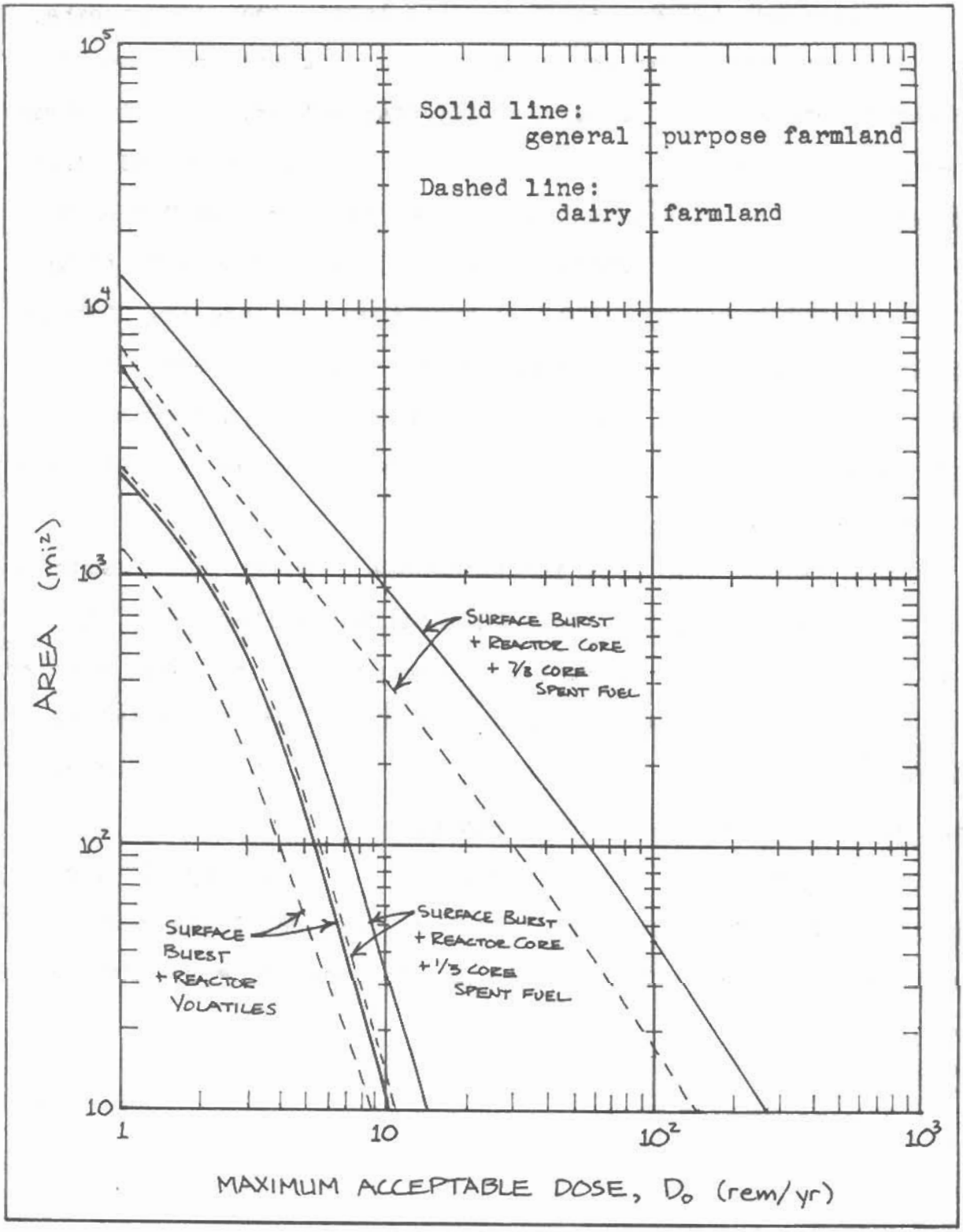

FIGURE 20: The area of agricultural land whose produce will result in a whole body dose greater than D_o if eaten at normal rates, after the produce has been washed to reduce contaminants by a factor of 50.

Although these areas are quite large, they are somewhat less than the areas that would have to be evacuate because of a greater dose received from ground contamination. Only in three cases, for the release of reactor volatiles onto dairy and mixed farmland, and the entrainment of the reactor core and 7/3 core spent fuel onto mixed farmland, would a person be able to return to the land to harvest a crop and live there henceforth, without receiving a greater dose from ground contamination than from ingestion of the crop. But it would be possible, and in most cases necessary, to only remain in the contaminated area long enough to harvest the crop.

The dose received from ingesting plants grown on contaminated land in subsequent seasons is substantially less less than that received by direct contamination, although it is somewhat greater than the direct deposition dose if the plants are decontaminated. Figure 7-21 shows the time dependent behavior of the crop damage from root uptake for subsequent seasons.

In summary, an attack on a reactor can be a very effecient method of contaminating foodstuffs, and can result in crop dmages 50 - 500 times larger than in the case of weapon fallout alone.

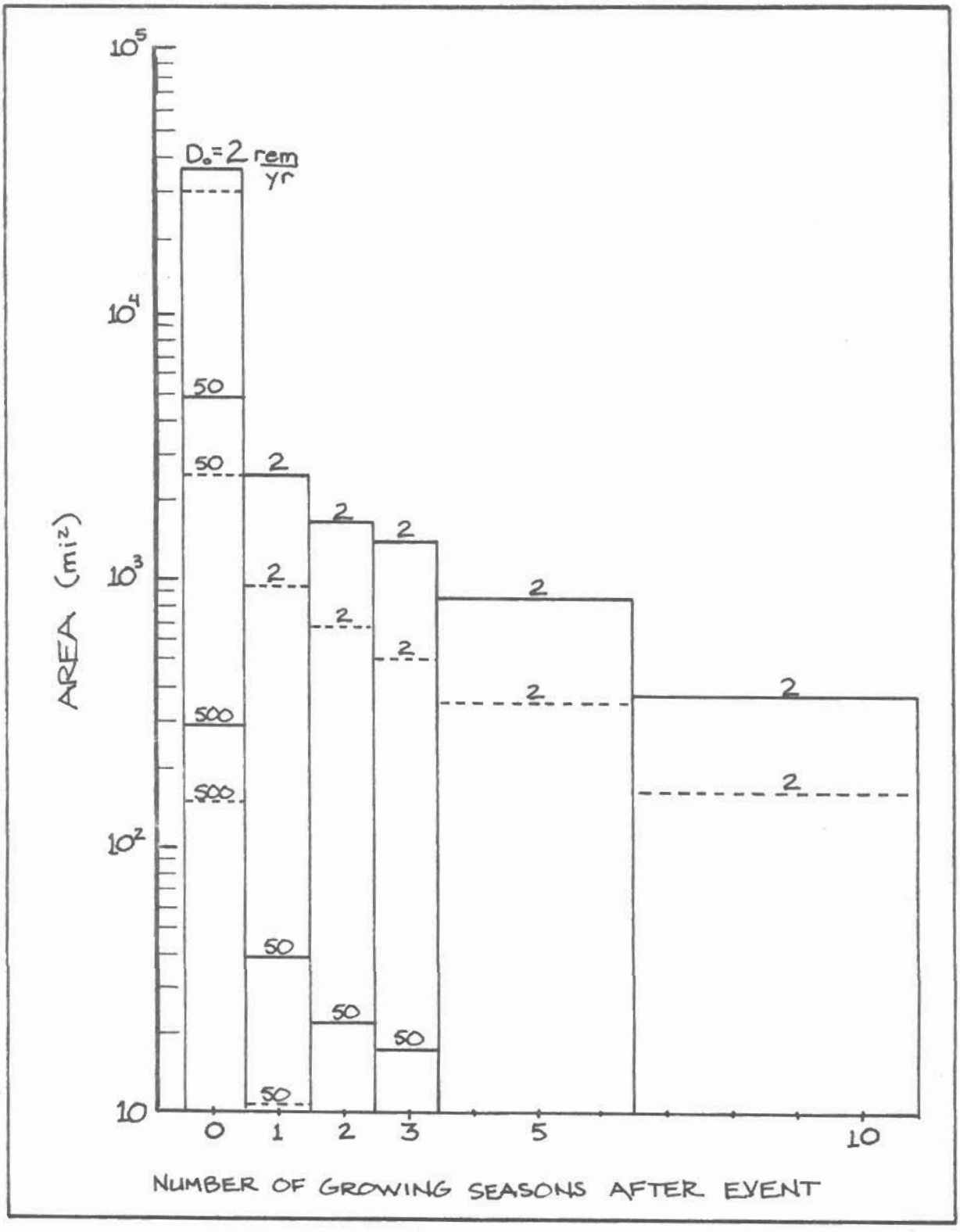

FIGURE 7-21: Agricultural land denial as a function of the growing season, for three values of D_o. Season "0" corresponds to food being grown at the time of the event.

CHAPTER 8

DAMAGE FROM A MELTDOWN

Another type of damage that can be inflicted by an attack on a nuclear reactor is the radiological contamination that results from the meltdown of the reactor core. As we have seen in the first section of this report, the detonation of a one-megaton weapon several miles from a reactor can damage safety systems, intake filters, outside power, and the containment structure itself, all of which can lead to a loss of coolant accident, with a release of radioactivity in about a half an hour. Indeed, if the weapon is detonated within 1½ miles of the reactor, the containment will be breached and radioactive aerosols from the reactor core will be released into the surrounding air. Because relatively little heat is released in this puff of radioactivity, the cloud will remain fairly close to the ground, and be carried along by the prevailing wind. As the cloud is carried downwind, people who are in its path may inhale the radioactive particles; they will also be exposed to contaminants that are deposited onto the ground as the cloud passes. If this radioactive release is capable of killing many people or contaminating a significant amount of land above that caused by the weapon alone, then an attacker may well choose the reactor as a target in war.

In order to predict the magnitude of the damage caused by a meltdown, I have chosen to adopt the same model used in the Reactor Safety Study.[1] As in the case of predicting contamination from weapon fallout, these models are highly idealized because of a lack of precise knowledge about the nature of the release and the atmospheric conditions at the time of the release. However,

these simple models are quite adequate for the comparisons made here, because any decision made by an attacker would be based on models very similar to those used here.

As the radionuclides escape the containment building and diffuse into the atmosphere, they form a plume which spreads in height and width as it travels downwind. If the rate of diffusion is uniform in all directions, then the plume will take the shape of a two-dimensional Gaussian distribution, which is illustrated schematically in Figure 8-1. If none of the material in the cloud is lost, deposited, or decays, then the concentration at any point downwind from the reactor is given by:

$$\chi = \frac{q}{\pi \sigma_y \sigma_z u} e^{\left[-\frac{y^2}{2\sigma_y^2} - \frac{z^2}{2\sigma_z^2}\right]} \qquad (8\text{-}1)$$

where X is the concentration (curies/meter^3), q is the source strength (curies/sec), u is the wind speed (meters/sec), z is the centerline height of the stabalized cloud (meters), and σ_y and σ_z are the standard deviations in the crosswind and vertical directions, and are both functions of the downwind distance, r.

As Figure 8-2 indicates, there are several ways in which a person who is immersed in this cloud can receive a dose of radiation. First, he may receive an external dose from the radionuclides in the surrounding air. Secondly, because the cloud itself remains very close to the ground, he may breathe in the radioactive contaminants. Thirdly, there is the dose which he will receive from the radionuclides which have been deposited onto the ground by the passing cloud. Associated with this mode of exposure is the dose from radionuclides that are resuspended in

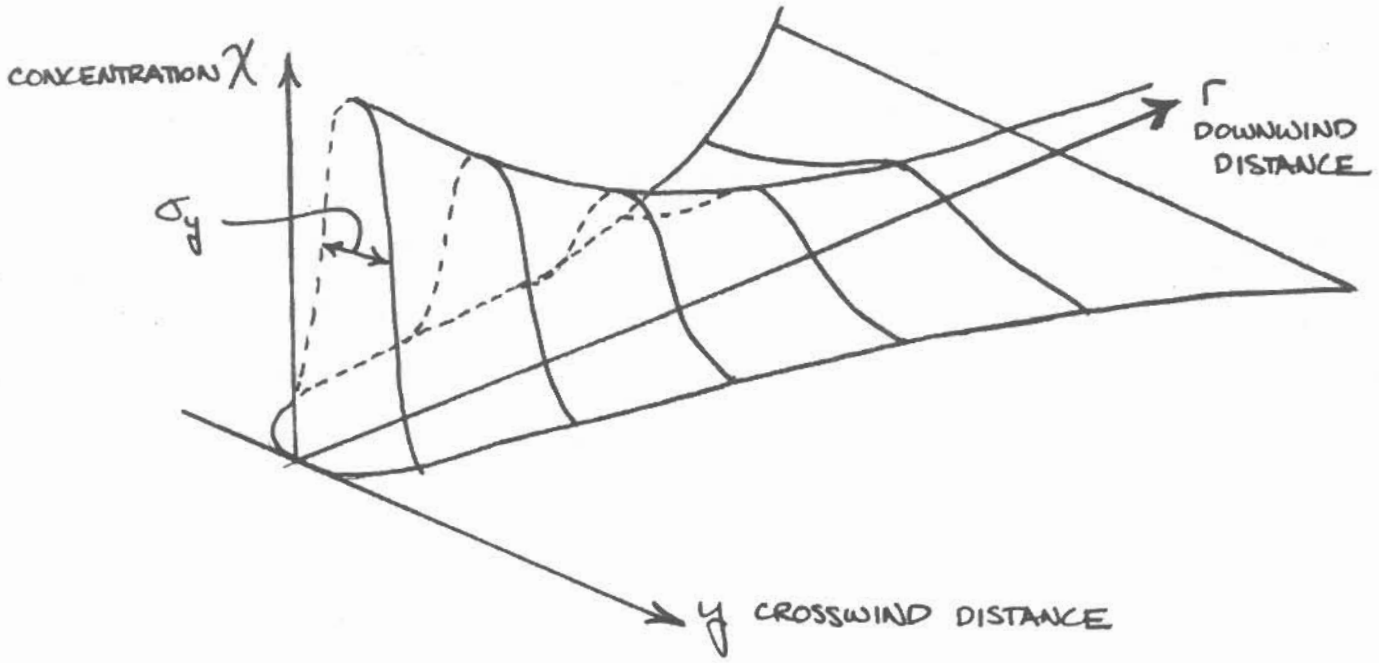

FIGURE 8-1: SCHEMATIC ILLUSTRATION OF THE VARIATION OF CONCENTRATION IN THE CROSSWIND DIRECTION.

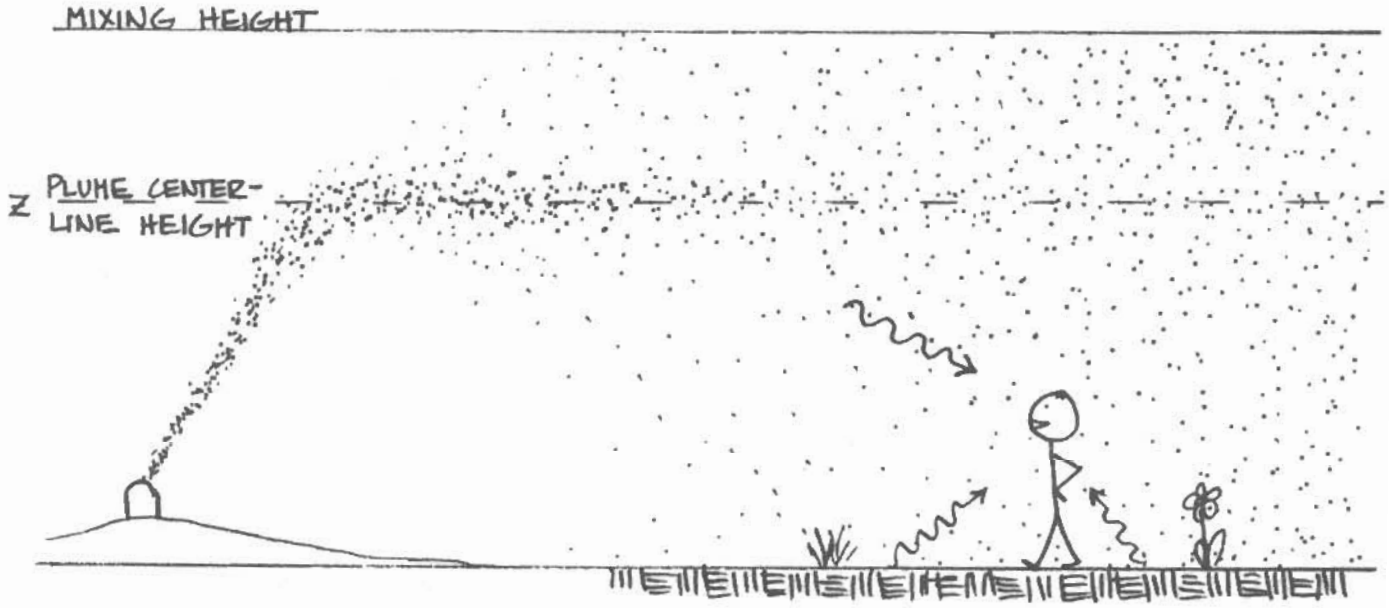

FIGURE 8-2: SCHEMATIC ILLUSTRATION OF THE VARIATION OF THE CONCENTRATION IN THE VERTICAL DIRECTION, AND DIFFERENT MODES OF EXPOSURE.

air and inhaled, and the dose from the ingestion of vegetation that has been contaminated. Notice that the first two modes of exposure can only occur when the cloud is still in flight; that is, during the first day, while the third mode of exposure continues for many years after the meltdown. Table $^{8-1}_{v}$ shows the relative importance of these modes of exposure in causing latent cancers.

It is apparent from Table $^{8-1}_{v}$ that the most important modes of exposure are the "total body" dose from radionuclides deposited onto the ground, and the dose to the lung from inhaled radionuclides. To simplify the analysis, only these two modes of exposure are considered here, and because of its similarity with the preceeding analysis of fallout contamination, the ground dose will be considered first.

In order to construct a realistic model of the deposition of contaminants onto the ground, we can define a deposition velocity, v_d , which describes the rate at which the radionuclides fall from the air onto the ground. If we multiply this deposition velocity by the concentration of contaminants directly above the ground, and by the total time it takes for the cloud to pass, then the result will be the density of contaminants on the ground, $d(r)$. But as it stands, the formula for the concentration in Equation $^{8-1}_{v}$ is not complete, because it does not take into account the depletion of the contaminants in the cloud as material is deposited onto the ground. In order to take this into account, Equation $^{8-1}_{v}$ must be multiplied by the following expression:

$$D(r) = \mathrm{EXP}\left[-\sqrt{\frac{2}{\pi}}\left(\frac{v_d}{u}\right)\int_0^r \frac{dr'}{\sigma_z(r')}\,\mathrm{EXP}\left[\frac{-z^2}{2\sigma_z(r')^2}\right]\right] \qquad (8-2)$$

Table 8-1

	Leukemia	Lung	Breast	Bone	GI tract	All Other	Whole Body
External cloud	0.2	0.5	0.5	0.1	0.1	0.3	3
Inhalation from cloud	0.5	59.0	10.0	0.2	1.0	0.2	15
External ground (<7 dys)	4.0	8.0	8.0	1.0	1.0	3.0	47
External ground (>7 dys)	2.0	2.0	6.0	1.0	1.0	2.0	30
Inhalation of resuspended contamination	0.1	3.0	0.1	0.1	0.1	0	2
Ingestion of contaminated foods	0.2	0.2	0.5	0.1	0.1	0.2	4
	7	66	16	2	3	6	100

The contribution of different modes of exposure to latent cancer fatalities. (Source: Reactor Safety Study, 13-24)

Then the density of contaminants at any point downwind will be given by:

$$d(r) = \frac{Q}{\pi \sigma_y \sigma_z} \left(\frac{U_d}{u}\right) D(r) \exp\left[-\frac{y^2}{2\sigma_y^2(r)} - \frac{z^2}{2\sigma_z^2(r)}\right] \qquad (8\text{-}3)$$

where Q is the total activity of the contaminants released (curies).

In order to evaluate this expression, we must experimentally determine the values of the deposition velocity, the centerline height of the cloud, and the relationships between the standard deviations and the downwind distance. Unfortunately, the data that exists is sparse and unconfirmed beyond a downwind distance of 20 kilometers, but in order to obtain meaningful results we must push these results into the range outside of their known validity.

Because there is relatively little heat released with the radioactive aerosols, the cloud remains close to the ground. The mean centerline height of the cloud is determined by the wind speed and by the heat released and the height of the mixing layer, and empirical relationships have been determined by several experimenters. For the heat heat releases considered here ($20\text{-}520 \times 10^6$ BTU/hr), and for normal wind speeds of 2 to 20 meters/second (5-45 mph), z ranges between 30 and 400 meters, with mean values of 50 to 250 meters.[2] z = 100 meters may be considered an acceptable average value for "typical" atmospheric conditions.

Values given in references for the deposition velocity vary greatly, ranging from 0.001 to 0.1 meters/sec, although 0.01 meters/sec. is generally believed to represent a "typical" situation.[3]

σ_y and σ_z have been determined for observations of plumes

for downwind distances less than ten kilometers. Table 8-2 shows some of the formulas which have been recommended in the Reactor Safety Study, for various atmospheric conditions.[4] Stability category A is the most unstable and F is the most stable; category D corresponds to the weather conditions which are most often encountered, and so this category will be taken to represent "typical" conditions.

Using these values, Equation 8-3 has been solved, and the results appear in Figure 8-3. These calculations are for points that are directly downwind for the reactor, that is, $y = 0$. Notice that for large distances, the results for a "typical" situation approach the realistic upper limit for the weather conditions. This is because when the deposition velocity is greater, the contaminants are deposited near the reactor site, and the concentration in the cloud is quickly depleted. On the other hand, if the deposition velocity is much less than the typical value, the contaminants will be deposited at a very slow rate, and the density will only exceed that given for "typical" values when the cloud is very dilute. In order to obtain the total density it is necessary to multiply the values given by Figure 8-3 by the total amount of material emitted, Q.

A systematic search of all possible values of the variables σ_y, σ_z, z, and (v_d/u) which are physically consistent has been conducted, and it has been found that the maximum upper limits are within a factor of two of the "typical" values given in Figure for $r \lesssim 15$ km.

Just as in the case of fallout prediction, one must know

TABLE 8-2

Stability Category	% Occurrence*	σ_y	σ_z
A	4%	$0.366\ r^{0.9031}$	$0.00024r^{2.09} - 9.6$
B	5%	$0.2751r^{0.9031}$	$0.055r^{1.098} + 2.0$
C	2%	$0.2089r^{0.9031}$	$0.113r^{0.911}$
D	39%	$0.1471r^{0.9031}$	$1.26r^{0.516} - 13$
E	32%	$0.1046r^{0.9031}$	$6.73r^{0.305} - 34$
F	18%	$0.0722r^{0.9031}$	$18.05r^{0.18} - 48.6$

The standard deviations in the crosswind and vertical directions as a function of r and the stability category.

*Atlantic coastal site.

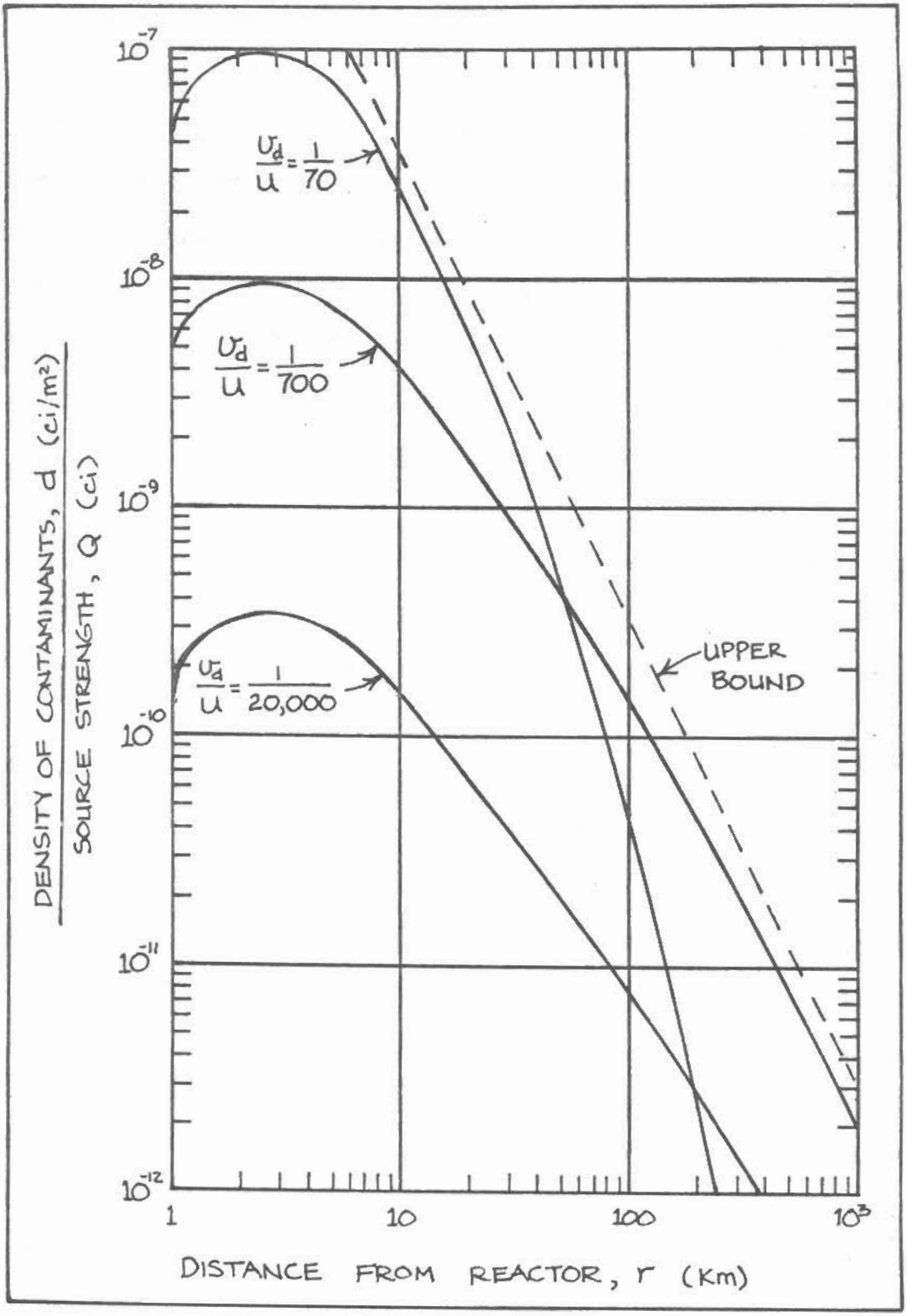

FIGURE 8-3: The density of the deposited contaminants as a function of distance for three values of (v_d/u), for stability category "D", and for a plume centerline height of 100 meters.

the decay function of the radionuclide mixture in order to predict the dose in a given amount of time. If it is assumed that a meltdown resulting from an attack will not be fundamentally different from that resulting from a reactor accident, then we can use the data given in the Reactor Safety Study for predicting the amounts of escaped radionuclides.[5] A list of the important radionuclides emitted in determining the ground dose is given in Table 8-3. The decay function is given by:

$$f(t) = f_w(t) \sum_{i=1}^{N} a_i c_i e^{-\lambda_i t} \qquad (8\text{-}4)$$

where $f_w(t)$ is given by Equation 7-6, a_1 is the proportion of the ith nuclide in the total mixture, and c_1 is a constant for each radionuclide which converts the activity into a dose-rate in rem/hour.[6] f(t) is plotted in Figure 8-4.

To convert this decay function into the dose that a person receives in a given time interval, it is necessary to integrate f(t) between the two times of interest. Figure 8-5 shows the integral of f(t) between one hour and t, F(1,t). To obtain the dose between times t_1 and t_2, take the difference $F(1,t_2) - F(1,t_1)$.

Just as in the case of estimating the damage done by fallout, I have computed the dose received in the first 96 hours after the arival of the contaminants, and these results appear in Figure 8-6. The land denial has also been calculated for the same maximum permissible doses, and appears in Figure 8-7.

Notice first of all that only small areas of land receive a large dose of radiation in the first 96 hours; in fact, these

TABLE 8-3

Radionuclides	Half Life (days)	Total Inventory ($\times 10^8$ curies)	Amount Released ($\times 10^8$ curies)
Cobalt 58	71	.0078	.003
Cobalt 60	1920	.0029	.001
Niobium 95	35	1.5	.0045
Zirconium 95	65	1.5	.0045
Ruthenium 103	40	1.1	.44
Ruthenium 106	366	.25	.10
Iodine 131	8.1	.85	.60
Cesium 134	750	.075	.03
Cesium 136	13	.030	.012
Cesium 137	11000	.047	.019
		5.363	1.214

Selected from an inventory of 54 radionuclides given in The Reactor Safety Study, Appendix VI, 3-3. Total release is 6 x 10^8 curies, corresponding to a PWR 1 release.

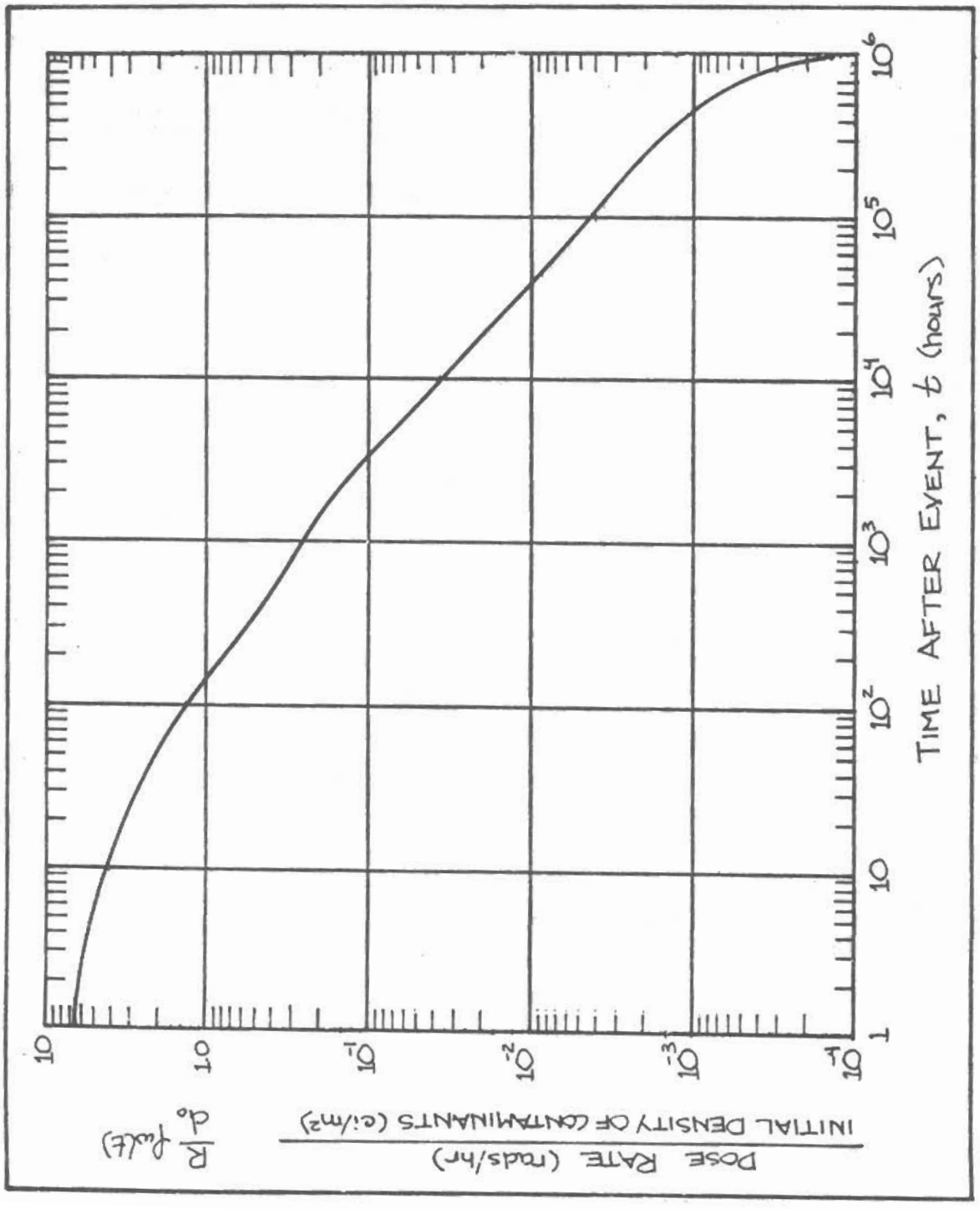

FIGURE 8-4: The decay of the dose rate with time for the radionuclides released in a PWR-1A reactor meltdown, as given by equation 8-4. Weathering included.

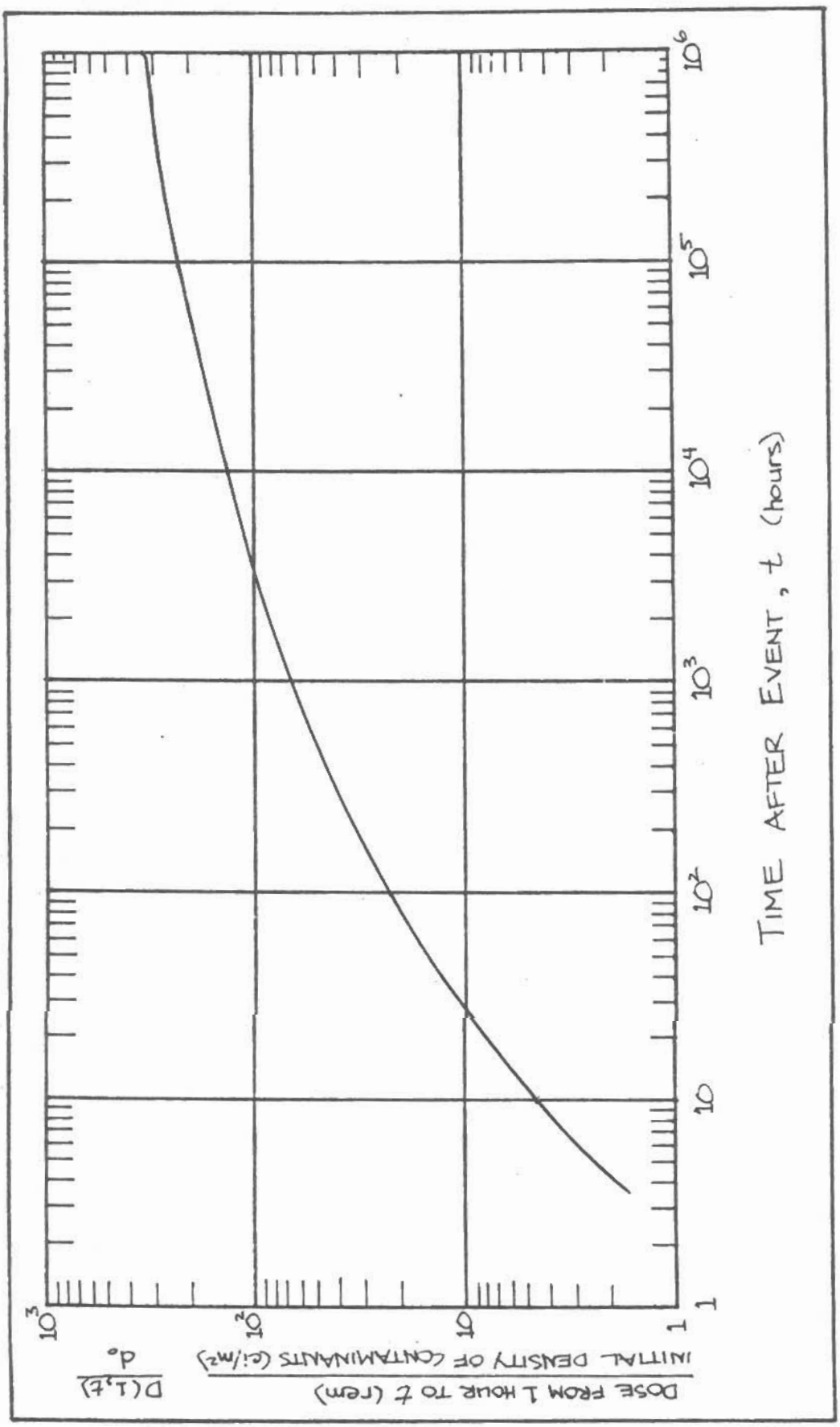

FIGURE 8-5: The integral of the function in Figure 8-4 from one hour to time t.

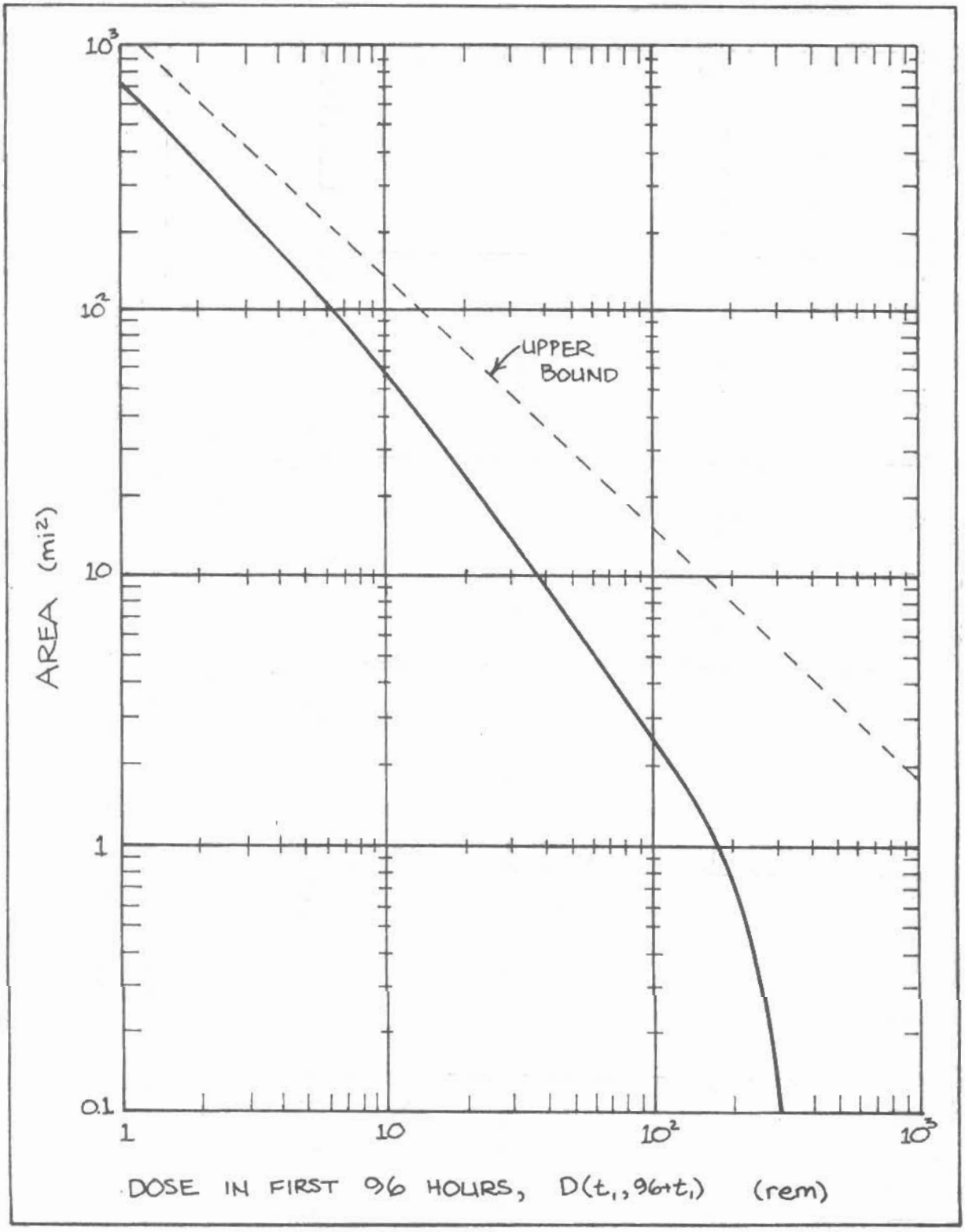

FIGURE 8-6: The area receiving a given ground dose in the first 96 hours from a meltdown. Solid line corresponds to "typical" conditions - $(v_d/u)=1/700$, $\bar{z}=100$, stability category "D".

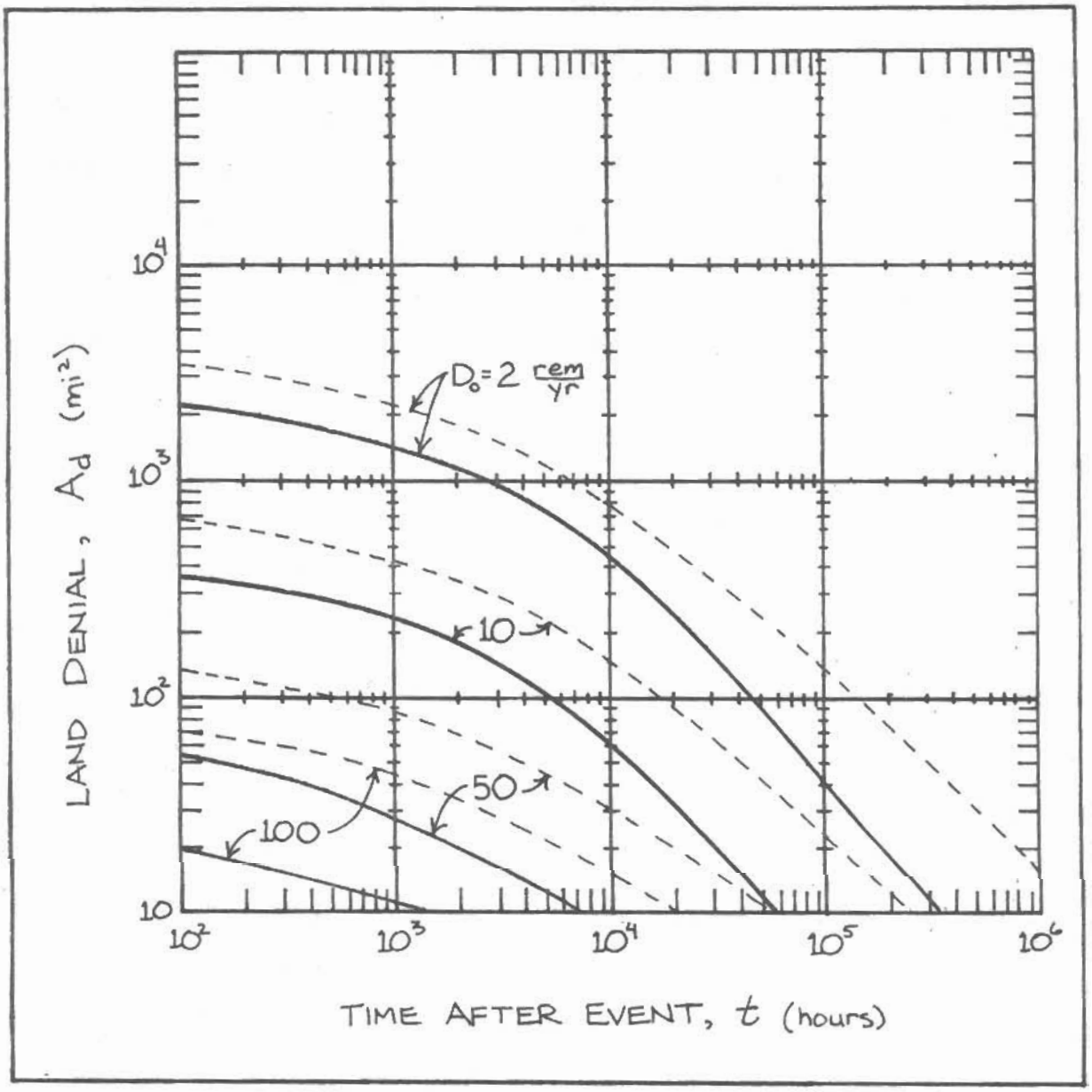

FIGURE 8-7: The land denial as a function of time for several values of D_o for a reactor meltdown, assuming "typical" conditions (solid lines). Dashed lines represent realistic upper bounds.

areas are at least 100, and more probably 1000 times smaller than the areas receiving the same dose from a surface burst weapon. Also notice that for short times after the attack, the magnitude of the land denial from the reactor meltdown is an order of magnitude less than that resulting from the surface burst of a one-megaton weapon, although after a few years the damage from the meltdown overtakes that from the weapon. From this point of view, the reactor is not an especially attractive target because it does not substantially increase the immediate damage inflicted by the attack. On the other hand, the weapon need not be surface burst in order to cause a reactor meltdown. If this is the case, the reactor may appear more attractive because the attack would afford a means of radiological contamination without ground-bursting the weapon, which reduces the damage done by air blast and thermal radiation by a factor of two. Even so, the attack must provide <u>additional</u> damage outside of the range of the weapon. In order to take complete account of the damage done by a meltdown, it is necessary to consider the dose that is inhaled by the downwind population.

We may also use the Gaussian plume model to predict the inhaled dose. If an average adult breathes a volume of air b per second, then the number of curies he will inhale during the passage of the cloud is bXt, where X is given by Equation 8-1, and t is the time it takes for the cloud to pass. If c is a constant which converts the number of curies per cubic meter of inhaled air into the dose in rem, then the total inhaled dose is given by:

$$D = cbXt = \frac{cb}{v_a}\left(\frac{d}{Q}\right)Q \qquad (8\text{-}5)$$

The breathing rate of a normal adult is about 1.0 cubic meters/hour, and (d/Q) can be read off Figure 8-3[7]. For the high doses of interest here, Equation 8-5[7] is quite insensitive to uncertainties in the deposition velocity, because such high doses occur at points close to reactor, before much deposition has occurred. The conversion factor c has been determined with a weighted average of the conversion factors of each radionuclide in the mixture; the individual conversion factors have been taken from Table VI D-2 of the Reactor Safety Study. The highest doses per inhaled curie are due to Ruthenium-106 and Cerium-144, which have conversion factors on the order of 3×10^5 rem/inhaled curie. The weighted average of all nuclides results in an average conversion factor of 1.4×10^4 rem/inhaled curie. As before, a total of 6×10^8 curies is assumed to be released in the meltdown. Substituting these values into Equation 5, we find that the total dose is $D = 2.4 \times 10^{11}(d/Q)$ for $v_d = 0.01$ meter/sec. Referring to Figure 8-3[7], we see that the maximum dose for typical conditions is 2400 rem, which occurs about 2 miles from the reactor. In comparison, 3000 rem is considered to be about the minimum dose to the lung which will cause death in less than a year. 50% fatalities are cause by a dose of about 4500 rem.[8] We can therefore conclude that for "typical" weather conditions, the inhaled dose will not contribute significantly to the number of fatalities from an attack on a reactor. It is wise to remember that almost everyone within an eight mile radius of a one-megaton nuclear detonation will be severely injured from other weapon effects. Even with the most favorable geometry, it is unlikely that a reactor meltdown will

produce a significant amount of additional prompt fatalities, because the plume would have to travel in excess of seven miles to encounter an unaffected population. Figure 8-8, which is taken from the Reactor Safety Study, shows that even for the most extreme weather conditions, the probability of death drops to zero only nine miles from the reactor.[9] Based on this and the calculated dose in the first 96 hours, we can conclude that a reactor meltdown will not significantly increase the prompt fatalities. However, as can be seen in Figure 8-7, an attack can be used to increase the land denial, but this increase will only be significant if the weapon is air burst.

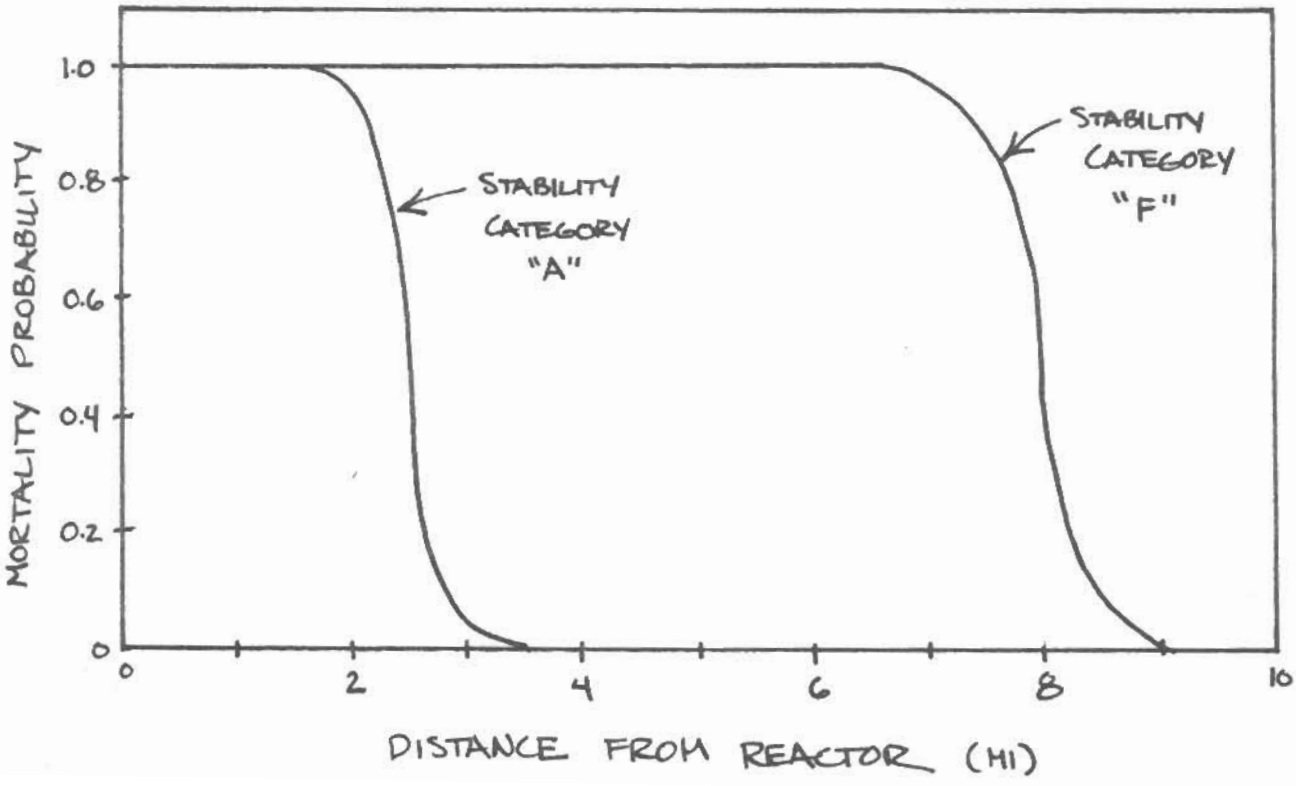

FIGURE 8-8- PROBABILITY OF MORTALITY FOR TWO EXTREMES OF ATMOSPHERIC STABILITY

CHAPTER 9

CONCLUSIONS

We now try to pull together the information presented in this report, and restate the question posed at the beginning: "Are nuclear reactors vulnerable to attack by nuclear weapons?"

To this we must answer a qualified "yes". If the attacker's objective is to cause great economic damage, contaminate vast tracts of land and the food supply, and if he can reliably deliver a large thermonuclear weapon within several hundred feet of the containment structure, then nuclear reactors <u>are</u> vulnerable to attack. Cratering a reactor will lead to a 70% increase in the lethal area, and a 50% increase in the area receiving radiation sickness. By attacking reactors as they exist today, the land denial in the short term can be increased by a factor of 3 to 10, and the total land denial will be 60 times larger than that caused by a weapon alone. The amount of contaminated farmland would also rise by a factor of 25-300.

If plans are carried out to increase on-site spent fuel storage, the damage can be increased dramatically; the total land denial would then be 160 times greater, and the farmland which is contaminated grows by a factor of 50 to 750. If reactors are located in twin or quad units, or in power parks, their vulnerability also increases substantially.

However, if the weapon is detonated 1,000 to 4,000 feet from the reactor, the vulnerability drops markedly. This corresponds to the range in which the reactor will be destroyed, and fission products will be released almost immediately, but the core is not

entrained in the radioactive cloud of the weapon. In this case, virtually no increase in the prompt effects will occur, and there will be very little increase in the total land denial (less than a factor of 2). Because of the amount of cesium released with the volatile fission products, there is a substantial increase in the amount of farmland contaminated - a factor of 20 to 150.

If the weapon is detonated between 5,000 and 20,000 ft, the additional damage from radiation becomes insignificant in the case of a surface burst, and only of marginal significance in the case of an air burst if only one reactor is attacked. Even under the worst circumstances, the effects of a meltdown would not add significantly to the prompt effects of the burst, and would result in a land denial in the short term which is 1/10 that of a surface burst alone.

At ranges where a breach of containment does not occur, but power generation is interrupted by a meltdown without release or by the collapse of supporting facilities, the vulnerability of the reactor is chiefly determined by the desire of the attacker to destroy energy production facilities, and by the cost of electricity. In this respect, reactors are only as vulnerable as any large-scale industrial operation with about the same capital investment and contribution to the GNP.

The accuracy which is needed to maximize the damage by the cratering of reactors is thought to be well within reach. In fact, current U.S. nuclear policy is based on the threat of a Soviet first-strike which would destroy all of our land based missiles. For such an attack to succeed, the warheads would

require accuracies of much less than 1,000 feet. One source assumes that by the year 2000 the Soviets will have 4,000 high-yield weapons with accuracies of about 50 feet.[1] The U.S. is now developing cruise missiles which have an accuracy of 50 ft. This is well within the range needed to crater a reactor (500-1000 ft).

The question of reactor vulnerability has only been touched by this report, and much more work needs to be done before reliable conclusions can be reached. There is no evidence in the open literature of plans to target reactor facilities by the U.S. or the Soviet Union, but this lack of evidence does not prove that reactors have escaped the attention of war planners. If further work indicates that the conclusions reached by this report are valid, then the risks posed by the generation and storage of radioactive materials must be brought into the current debates on both nuclear power and nuclear warfare. The severity of this issue cannot be pressed enough; targeting reactor facilities can prove to be an efficient means of desolating entire states.

1) R.L. Leggett, "Two Legs Do Not a Centipede Make", Armed Forces J. Int., 112, 6, 30 (Feb. 1975).

LIST OF SYMBOLS USED

A	Area (mi^2, ft^2, or km^2)
A_d	Land denial (mi^2)
a	Width of flat slab (Chap. 3; ft) Diameter of an ejecta missile (Chap. 4; ft)
a_i	Fraction of the ith nuclide in the mixture
a_m	The maximum ejecta diameter at range r (ft)
a_o	The ejecta diameter which corresponds to momentum P_o (ft)
b	Length of flat slab (ft) Breathing rate (Chapter 8; m^3/s)
$C(\mu)$	the ratio (R_m/f) corresponding to a ductility ratio μ
C_d	Drag Co-efficient
C_L	Seismic loading velocity (ft/s)
C_S	Seismic velocity (ft/s)
c	Dose conversion factor (rem/hr/curie/m^2)
c_i	The factor c for the ith nuclide
c_o	Speed of sound (ft/s)
CF	Dose conversion factor (curies/m^2/curie)
D	Dose (rad or rem)
D(r)	Depletion fuction
D_a	Apparent depth of crater
D_c	Total thickness of concrete slab (in)
D_o	Maximum acceptable dose per year (rem/year)
DC	Dose conversion factor (rem/curie ingested)
d	Effective thickness of slab (Chapter 3; in) Depth (Chapter 4; ft)
$d(r)$	Density of deposited contaminants (curies/m^2)
d_o	Initial density of deposited contaminants (curies/m^2)

E	Modulus of elasticity
F	Force (Chapter 3; lb) Constant; F=1 for soil, F=2 for hard rock (Chap. 4) Constant related to the effective wind speed (Chap. 7)
$F(t)$	Integrated decay function
f	Thermal partition function (Chap. 2) Fraction of energy derived from fission (Chap. 7)
$f(t)$	Decay function
f_s	Steel ratio
$f_w(t)$	Weathering function
$g(\epsilon)$	fraction of total energy emitted between ϵ and $d\epsilon$.
I	Impluse (psi-sec)
$\bar{I}$	Expected number of missile impacts
I_p^+	Incident positive phase impulse (psi-sec)
I_r	Reflected implulse (psi-sec)
K_{lm}	Transformation factor
k	Spring constant (lb/ft)
M	Mass ($lb\text{-}s^2/ft$)
$M(a_o)$	Total mass of missile with diameter greater than a_o (lb)
M_e	Total mass of ejecta (lb)
M_o	Ultimate moment (ft-lb/ft)
M_{oh}	Ultimate moment of horizontal tendons
M_{ov}	Ultimate moment of vertical tendons
M_{Pfa}	Total Positive ultimate moment along short edge
M_{Pfb}	Total positive ultimate moment along long edge
$\bar{m}$	Average missile mass (lb)
m_m	Maximum missile mass at a range r (lb)
m_o	Missile mass corresponding to a momentum P_o (lb)
N	Number of neutrons per unit area (n/cm^2)

$\bar{n}$	Average number of missiles
P	Pressure above ambient (psi) Momentum (lb-ft/s)
P	Probability
P_b	Missile momentum needed to breach containment (lb-ft/s)
P_i	Incident Overpressure (psi)
P_m	Maximum Overpressure (psi)
P_o	ambient overpressure (psi) Standard missile momentum (lb-ft/s)
P_r	Reflected pressure (psi)
P_s	Stagnation pressure (psi)
P_1	Pressure of first triangular pulse (psi)
P_2	Pressure of second triangular pulse (psi)
Q	Heat absorbed per gram of concrete (cal/gm) Dynamic pressure (psi) Total activity released (curies)
Q_m	Maximum dynamic pressure (psi)
q	rate of release (curies/s)
R	Dose rate (rad/hr, rem/hr)
R_a	Radius of apparent crater (ft)
R_m	Maximum force or resistance (lb)
R_1	Unit-time dose rate (rad/hr)
r	Distance from ground zero (ft, mi) Distance downwind (mi, km)
r_a	Radius of radioactive cloud (mi)
r_o	Twice the range required to reach the terminal velocity (ft)
T	Period (sec)
$T_{\frac{1}{2}}$	Half-life (hours)
t	time (seconds, hours)
t_p^+	Positive overpressure phase duration (sec)

t_q^+	Positive dynamic pressure phase duration (sec)
t_s	Stagnation time (sec)
t_{d_1}	Duration of first triangular pulse (sec)
t_{d_2}	Duration of second triangular pulse (sec)
t_1	Time it takes fallout to reach a point r (hours)
U	Velocity of shock front (ft/s)
u	Wind speed (mi/hr or m/s)
V	Volume of crater (ft^3)
V_1	Volume of crater in first layer (ft^3)
V_2	Volume of crater in second layer (ft^3)
v	velocity (ft/s)
v_d	Deposition velocity (m/s)
v_o	Velocity of missile corresponding to momentum P_o (ft/s)
W	Yield of weapon in kilotons
w	Maximum width of iso-dose contours (mi)
X	Concentration of contaminants ($curies/m^3$)
x	Distance into containment wall (cm)
x_m	Maximum horizontal acceleration (g's)
y	Displacement (ft) Crosswind direction (m)
y_e	Elastic limit (ft)
y_m	Maximum displacement (ft)
y_m	Maximum vertical acceleration (g's)
z	Plume centerline height (m)
γ	Specific heat ratio Density (lb/ft^3)
ϵ	Energy (ergs)
Θ	Angle of ejection

λ	Decay constant (hours^{-1})
μ	Mass absorption co-efficient (cm^2/gm) Ductility factor (y/y_e)
σ_c	Concrete compression strength (psi)
σ_s	Yield strength of steel (psi)
σ_t	Plastic strength of tendons (psi)
$\sigma_y(r)$	Standard deviation in the crosswind direction (m)
$\sigma_z(r)$	Standard deviation in the vertical direction (m)
τ	Transmittance

REFERENCES

1. Beyea, Jan and Frank von Hippel, Nuclear Reactor Accidents: The Value of Improved Containment, Center for Energy and Environment Studies, Princeton Univ., January, 1980.

2. Biggs, J.M., Structural Dynamics, McGraw-Hill, 1964.

3. Blomeke, J.O., and Mary F. Todd, Uranium-235 Fission-Product Production as a Function of Thermal Neutron Flux, Irradiation Time, and Decay Time, Oak Ridge National Laboratory, ORNL-2127, 1957.

4. Brode, H.L., First Supplement to Preliminary Safety Analysis Report, Brunswick Steam Electric Plant, Units 1 & 2, Carolina Power & Light Company, U.S. AEC Docket Numbers 50-324 and 50-325, 1968.

5. Brode, H.L., Height of Burst Effects at High Overpressures, Rand, RM-6301-DASA, 1970.

6. Brode, H.L.,"Review of Nuclear Weapons Effects", Annual Review of Nuclear Science, 18, 153, 1968.

7. Brode, H.L., A Review of Nuclear Explosion Phenomena Pertinent to Protective Construction, Rand R-425-PR, May 1964.

8. Chester, C.V. and R.O. Chester, "Civil Defense Implications of a Pressurized Water Reactor in a Thermonuclear Target Area", Nuclear Applications and Technology, Vol. 9, December 1970.

9. Chester, C.V. and R.O. Chester, "Civil Defense Implications of the U.S. Nuclear Power Industry During a Large Nuclear War in the Year 2000", Nuclear Technology, Vol. 31, December, 1976.

10. Crawford, Robert E., et al, The Air Force Manuel for Design and Analysis of Hardened Structures, Air Force Weapons Laboratory, AFWL-TR-74-102, 1974.

11. Design of Structures to Resist the Effects of Atomic Weapons, U.S. Army Corps. of Engineers Manuel EM1110-345-415, 1957.

12. Etherington, Harold, ed., Nuclear Engineering Handbook, McGraw-Hill, 1958.

13. Fetter, Steven and Kosta Tsipis, Catastrophic Nuclear Radiation Releases, PSTIS Report #5, MIT, 1980.

14. Gault, D.E., Spray Ejected from the Lunar Surface by Meteoriod Impact, Ames Research Center, NASA TN D-1767, 1963.

15. Day, T.P., et al, Ejecta Distribution from Flat Top I Event, Boeing, POR-3007, October 1965.

16. Geiger, W., "Generation and Propagation of Pressure Waves due to Unconfined Chemical Explosions and Their Impact on Nuclear Power Plant Structures", Nuclear Engineering and Design, 27, 1974.

17. Glasstone, Samuel and Philip J. Dolan, The Effects of Nuclear Weapons, U.S. Department of Defense, 1977.

18. Habip, L.M. Characterization of Structural Damage Caused by Extreme Dynamic Loads, International Conference on Structural Mechanics, J10/9, 1978.

19. Kot, C.A. and P. Turula, Air Blast Effects on Concrete Walls, Argonne National Laboratory, ANL-CT-76-50, 1976.

20. Kot, C.A., et al, Effects of Air Blast on Power Plant Structures and Components, Argonne National Laboratory, ANL-CT-78-41, 1978.

21. Melin, J.W. and S. Sutcliffe, Development of Procedures for Rapid Computation of Dynamic and Structural Response, Univ. of Illinios, 1959.

22. Preliminary Safety Analysis Report, First Supplement, Brunswick Steam Electric Plant, Units 1 & 2, Carolina Power & Light Company, U.S. Docket Nos. 50-324 and 50-325, 1968.

23. Reactor Safety Study, United Staes Nuclear Regulatory Commission, Appendix VI, October 1975.

24. Tsipis, Kosta, Nuclear Explosion Effects on Missile Silos, Center for International Studies, MIT, C78-2, 1978.

25. Sauer, F.M., et al, Nuclear Geoplosics, A Sourcebook of Underground Phenomena and Effects of Nuclear Explosions, Part IV, DASA-1285(IV), May 1964.

NOTES

(The first number refers to the list of references on pages 157 and 158)

Chapter 2

1) 17, 8.117b.
2) 10, p. 633.
3) 6, p. 177.
4) 10, p. 564
5) 17, 7.98.
6) 17, 7.87.
7) 7, p. 12.
8) 17, 11.50.

Chapter 3

1) 6, p.180.
2) 5
3) 17, Chap. 3
4) 6, p. 180.
5) 17, 3.55.
6) 17, 3.56.
7) 5, p. 17.
8) 17, 3.55.
9) 17, 3.57
   7, p.36,37.
10) 17, 4.42.
11) 17, 4.57-66.
12) 20, p. 28.
13) 11

Chapter 3 (cont.)

14) 21
15) Conversation w/ J. Biggs, O. Buyukozurk, M. Fardis
16) 2, p. 307.
17) 17, 5.139a, 5.140
18) 16, p. 198.
19) 18, p. 13.
20) 8, p. 792.
21) 6, p. 186.
22) 5, p. 34
23) 8, p. 793.

Chapter 4

1) 6, p. 195.
2) 17, 6.70 et seq.
3) 10, p. 118.
4) 10, p. 121.
5) 17, 7.20.
6) 17, 2.16.
7) 10, p. 152.
8) 4, p. 12-4.
9) 14
10) 15

Chapter 4

11) 10, p. 151.
12) 10, p. 150.
13) 10, p. 139.
14) 17, 6.75.
15) 4, p. 12-3.
16) 8, p. 788.
17) 20, p. 18, 26.

Chapter 5

1) 25
2) 7, p. 52, 53.
3) 10, p. 248.
4) 7, p. 53.
5) 22, p. 1-2

Chapter 7

1) 17, 9.79 et seq.
2) 17, 9.93.
3) 17, 9.97.
4) 12, p. 7-28.
5) 23, p. 8-8.
6) 17, 9.16.

Chapter 7 (cont.)

7) 17, 9.159,
   23, p. 3-3.

8) 3.

9) 23, p. 3-3, c-6.

10) 17, 2.16.

11) 23, p. E-30, 38

12) 23, p. 8-21.

13) 17, 9.124.

14) 23, p. 3-3.

15) 23, p. 10-5.

Chapter 8

1) 23, Chap. 4 & 5
   App. A & B.

2) 1, Fig. II-3.

3) 23, p. 6-2.

4) 23, p. A-5.

5) 23, p. Chap. 3.

6) 23, Table VI C-2.

7) 1, p. RII-4.

8) 23, p. F-4

9) 23, p. 13-9.